12/80
2/81
5/81
9.21.82

TESTING OF THE PERMANENT MAGNET MATERIAL Mn-Al-C FOR POTENTIAL USE IN PROPULSION MOTORS FOR ELECTRIC VEHICLES.

(Topical Report on Task 5 of Contract DEN3-189)

by Z. A. Abdelnour, H. F. Mildrum and K. J. Strnat

12 November 1980

prepared for the

NATIONAL AERONAUTIC AND SPACE ADMINISTRATION

NASA Lewis Research Center, Contract DEN3-189

SCHOOL OF ENGINEERING
and
RESEARCH INSTITUTE

UNIVERSITY OF DAYTON

DAYTON, OHIO

TESTING OF THE PERMANENT MAGNET MATERIAL Mn-Al-C FOR POTENTIAL USE IN PROPULSION MOTORS FOR ELECTRIC VEHICLES.

(Topical Report on Task 5 of Contract DEN3-189)

by Z. A. Abdelnour, H. F. Mildrum and K. J. Strnat

12 November 1980

prepared for the

NATIONAL AERONAUTIC AND SPACE ADMINISTRATION
NASA Lewis Research Center, Contract DEN3-189

SCHOOL OF ENGINEERING
and
RESEARCH INSTITUTE

TESTING OF THE PERMANENT MAGNET MATERIAL Mn-Al-C FOR POTENTIAL USE IN PROPULSION MOTORS FOR ELECTRIC VEHICLES

(Topical Report on Task 5 of Contract DEN 3-189)

TABLE OF CONTENTS

ABSTRACT: The development of Mn-Al-C permanent magnets is briefly reviewed. The general properties of the material are discussed and put into perspective relative to alnicos and ferrites. The commercial material now available from the Matsushita Electric Industrial Co. is described by the manufacturer's data.

The traction-motor designer's demands of a permanent magnet for potential use in electric vehicle drives are reviewed. From this, a list of the needed specific information is extracted. A plan for experimental work is made which would generate this information, or verify data supplied by the producer. These planned tests and measurements were executed in our laboratory.

The results of these measurements are presented in the form of tables and graphs. The data is discussed and interpreted. The tests determined magnetic design data and some mechanical strength properties. Easy-axis hysteresis and demagnetization curves, recoil loops and other minor-loop fields were measured over a temperature range from -50°C to +150°C. Hysteresis loops were also measured for three orthogonal directions (the easy and 2 hard axes of magnetization). Extruded rods of three different diameters were tested. The nonuniformity of properties over the cross section of the 31 mm diameter rod was studied. Mechanical compressive and bending strength at room temperature was determined on individual samples from the 31 mm rod.

This report presents the data as measured, in considerable detail. In this form it would be of use in motor design calculations. Simpler summary graphs and tables that allow one to get a quick picture of the behavior of Mn-Al-C magnets in general will be prepared and presented in a later report. If the use of this material in motors is seriously considered, more information about the temperature dependence of the flux at different operating points, irreversible losses on heating, and the long-term flux stability at elevated temperatures should be generated. The present contract did not provide for such extended studies, but suitable samples were obtained.

TESTING OF THE PERMANENT MAGNET MATERIAL Mn-Al-C FOR POTENTIAL USE IN PROPULSION MOTORS FOR ELECTRIC VEHICLES.

(Topical Report on Task 5 of Contract DEN3-189)

INTRODUCTION: Task 5 of this contract calls for an experimental characterization of the magnetic and some mechanical properties of the new permanent magnet material, Mn-Al-C. This work has now been completed and the results are herewith reported. However, to put our data into the proper perspective and make them more meaningful, the report sections on our experimental results are preceded by a general background discussion of Mn-Al-C, a review of the properties reported for it in the literature, information on the availability of the material, and some economic considerations. This discussion is based on information collected under Task 2, so some of those comments will be duplicated in a later report on Task 2, "Review of Permanent Magnets."

BACKGROUND INFORMATION ON Mn-Al-C MAGNETS

In the last few years the Matsushita Electric Industrial Co. in Japan has developed to commercial maturity a permanent magnet material which is based on a manganese-aluminum intermetallic phase. [1,2] Basically the same material had first caused excitement as a potential new permanent magnet about twenty years ago. Several industrial magnet laboratories (including those of the Indiana General Corporation in the U.S.[3] and the Philips Company in Holland [4]) attempted then to develop useful properties and fabrication methods, but the results were disappointing. No commercial production resulted, and work in the U.S. was discontinued. The principal problem was that of obtaining a sufficiently good metallurgical grain orientation which would result in a single-easy-axis magnetic anisotropy and, as a consequence, should yield good remanence, squareness of the intrinsic magnetization curve in the second quadrant, and a high energy product.

Development work continued, however, in Japan. As the result of a determined effort in the last decade, scientists at Matsushita developed a technique of warm extrusion and heat treatments which results in a favorable crystal texture[5] and in technologically interesting magnetic properties. Chemically, the material was slightly modified by the addition of small amounts of carbon and nickel. (The C metallurgically stabilizes the hardmagnetic phase, and the Ni facilitates extrusion.)

In terms of their room temperature magnetic properties, the best magnets of this kind (as described in Matsushita publications) combine moderately high remanence values ($B_r \approx 6$ kG), approaching those of Alnico 8 HC, with a coercive force ($H_c \approx 2.7$ kOe) in the range of that of high-energy hard

ferrites. This H_c is four times that of Alnico 5, or 1.5 times that of Alnico 8. The energy product of the best Mn-Al-C (7 - 7.5 MGOe) is comparable to that of grain-oriented Alnico 5. The material is not brittle like Alnico or ferrite; it has a moderate degree of ductility and is machineable on a lathe or milling machine with carbide-tipped tools. These are unusual mechanical properties for good permanent magnet materials, which must normally be shaped by grinding or electric discharge machining, or by other special techniques suitable for hard and brittle materials.

However, all these advantages (there are also some drawbacks; see below) might not have sufficed to give the material a promising commercial future in competition with the well-established Alnico magnets, had it not been for a cobalt supply crisis which developed in 1977-78. Cobalt is the principal alloying partner of iron in the higher-grade Alnicos (24-38% Co). Cobalt is a by-product of either copper or nickel production, and the United States has relied heavily on the African countries, Zaire and Zambia, as its cobalt suppliers. For a variety of reasons, the price of cobalt quintupled between mid-77 and mid-79, from about $5.00 to $25.00 per pound, and there was a time when manufacturers found it difficult to purchase cobalt even at this highest price. In contrast, manganese and aluminum - the principal constituents of the magnet material discussed here - are at present quite inexpensive (about $0.60/lb.), and the raw materials are plentiful. (It should be noted, however, that the U.S. presently imports practically all its manganese.)

In any case, due to the cobalt shortage, magnet users and producers have looked for potential replacements for Alnico, and the Mn-Al-C magnets are one attractive possibility.[6]

On the negative side, it must be said that the Mn-Al-C has a very low Curie temperature, ~290°C, compared with 700°C to 800°C for the Alnicos and 450°C for the ferrites. This has the consequence that all magnetic design parameters of these magnets are strongly temperature dependent, and the values of B_r, H_c, $(BH)_{max}$, etc., fall off rapidly as the magnet is heated above room temperature. Another apparent drawback at the present time is that the warm extrusion is a difficult process requiring heavy machines and therefore large capital investment; short lifetime of the extrusion dies appears to be a problem too. This has the consequence that the present price of Mn-Al-C magnets is in the same range as that of oriented Alnico 5. It is quite possible that, in spite of the low raw material price, Mn-Al-C may remain a relatively expensive magnet material in the long run.

MATERIAL AVAILABLE FROM MATSUSHITA ELECTRIC INDUST. COMP.[7]

The need for the extrusion step puts restrictions on the shapes and sizes in which the material can be manufactured. The material is always extruded in the form of a long rod of relatively small and simple cross-section, with the easy direction of magnetization along the extrusion axis. (But note that Matsushita has also published a laboratory method of producing a lower-energy magnet featuring an isotropic easy plane of magnetization perpendicular to the extrusion axis.[8] This is achieved by cutting a slice from the extruded bar and subjecting it to additional plastic deformation steps. Such a material could have application in small size, multi-pole structures such as the rotor in certain stepper motors.) In its laboratory pilot production, Matsushita has apparently produced a variety of rods of circular cross section, ranging from about 4 mm to 31 mm diameter. Some of these sizes are now going into a larger-scale commercial production (including 4 mm, 6.5 mm and 31 mm rods). Engineering samples of sufficient quantity for the evaluation in motors were promised to the General Electric R&D Center and possibly other U.S. customers for delivery in October 1980. Bars of rectangular cross section 5 x 10 mm were said to have been extruded successfully, but the problems of die wear and breakage are apparently so severe that no commercial production is contemplated at present.

According to information given us by Mr. Sakamoto during his visit at the University of Dayton in May, 1980, and earlier conversations with him and Mr. Kubo during K. Strnat's visit to the Matsushita Research Center at Osaka in June, 1979, Mn-Al magnets have been in a pilot line production there for 3-1/2 years now. Several million pieces of ~1 gram weight, cut from 4 mm and 6.5 mm extruded bars, have been sold to electric clock manufacturers. (This is a total quantity of several tons.) Slices from 24 and 31 mm diameter bars were used in commercial loudspeakers by another division of the Matsushita Company. A "pancake", axial-field electric motor for a bicycle drive is apparently also in commercial production. It uses the 31 mm diameter discs.

A new commercial manufacturing plant has recently been built by Matsushita about 100 miles from Osaka. It was scheduled to begin production in the summer of 1980. The production plan includes 10 diameters of circular rods, from 4 to 31 mm.

Matsushita continues to be the only source for Mn-Al-C magnets in the world. Apparently, no other company has been licensed by Matsushita for their patented extrusion process; and although the laboratories of Brown, Boveri (Switzerland), Colt Industries, General Electric, General Motors and the Indiana General Corporation say that they are doing some R and D work, there is no prospect for a commercial production outside Matsushita in the near future.

TYPICAL PROPERTIES ADVERTISED BY MATSUSHITA

Table 1 and Figure 1 are reproduced from an illustrated Panasonic announcement and data sheet received in May 1979. The sheet was undated, but the properties agree well with those given in Ref. 2 (July 1977), from which Table 2 is taken. Note that Table 2 contains some additional information not in Table 1.

TABLE 1·

Specifications (Preliminary)

Item	Symbol	Unit	Mn Al C Magnet (anisotropic)
Maximum Energy Product	(BH)max	x10⁶ G Oe	5 0 - 6 0
Residual Induction	Br	G	5 200 - 6 000
Coercive Force	Hc	Oe	2 000 - 2 600
Permeance Coefficient at (BH)max	Bd/Hd	G/Oe	2 3
Average Recoil Permeability	μ_r	G/Oe	1 0 - 1 2
Reversible Temperature Coefficient at Br		%/°C	- 0 12
Curie Temperature	Tc	°C	300
Density	d	g/cm³	5
Resistivity	ρ	x10 ⁶Ω cm	80
Coefficient of Thermal Expansion		x10 ⁶/°C	18
Hardness (Rockwell C)	HRc	—	50 - 55
Tensile Strength		kg/mm²	> 30
Compressive Strength		kg/mm²	> 200
Transverse Strength		kg/mm²	> 20

FIGURE 1:

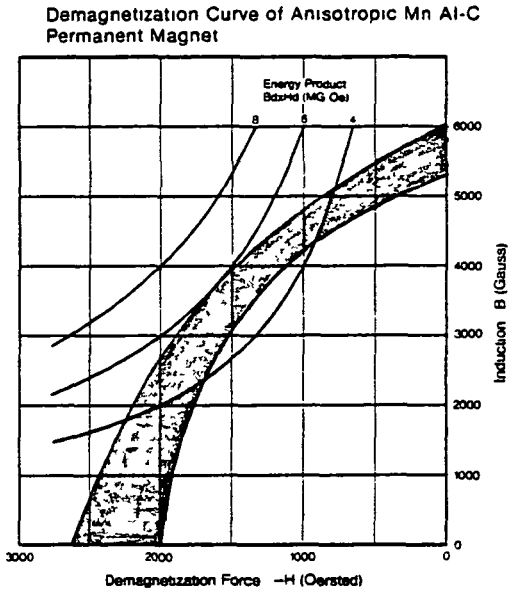

TABLE 2: Summary of properties (Ref. 2)

Item	Symbol	Unit	Mn-Al-C magnet (anisotropic)
Residual Induction	(Br)	G	5200~6000
Coercive Force	(Hc)	Oe	2000~2600
Maximum Energy Product	(BH)max	× 10⁶G·Oe	5 0~6 0
Band H at (BH)max	(Bd)	G	3600
	(Hd)	Oe	1550
Permeance Coefficient at (BH)max	(Bd/Hd)	G/Oe	2.3
Average Recoil Permeability	(μr)	G/Oe	1 0~1 2
Recoil Energy Product	(Er)	× 10⁶G·Oe	2.2
Reversible Temperature Coefficient at Br		%/°C	-0 12
Curie Temperature	(Tc)	°C	300
Absolute Maximum Temperature		°C	500
Density	(d)	g/cm²	5 1
Resistivity	(ρ)	× 10 ⁶Ω·cm	80
Coefficient of Thermal Expansion		× 10⁻⁶/°C	18
Specific Heat		Cal/g°C	0 15
Hardness (Rockwell C)	(HRc)	-	50~55
Tensile Strength		kg/mm²	> 30
Compressive Strength		kg/mm²	> 200
Transverse Strength		kg/mm²	> 20
Machinability		-	machinable

FIG. 2· Demagnetization Curves for Anisotropic Mn-Al-C Magnet at Different Temperatures. (From Reference 1, Ohtani et al.)

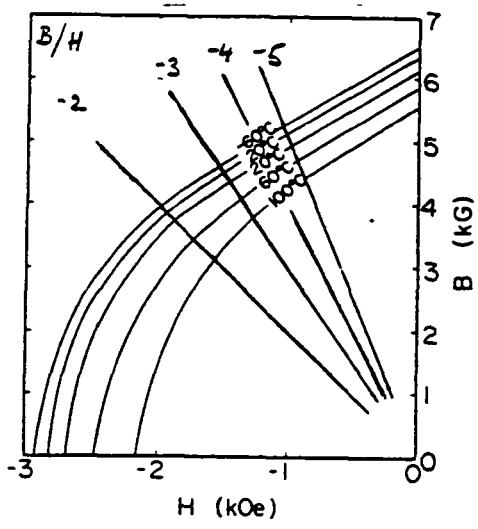

Another 1977 news release[9] gave somewhat more optimistic upper limits for the remanence (6200G) and energy product (7 MGOe). The demagnetization curves at different temperatures shown in Fig. 2 are from Ref. 1 (we drew in the B/H load lines). They belong to a magnet that has 7 MGOe at +20°C.

Mr. Yoichi Sakamoto provided us with machining instructions for turning Mn-Al-C magnets on a lathe. These are reproduced here as Table 3. Mr. Y.S. stated that on ordinary SiC cutoff wheel may be used, too, and we have also successfully cut the material with an electric discharge machine (EDM).

DATA REQUIREMENTS FOR TRACTION-MOTOR USE OF Mn-Al-C AND THE GENERAL PLAN FOR OUR EXPERIMENTAL STUDIES

1. For the contemplated use of Mn-Al-C magnets in the rotors of traction motors, it would be desirable to have a high air-gap flux density of about 6 k G. However, if the magnet is placed directly at the gap, as in the GE axial-field, "advanced motor" design,[10] B_{gap} is only about 3 to 4 kG if the material is used close to its maximum volumetric efficiency. The high motor currents possible during vehicle climb or in a stall/start condition, and the self-demagnetizing fields due to the air gaps, require that the magnet have a high resistance to demagnetization. The coercive force of Mn-Al-C, ~2600 Oe at room temperature, is relatively favorable compared to the values for Alnico grades (600-1900 Oe).

Nevertheless, the combination of B_r and H_c offered by Mn-Al-C is said to require the use of large magnet blocks in the motors. These are cubes or trapezoidal prisms of about 1 inch edge length. Considering the production limitations on Mn-Al-C shapes and sizes, each such block must be assembled from several pieces that have to be cut from the 31 mm cylindrical extruded stock. In the process, certain inner portions of the bar are selected for use, while some of the outer rim will be cut off and discarded. It is thus desirable to know if there is a variation of properties over the cross section. One aspect of our experimental study addressed this question.

2. The flux direction in the magnet is not always or in every volume element parallel to the easy axis of magnetization[11] (i.e., the extrusion axis in Mn-Al-C). Attempts to take this fact quantitatively into account in the design of machines require a detailed knowledge of the magnetization characteristics of the permanent magnet, not only for the easy-axis magnetization direction for which they are usually published by the manufacturer, but for three mutually perpendicular directions.[12] We undertook it to describe the magnetic anisotropy by measuring major hysteresis loops for the extrusion axis, the radial and the circumferential ("transverse") directions of the 31 mm extruded bar. This was done at several temperatures, and at room temperature for two locations on the bar cross section.

TABLE 3: MACHINING CONDITIONS FOR THE ANISOTROPIC Mn-Al-C PERMANENT MAGNET USING A LATHE

Bit ---------- Cementated Carbide Bit
Rotating Speed ---------- 1,115 r.p.m.
Feed ----------0.02-0.03 mm/rev.
Depth of Cut ---------- 2.0 mm(rough), 0.25 mm(finish)
Nose Radius of Bit ------- 0.1-0.2 mm
Shape of bit

• Surface Cetting ----- Point Nose Straight Tool

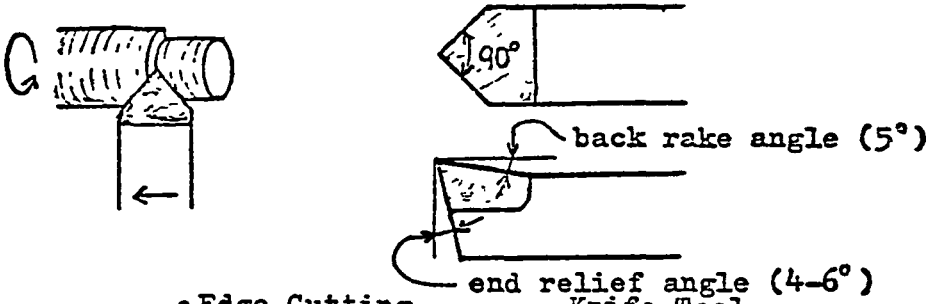

• Edge Cutting ------- Knife Tool

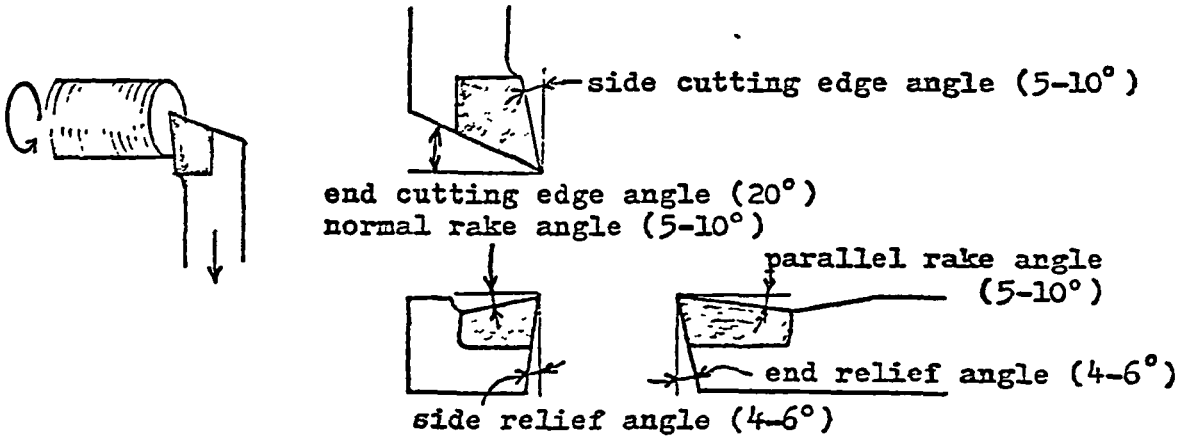

• Drilling ---------- Straight Drill (all cemented carbide drill)

Received June 26, 1980
from Mr. Sakamoto of:

Matsushita Electric Industrial Co., Ltd.
CENTRAL RESEARCH LABORATORIES
MORIGUCHI OSAKA 570 JAPAN
TEL OSAKA(06)909 1121 CABLE MATSUDEN MORIGUCHI" TELEX MATUSITA J 63426

3. According to the motor designers we interviewed on this question, the new vehicle traction motors are designed to operate at winding temperatures of about 150°C. Peak temperatures of 180°C to 200°C might be tolerable from the point of view of electrical insulation and structural integrity. Although the magnets will generally be cooler, they certainly could get as hot as about 150°C unless special provisions are made for cooling them. Because of its low Curie temperature, Mn-Al-C shows fairly severe flux losses on heating. While the generally reported temperature coefficient of $B_r(H=0)$ is moderate (- 0.12% per °C, average between 0 and 100°C) inspection of the set of curves in Fig. 2 shows that the intrinsic coercive force and hysteresis loop shape deteriorate much more rapidly on heating than does the zero-field remanence. As a consequence, the temperature coefficient of the useful flux density, B_d at a realistic operating point of perhaps $B_d/H_d = -2.3$ to -2.5, is going to be much less favorable. Also, the losses above 100°C will rise at an increasing rate. The severe loss of ${}_MH_c$ on heating means a poor resistance to demagnetization under the combined influence of motor overheating and large currents during a prolonged steep climb, an operating condition that must be expected on occasion. The designer, who must protect the magnet against demagnetization under such worst-case conditions, thus needs detailed information about the temperature dependence of the hysteresis curves and recoil loops. While low temperatures do not pose a threat to the stability of Mn-Al-C magnets, their characteristics down to the lowest expected environmental temperatures should also be known. With these requirements in mind, we measured demagnetization curves B vs. H and (B-H vs. H over the range from -50°C to +150°C.

4. The variable effective air gap during motor operation, current surges occuring for any reason, or partial disassembly of the motor cause the magnet material to change its operating permeance, to "recoil," and thus to work on a minor hysteresis loop in the second quadrant of (B-H) vs. H. We have measured recoil loop fields (full recoil to H=0) at several different temperatures in order to allow designers to accurately assess the effects of such operating point changes.

For some samples (at room temperature only) an extended minor-loop field was plotted with the recoil lines continuing through the first quadrant to the full original forward magnetizing field. These curves will be useful in determining how to initially charge the magnets in the fully or partially assembled motor, or how to remagnetize them after accidental demagnetization, or in similar operations. Minor loop fields were plotted only for the extrusion axis, i.e., the normal magnetization direction.

MAGNET SAMPLES USED IN OUR TESTS AND SUMMARY OF MEASUREMENTS MADE ON THEM

The following is a description of the samples as received and as they were prepared for the measurements by us. We also present tables of the commonly given room-temperature quantities as reported by the Matsushita Research Laboratory and measured by us. This section will also serve as a guide to the following recorder plots and graphs which show the detailed results of our measurements.

Sample Group I

● Material supplied: Three cylinders, 6.4 mm diameter x 8 mm long, magnetized along axis. Cut from 6.5 mm extruded rod stock by Matsushita. Received at Osaka on June 3, 1979. These samples were machined and selected by Matsushita. Room temperature hysteresis loops were measured and provided with the samples. The cylinders were marked as No. 6, 7 and 8.

● Reported composition: 70 wt. % Mn, 29.5% Al, 0.5% C. (Letter from Mats.)

● Salient Room-Temperature Magnetic Properties:

Data By:		Matsushita (26°C)			Univ. of Dayton (25°C)		
Identification		B_r	$_MH_c$	$(BH)_m$	B_r	$_MH_c$	$(BH)_m$
Mat.	U. Dayton	kG	kOe	MGOe	kG	kOe	MGOe
No. 6	M-1483	5.95	2.63	6.0	6.17	2.72	6.4
No. 7	M-1481	5.96	2.61	--	6.17	2.74	6.5
No. 8	M-1482	5.98	2.75	--	6.18	2.82	6.5

● Comments on these results:

Note that Matsushita reported conservative numbers. We measured slightly higher values for remanence, coercivity and energy product. This is unusual. We normally find the claims of vendors exaggerated and measure lower properties than reported by the producers.

- Measurements made on these samples:

1. Major hysteresis loops at room temperature (RT = 25°C), for all three cylinders. Intrinsic loop, (B-H) vs. H, directly recorded. Normal demagnetization curve, B vs. H, manually drawn. (Figures 3, 4 & 5)

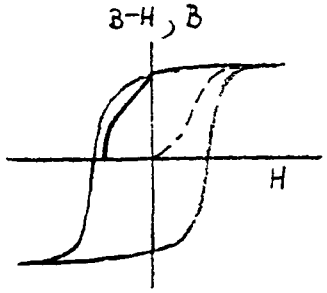

2. Recoil loop fields, 2nd quadrant (abbrev. Q-2) curves (B-H) vs. H (directly recorded) and B vs. H (manually replotted from B-H curves). For sample M-1482 (No. 8) only; 25°C. (See Figure 6)

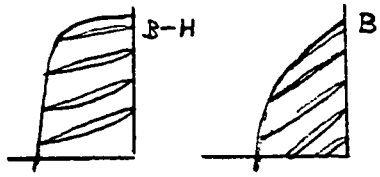

3. Minor loop field, (B-H) vs. H. From Q-2 and Q-3 back to +H peak. For sample M-1482 (No. 8) only. At 25°C. (See Figure 7)

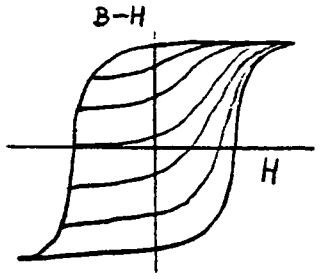

Sample Group II:

- Material supplied: One disc, ~31 mm diameter x 6 mm thick, magnetized through thickness = cylinder axis = extrusion direction. Cut at Matsushita from ~31 mm extruded rod stock. (Pilot plant product, probably early 1979). Received at Osaka on June 3, 1979.

- Samples machined at U. Dayton for magnetic measurements: Two cylinders, 6.35 mm (1/4") diameter x 6 mm long were EDM machined from two locations, the center of the disc and near the rim, as shown in the sketch.

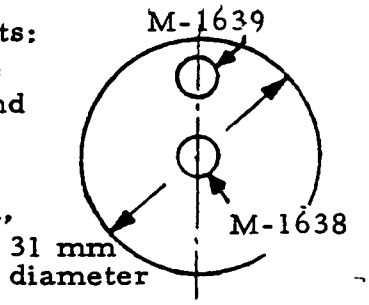

- Reported "typical" composition: 69.5 wt. % Mn, 29.3% Al, 0.5% C, 0.7 wt. % Ni.

- Salient Room Temperature Magnetic Properties:

Matsushita (22°C)				University of Dayton (25°C)				
B_r kG	M^H_c kOe	B^H_c kOe	$(BH)_m$ MGOe	Sample Identification	B_r kG	M^H_c kOe	B^H_c kOe	$(BH)_m$ MGOe
5.7	2.7	2.3	5.1	M-1638	5.48	2.91	2.44	5.1
Measured on the whole disc				M-1639	5.85	2.93	2.52	6.0

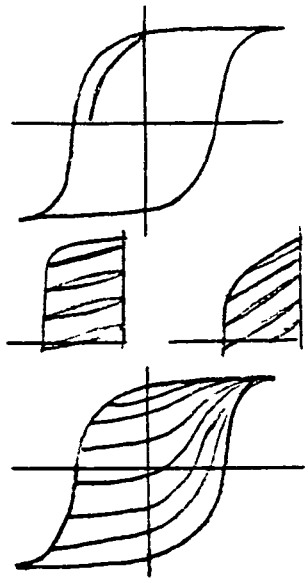

- Measurements made on these samples:

  1. Major hysteresis loops at RT (25°C) for both samples, (B-H)vs. H. demag. curve B vs. H manually drawn in. (Figures 8 & 9)

  2. Recoil loop fields, Q-2, (B-H)vs. H and B vs. H . For center sample M-1638 only, 25°C (See Figure 10)

  3. Minor loop field, (B-H) vs. H, from Q-2 and Q-3 back to +H peak. For center sample M-1638 only, 25°C (See Figure 11)

- Objectives of tests:

  1. To study the variation of properties over the cross section of the extruded rod.

  2. To study the dependence of the magnetic properties on the diameter of the extruded stock.

  3. To generate minor and recoil loop fields characteristic of the largest diameter rod stock (31 mm) in pilot production before June 1979. (Compare with minor loops of the small, 6.5 mm rod stock of Sample Group I.)

- Notes on results:

  1. Again, it appears that Matsushita reported properties conservatively. Our weighted average energy product value would be almost 6 MGOe, compared with Matsushita's 5.1 MGOe.

  2. The B_r and $(BH)_{max}$ for the 31 mm rod are poorer than those of the 6.5 mm rod stock. It appears that the smaller the diameter of the extruded bar, the better is the grain orientation achieved, and therefore the remanence, loop squareness and energy product.

  3. There is a radial gradient of the properties. B_r and $(BH)_{max}$ near the rim are about 7% and 18% higher than the respective quantities at the center of the rod. This is certainly due to better crystal orientation. It is likely that the greater shear stresses near the die wall during the extrusion process favor the formation of the desired crystal texture there.

Sample Group III:

- Material supplied: Discs, 31 mm diameter x 8.15 mm thick, magnetized through thickness = cylinder axis = extrusion direction. Cut at Matsushita from 31 mm extruded rod stock. (Commercial product, early 1980). Received by mail from Mr. Sakamoto in June, 1980. (Letter dated 5/29/80.)

- Samples machined from Disc B at Inland Motor/Kollmorgen and the University of Dayton:

  (a) Three cubes, along a diameter; one at center of disc, two symmetrically located halfway between center and rim. Edge length 8.13 mm (0.320 inch). Axes parallel to extrusion direction, a radius, and a tangent to the circumference ("transverse direction" for outer cubes)

  (b) Two bars of cross section 3.18 x 3.18 mm (0.125 inch) and ~27 mm length, located as shown in sketch.

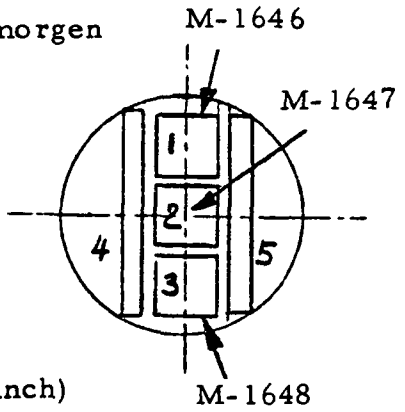

- Salient Room Temperature Magnetic Properties:

Matsushita (27°C)				University of Dayton (25°C)				
B_r kG	M^H_c kOe	B^H_c kOe	$(BH)_m$ MGOe	Sample Identification	B_r kG	M^H_c kOe	B^H_c kOe	$(BH)_m$ MGOe
5.45	3.15	2.55	5.0	M-1646	5.84	2.85	2.43	5.4
Measured on the whole disc. (Identified as sample B)				M-1647	5.86	2.87	2.42	5.3

- Note concerning the magnetic measuring method:

The UD values in the above table are from hysteresis loops measured with a (B-H)-compensated coil arrangement. It uses a close-fitting, centered, surface H-coil that inductively senses dH/dt for both the H deflection and the H-flux compensation. For the measurements of the temperature and direction dependence of properties, another coil fixture was used which contains a square H-coil identical to the B-coil, and where these coils are side-by-side rather than concentric. The absolute accuracy of the concentric coils is better than for the side-by-side ("dual coil") arrangement. However, only the latter allows controlled temperature variation. The use of these different coil arrangements is the main reason for the minor

variations between magnetization curves measured on the same sample at the same temperature. The curves are presented as-measured, and no attempt was made to normalize all values to the concentric-coil values as a standard. For most purposes, the differences are negligible.

- Measurements made on the cubic samples.

1. Major hysteresis loops at RT (25°C) for all three cubes: (B-H) vs. H measured and B vs. H calculated. Note that equivalent measurements were made with the concentric coils and with the dual coil. The latter was first used by itself with the sample in direct contact with the yoke poles, and then inside a heating/cooling fixture which contains fixed extension pole prices that may introduce minor air gaps. (Figures 12 through 20)

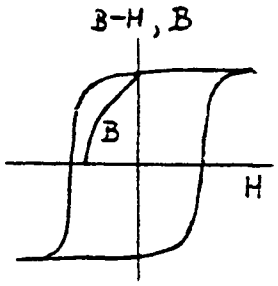

2. Q-2 recoil and full minor-loop fields at RT as before, for easy axis only, using the dual coils with heating/cooling fixture in place. (Figures 21 through 26)

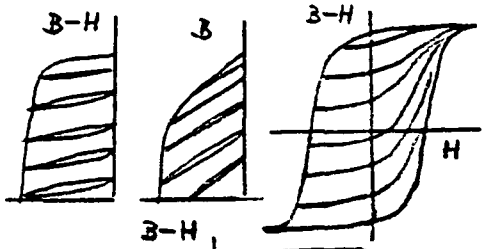

3. Major hysteresis loops for all three cube axes at RT, using the concentric and the dual coils with fixture. (Anisotropy measurement.) On 3 cubes. (Figures 27 through 32)

4. Easy-axis major loops (B-H) and B vs. H at the temperatures -50°C, 0°C, (+25°C, see No. 1) +50°C, +100°C and +150°C. Dual coils with fixture. 3 cubes. (Figures 33 through 47)

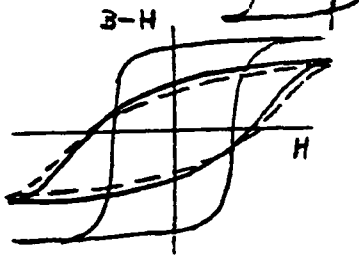

5. Major hysteresis loops for all three cube axes at -50°C, 0°C, (+25°C), +50°C, +100°C and +150°C. Dual coils with fixture. 3 cubes. (Figures 48 through 62)

6. Q-2 recoil loop fields (B-H and B) for the same temperatures. Dual coils with fixture. Easy axis. All 3 cubes. (Figures 63 through 77)

7. Q-2 demagnetization curves (B-H and B) for all temperatures, summary graphs (recorded independently). Dual coil with fixture. Easy axis. All 3 cubes. (Figures 78, 79 & 80)

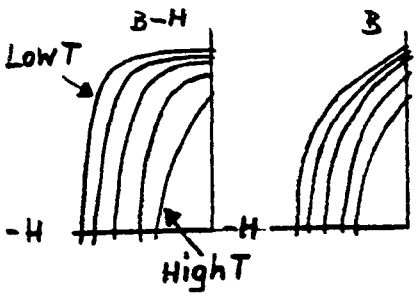

Sample Group IV:

- Material supplied: Two cylinders, 6.35 mm diameter x 30 mm long. Magnetized in long direction = cylinder axis = extrusion direction. Machined at Matsushita from 24 mm extruded rod stock. (Presumably pilot line product, early 1980). Sample location on bar cross section as shown in sketch.
  Received from Mr. Sakamoto in June, 1980. (Letter dated 6/10/1980.)

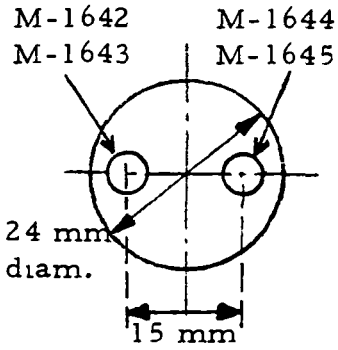

- Samples cut at U. Dayton for magnetic measurements: Four cylinders of different length from each of the two bars. (D= 6.35 mm = 1/4 inch).

Length	mm	~8.8	~7.1	~5.6	~4.2
L/D	--	1.40	1.12	0.89	0.66
B_d/H_d	G/Oe	~5	~4	~3	~2

Relationship between L/D and B_d/H_d based on the ballistic demagnetizing factor of Joseph.[14]

- Reported "Typical" Composition (per Matsushita letter): 69.5 wt. % Mn, 29.3 % Al, 0.5 % C, 0.7 wt. % Ni

- Salient Room Temperature Magnetic Properties

Sample Identification	Length mm	B_r kG	$_MH_c$ kOe	$_BH_c$ kOe	$(BH)_m$ MGOe
Matsushita (27 °C) - Average for 24 mm extruded rod.					
Extruded Rod	--	5.45	3.3	2.75	5.4
Univ. of Dayton (25 °C) - 2 samples cut from 6.35 mm cylinder.					
M-1642	8.84	5.69	3.44	2.83	5.8
M-1643	5.59	5.66	3.46	2.83	5.7
M-1644	8.84	5.72	3.44	2.85	5.9
M-1645	5.56	5.64	3.42	2.79	5.6
Average Values	--	5.68	3.44	2.83	5.75

● Note concerning the measuring method: The hysteresis loop measurements on these samples (as on the 1/4" cylinders of Sample Groups I and II) were made with a (B-H)-compensated coil arrangement with a closely fitting, concentric surface H-coil used for the H-deflection and the H-flux compensation. The pole faces of the magnetizing yoke (Varian 4" DC laboratory electromagnet) were in close contact with the sample ends. (B-H) was calibrated against pure iron standards of dimensions close to the samples. The saturation of Fe was taken as 21,580 Gauss.

● Measurements made on these samples:
At room temperature only, full hysteresis loops (B-H) vs. H were recorded, and Q-2 demagnetization curves B vs. H were calculated and manually drawn into the recorder graphs. This was done for two of the four samples of different length which were cut from each of the two 1/4" rods received. (See Figures 81 to 84 and the above table.)

● Objectives of the tests:

1. To characterize material from the third extruded rod diameter available to us, i.e., 24 mm rod stock. (Compare with 6.5 mm and 31 mm measured before.)
2. To document the initial room-temperature properties of these samples on which we plan to make open-circuit flux stability studies at a later date.
3. To compare again our measurements with those of Matsushita.
4. To demonstrate the slight variation of our measured values for B_r and $(BH)_{max}$ on the length of the sample for presumably identical material.

● Notes on the results:

1. Again, we measure slightly better properties (all! See table) than Matsushita reported: +4% for B_r and ${}_M H_c$, +3% for ${}_B H_c$, and +6.5% for $(BH)_{max}$.
2. There is a slight dependence of the properties - measured with our coil arrangement – on the length of the sample. It is in the sense that the measured values of B_r, ${}_B H_c$ and $(BH)_{max}$ are slightly lower for the shorter samples than for longer ones. Comparing the 8.8 mm and the 5.6 mm cylinders, the differences were ~1% for B_r, ~1.2% for ${}_B H_c$, and ~3.5% for $(BH)_{max}$, not much more than the reproducibility limits. ${}_M H_c$ is independent of the sample geometry within the error limits, as it should be.

3. The remanence and energy values for this 24 mm rod stock lie between those of the 6.5 mm rod and those of the 31 mm rod, but closer to the latter. Using the Matsushita figures (because they are averages over the whole rod cross section), the salient properties compare as follows:

Rod Diameter	B_r	$_M H_c$	$(BH)_m$
mm	kG	kOe	MGOe
6.5	5.95	2.63	6.0
24	5.45	3.30	5.4
31	5.45	3.15	5.0

● Plans for future experiments on these samples:
We hope to conduct temperature cycling and elevated temperature/long-term flux stability studies on the samples of Group IV. In these, the open-circuit remanent flux would be measured at different temperatures, and as a function of time-at-temperature, with a resolution of 0.01%. The different L/D ratios determine different B_d/H_d operating permeance and allow one to simulate the circuit behavior of the magnet at different operating points.

The present contract does not provide for such stability studies.

MECHANICAL TESTS

1. Machining Experience

During the machining of test samples it became obvious that the extruded Mn-Al-C (Ni) alloy is not really ductile at room temperature. While it can certainly be machined with carbide tools according to Matsushita's instruction, the workpiece chipped severely during drilling on the exit side. In spark-erosion machining (EDM), too, a piece broke off the corner of one cube. The latter fracture may have started at a flaw that was present in the 31 mm disc from the extrusion process. The fracture surfaces look like those of ceramics and are indicative of brittle fracture.

2. Bending Test for Flexural Strength

According to the test plan, room-temperature bending tests were performed on two specimens cut from a 31 mm disc. (Sample Group III; see sketch on page 12 for sample location, specimens 4 and 5.) However, only the ultimate strength was determined. The samples were too small to instrument them for elastic modulus and Poisson's ratio measurements, as was originally intended.

The flexural tests were performed on prismatic bar specimens of 3 x 3 x ~26 mm (0.13 x 0.13 x ~1 in) size, with the load applied parallel and perpendicular to the magnetization = extrusion direction. The long direction of the bar was essentially along a diameter of the 31 mm disc, i.e., a magnetically hard axis. The samples were magnetized.

Four-point flexure testing was used in preference to a uniaxial tension test for several reasons. Uniform-stress, uniaxial tensile tests using the familiar "dogbone" shaped specimens would be too wasteful of material. We did not have enough to make standard-size samples. Moreover, direct tension tests are very susceptible to parasitic stresses resulting from eccentric loading, and to cracking of specimens in the test grips, in the case of brittle materials.

In contrast, the four-point flexure test uses a very simple specimen geometry and permits the use of quite small samples. Under load, a constant moment is developed between the two inner load points. Consequently, a uniform surface stress is developed over a significant portion of the sample and valid test data can be obtained for failures which occur anywhere in that region. To minimize errors from fixture misalignment, friction effects, and contact point wedging, a kinematically designed bend fixture is employed. This fixture incorporates the basic design features recommended by the NATO Advisory Group for Aerospace Research and Development. A universal testing machine is used to load specimens at a rate intended to produce failure in not less than two minutes.

From the machining experience described above we had reasons to suspect that the material is indeed relatively brittle. The fracture mode of the flexure test bars confirmed this. The broken surfaces again look like those of the machining fractures, and there is no evidence of plastic deformation before failure of the bars.

The test results are given in the table below:

Specimen Type	Dimensions b[mm]	d[mm]	Load [kgf]	Ultimate Strength [MPa]	[kgf/mm^2]	[kpsi]
F $\parallel$ M	3.23	3.24	27.3	150.8	14.8	21.9
F $\perp$ M	3.34	3.21	31.6	171.0	16.8	24.8

3. Compressive Strength Test:

The testing plan provided that one of the cubes cut from the 31 mm diameter stock, Sample Group III, should be subjected to a compressive strength test. This has not yet been done. Since we will be destroying a magnetic test sample (M-1647) we wanted to be sure that it will not be needed for more magnetic property measurements before doing so. The results will be included in a later report.

The sample will be loaded in a compression fixture with the force parallel to the extrusion direction = magnetic easy axis = thickness of the cylindrical disc A-3. A stress-strain curve will be recorded. Numerical values for the elastic modulus, elastic limit, yield point and ultimate strength will be derived from the curve.

REFERENCES:

1. T. Ohtani et al., "Magnetic Properties of Mn-Al-C Permanent Magnet Alloys." IEEE Trans. Magnetics, MAG-13, (1977), p. 1328.

2. T. Kubo et al., "Anisotropic Mn-Al-C Alloy Permanent Magnets can be Machined and Mass Produced." JEE, No. 127 (July 1977), p. 50. (DEMPA Publications, Inc., Tokyo, Japan)

3. M.A. Bohlmann, "Manganese-Aluminum for Permanent Magnet Material." Tech. Docum. Report ASD-TDR-63-422 (1963), Wright-Patterson AF Base, Ohio.

4. A.J.J. Koch et al., J. Appl. Phys. 31 (1960) p. 75 S.

5. Y. Sakamoto et al., "Crystal Orientation and its Formation Process of an Anisotropic Mn-Al-C Permanent Magnet." J. Appl. Phys. 50 (1979), p. 2355.

6. G.Y. Chin et al., "Impact of Recent Cobalt Supply Situation on Magnetic Materials and Applications." IEEE Trans. Magnetic, MAG-15 (1979) p. 1685.

7. The Information about Matsushita's production program and future prospect given in this section is based primarily on conversations with two Matsushita engineers, Mr. T. Kubo and Mr. Y. Sakamoto, in June 1979 and In May 1980.

8. Y. Sakamoto et. al,, "New MnAlC Permanent Magnets Exhibiting Macroscopically-Plane Magnetic Anisotropy." IEEE Trans. Magnetics, MAG-16 (1980) p. 1056.

9. Matsushita (National/Panasonic) News Release, MEP-77-7, dated March 4, 1977.

10. G. Kliman, General Electric Comp., Corp. R. and D. Center. Personal communication (July 1980)

11. P. Campbell, "The Magnetic Circuit of an Axial Field D.C. Electrical Machine." IEEE Trans. Magnetics, MAG-11 (1975) p. 1541.

12. P. Campbell, "Permanent-Magnet Motors for Electric Vehicles." Electric Vehicle Developments, No. 3 (Sept. 1979) p. 1. IEE, London.

13. F. Echolds, Garrett Airesearch Mfg. Co. Verbal information (May 1980).

14. R. E. Joseph, "Ballistic Demagnetizing Factor in Uniformly Magnetized Cylinders." J. Appl. Physics, 37 (1966) p. 4639.

APPENDIX

HYSTERESIS LOOPS, DEMAG. CURVES, MINOR LOOP FIELDS

FIGURES 3 THROUGH 84

PAGES A-1 THROUGH A-82

SAMPLE IDENTIFICATION		Figures	Page
Sample Group I	Cylinders from 6.5 mm rod	1 - 7	A-1 to A-5
Sample Group II	Cylinders from 31 mm rod	8 - 11	A-6 to A-9
Sample Group III	Cubes from 31 mm rod		
	(a) Room temperature data	12 - 32	A-10 to A-23
	(b) Data for -50°C to +150°C	33 - 80	A-31 to A-78
Sample Group IV	Cylinders from 24 mm rod	81 - 84	A-79 to A-82

SUMMARY OF THE AVERAGE MAGNETIC PROPERTIES OF CUBE M-1646

			Measurements at 25°C with 3 different coils.			Measurements at low and high temperatures. Dual coil with heating/cooling fixture.					
			CONC. COILS	DUAL COIL W/O Heat Fixture	DUAL COIL With Heat Fixture	-50°C	0°C	+25°C	+50°C	+100°C	+150°C
FROM HYSTERESIS LOOPS MEASURED WITH FIELD PARALLEL TO THE EXTRUSION AXIS (= EASY AXIS)		B_r [kG]	5.84	5.79	5.77	6.12	5.89	5.77	5.64	5.25	4.78
		$_M H_c$ [kOe]	2.85	2.88	2.85	3.36	3.04	2.85	2.59	2.06	1.46
		$_B H_c$ [kOe]	2.43	2.45	2.39	2.74	2.53	2.39	2.22	1.82	1.31
		H_K [kOe]	1.35	1.32	1.30	1.48	1.38	1.30	1.22	1.00	0.70
		$(BH)_{max}$ [MGOe]	5.4	5.3	5.2	6.1	5.5	5.2	4.9	3.8	2.7
H ⊥ EXTRUSION AXIS *	R	B_r [kG]	3.06	--	2.94	3.15	3.06	2.94	2.92	2.67	2.34
	T		3.00	--	2.91	3.15	3.06	2.91	2.86	2.67	2.31
	R	$_M H_c$ [kOe]	3.49	--	3.43	4.00	3.69	3.43	3.24	2.64	1.98
	T		3.45	--	3.43	4.00	3.67	3.43	3.24	2.61	1.98

* R = Radial Direction; T = Tangential Direction.

SUMMARY OF THE AVERAGE MAGNETIC PROPERTIES OF CUBE M-1647

			Measurements at 25°C with 3 different coils.			Measurements at low and high temperatures. Dual coil with heating/cooling fixture.					
			CONC. COILS	DUAL COIL W/O Heat Fixture	DUAL COIL With Heat Fixture	-50°C	0°C	+25°C	+50°C	+100°C	+150°C
FROM HYSTERESIS LOOPS MEASURED WITH FIELD PARALLEL TO THE EXTRUSION AXIS (= EASY AXIS)		B_r [kG]	5.86	5.78	5.76	6.08	5.91	5.76	5.64	5.30	4.78
		M^{H_c} [kOe]	2.87	2.86	2.85	3.34	3.07	2.85	2.61	2.08	1.47
		B^{H_c} [kOe]	2.42	2.39	2.40	2.73	2.54	2.40	2.23	1.81	1.31
		H_K [kOe]	1.32	1.27	1.28	1.45	1.35	1.28	1.20	0.98	0.69
		$(BH)_{max}$ [MGOe]	5.3	5.2	5.1	6.0	5.6	5.1	4.8	3.9	2.7
H ⊥ EXTRUSION AXIS *	R	B_i [kG]	3.04	--	2.99	3.23	3.06	2.99	2.91	2.72	2.38
	T		3.02	--	2.93	3.15	3.06	2.93	2.91	2.64	2.35
	R	M^{H_c} [kOe]	3.45	--	3.44	4.04	3.62	3.44	3.27	2.65	1.97
	T		3.44	--	3.41	3.92	3.62	3.41	3.27	2.59	1.97

* R = Radial Direction, T = Tangential Direction.

SUMMARY OF THE AVERAGE MAGNETIC PROPERTIES OF CUBE M-1648

			Measurements at 25°C with 3 different coils.			Measurements at low and high temperatures. Dual coil with heating/cooling fixture.					
			CONC. COILS	DUAL COIL W/O Heat Fixture	DUAL COIL With Heat Fixture	-50°C	0°C	+25°C	+50°C	+100°C	+150°C
FROM HYSTERESIS LOOPS MEASURED WITH FIELD PARALLEL TO THE EXTRUSION AXIS (= EASY AXIS)		B_r [kG]	5.84	5.76	5.76	6.05	5.87	5.76	5.62	5.30	4.78
		M^{H_c} [kOe]	2.88	2.84	2.84	3.32	3.05	2.84	2.59	2.08	1.47
		B^{H_c} [kOe]	2.44	2.44	2.40	2.72	2.54	2.40	2.23	1.84	1.31
		H_K [kOe]	1.35	1.29	1.28	1.45	1.38	1.28	1.23	1.03	0.70
		$(BH)_{max}$ [MGOe]	5.3	5.1	5.2	5.9	5.6	5.2	4.9	4.0	2.7
H ⊥ EXTRUSION AXIS *	R	B_r [kG]	3.02	--	2.92	3.15	3.06	2.92	2.87	2.64	2.32
	T		3.02	--	2.92	3.14	3.06	2.92	2.85	2.63	2.32
	R	M^{H_c} [kOe]	3.49	--	3.44	4.02	3.67	3.44	3.21	2.62	1.97
	T		3.45	--	3.44	3.99	3.67	3.44	3.20	2.59	1.97

* R = Radial Direction; T = Tangential Direction.

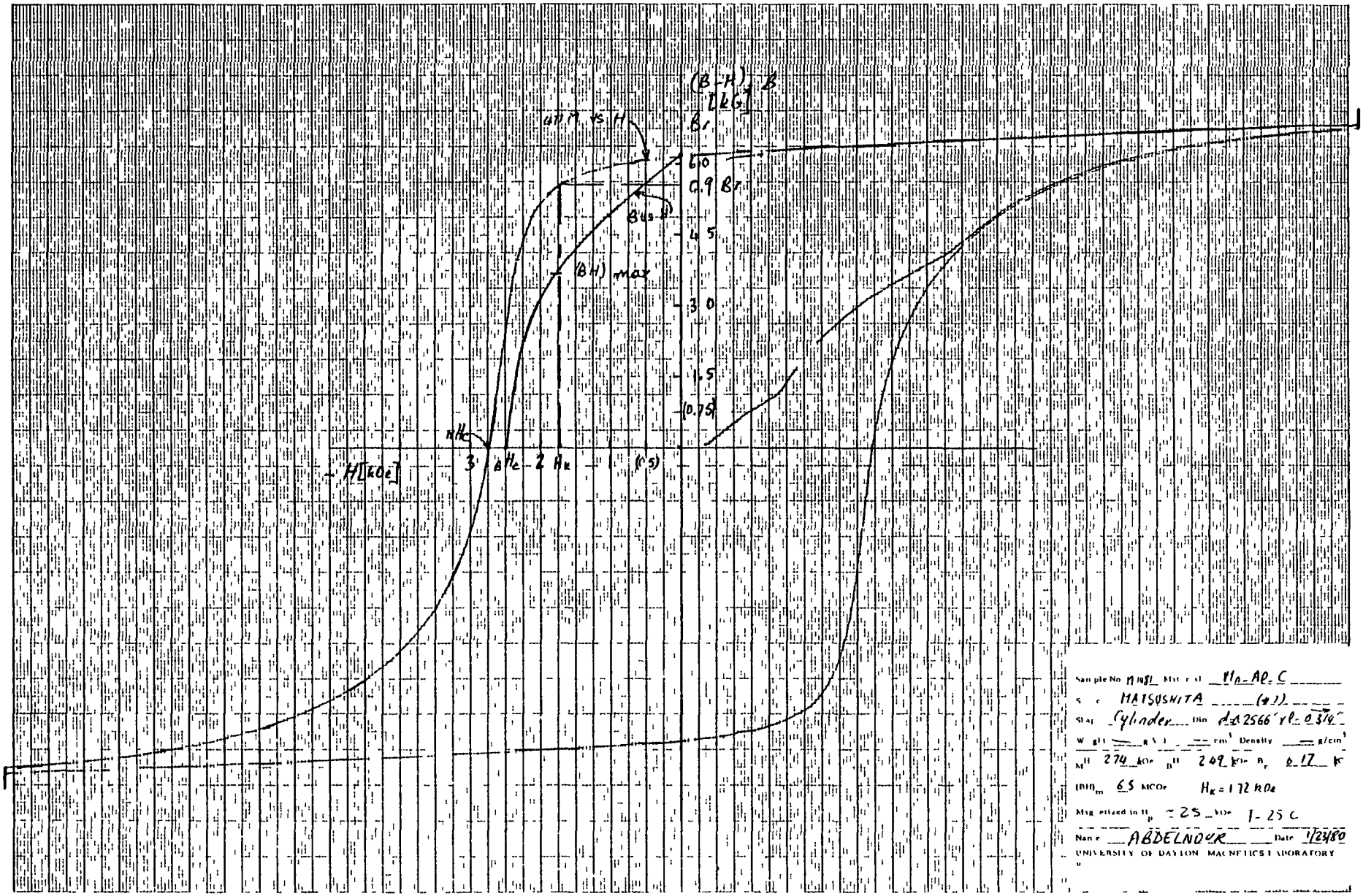

Fig. 3 Major Hysteresis Loops For Cylinder M-1481 at 25°C.

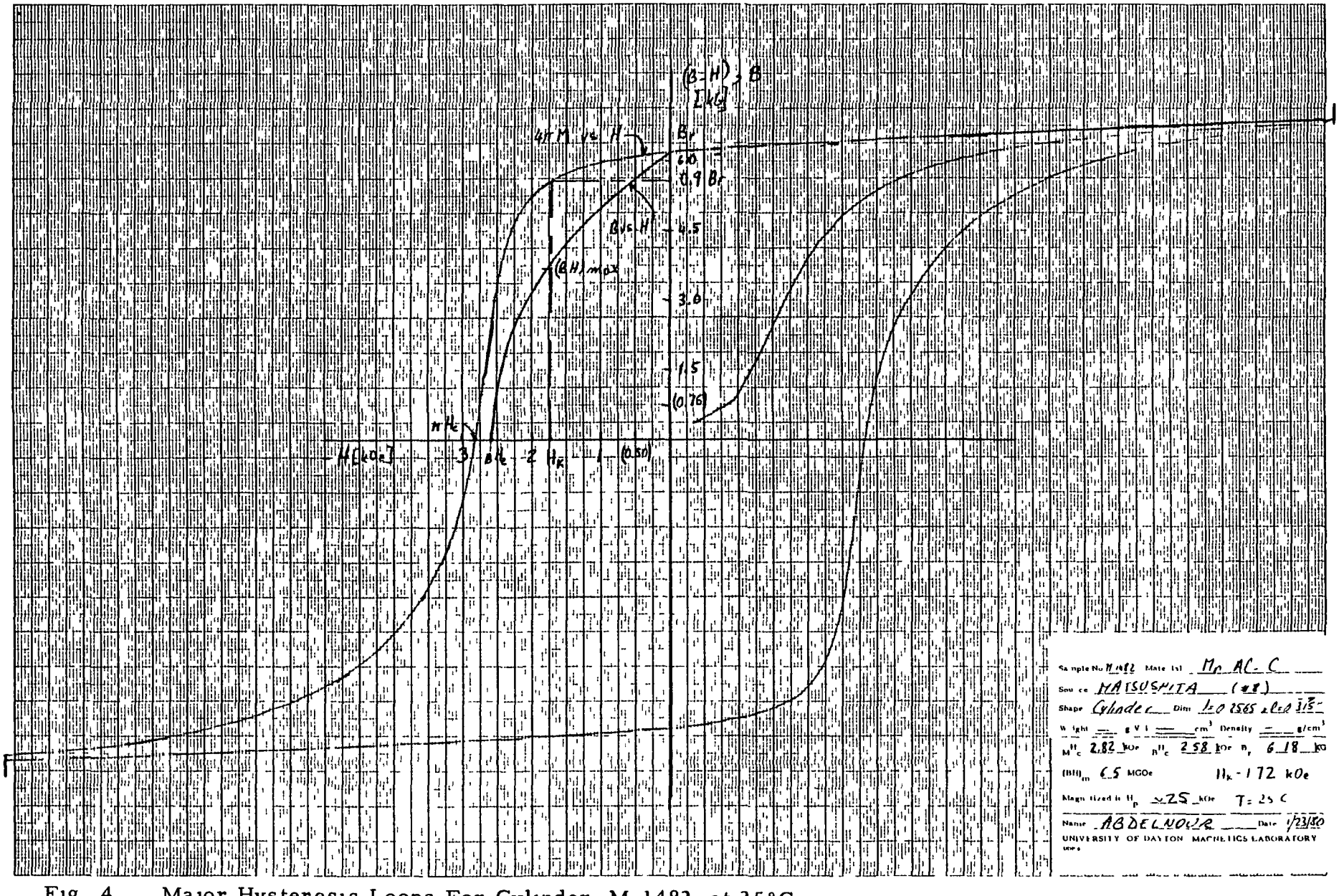

Fig. 4 Major Hysteresis Loops For Cylinder M-1482 at 25°C.

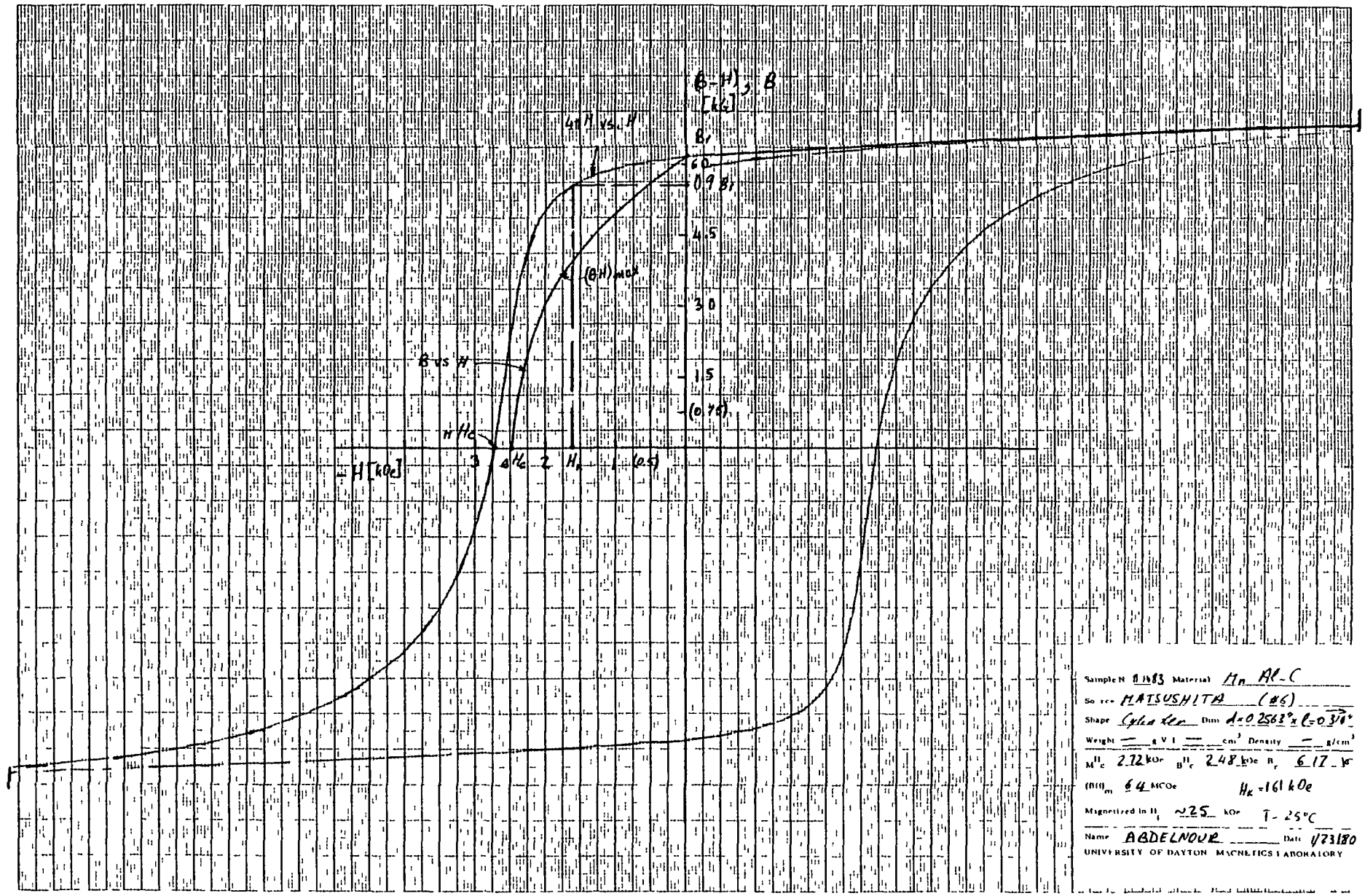

Fig. 5 Major Hysteresis Loops For Cylinder M-1483 at 25°C.

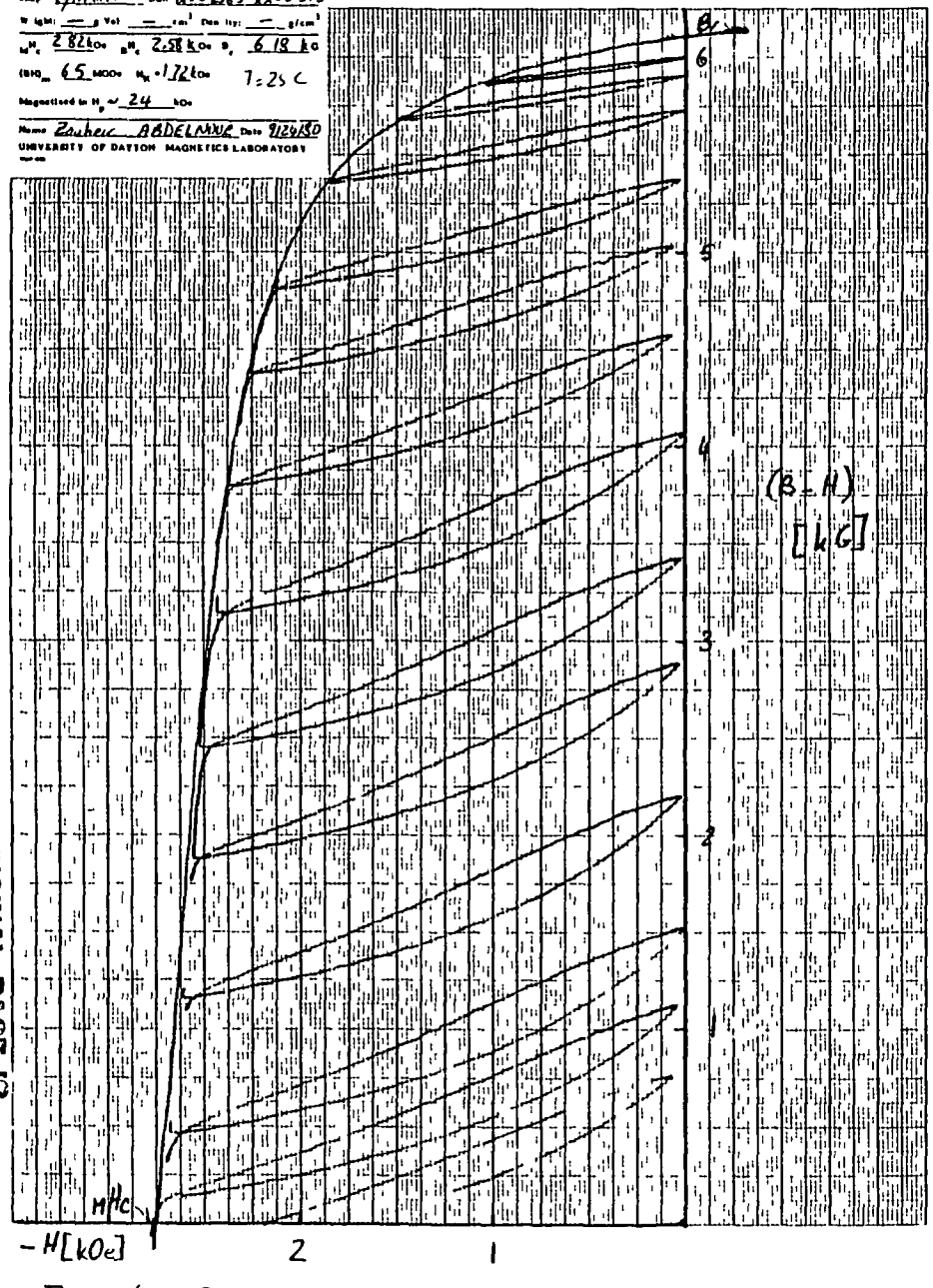

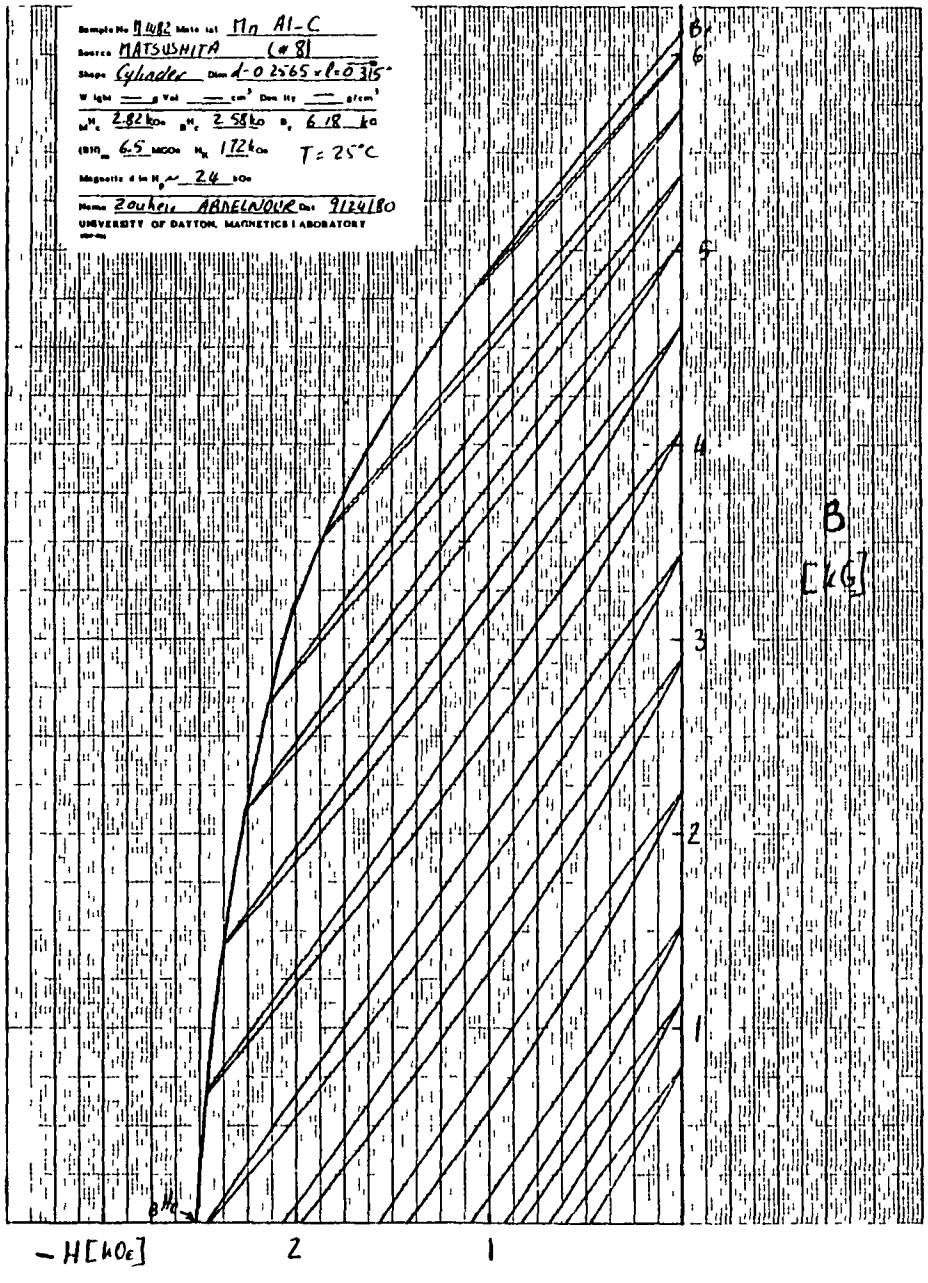

Fig. 6 Q-2 Recoil Loops, (B-H) &B, For Cylinder M-1482 at 25°C

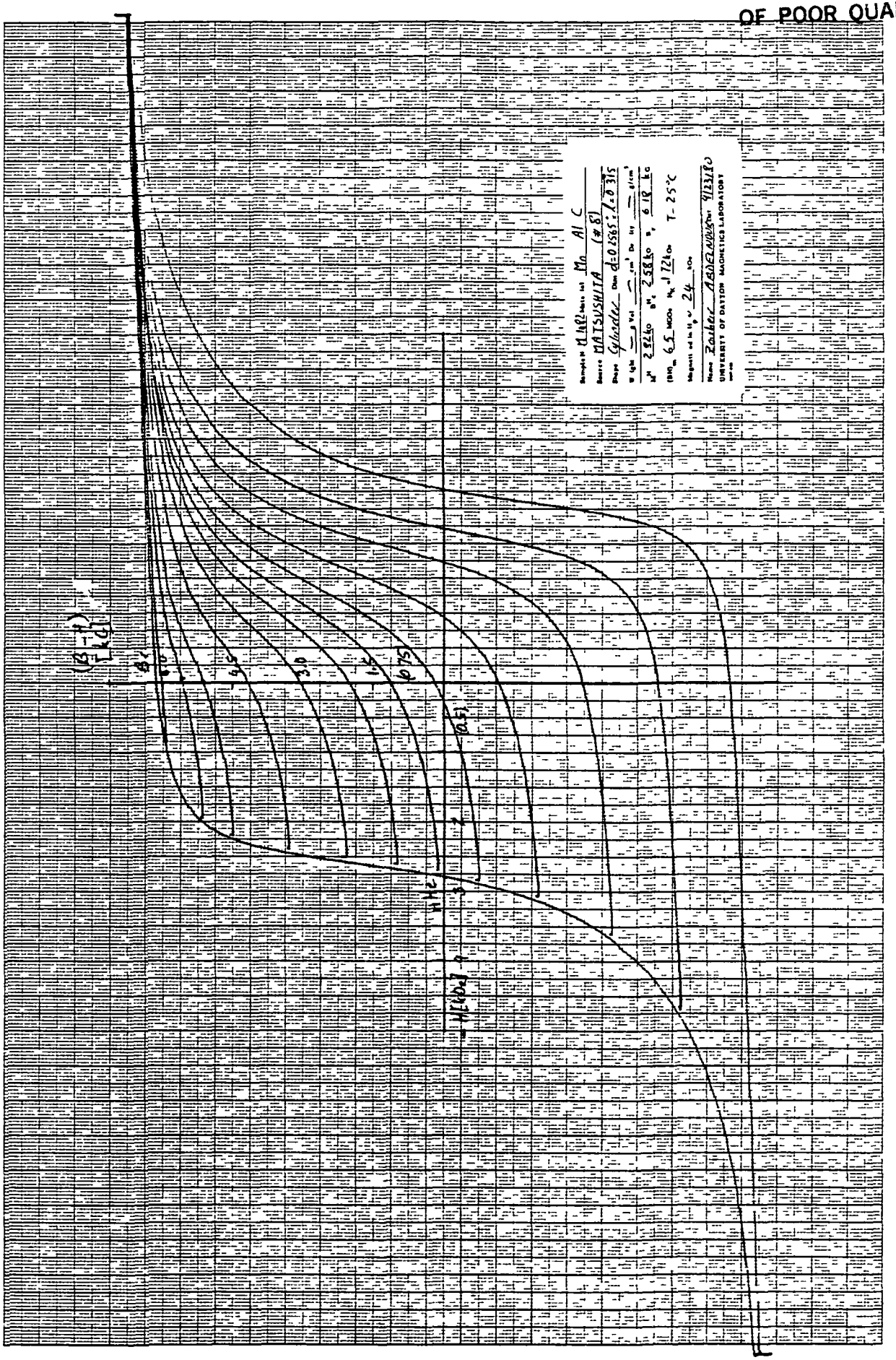

Fig. 7 Full Minor-Loop Field For Cylinder M-1482 at 25°C.

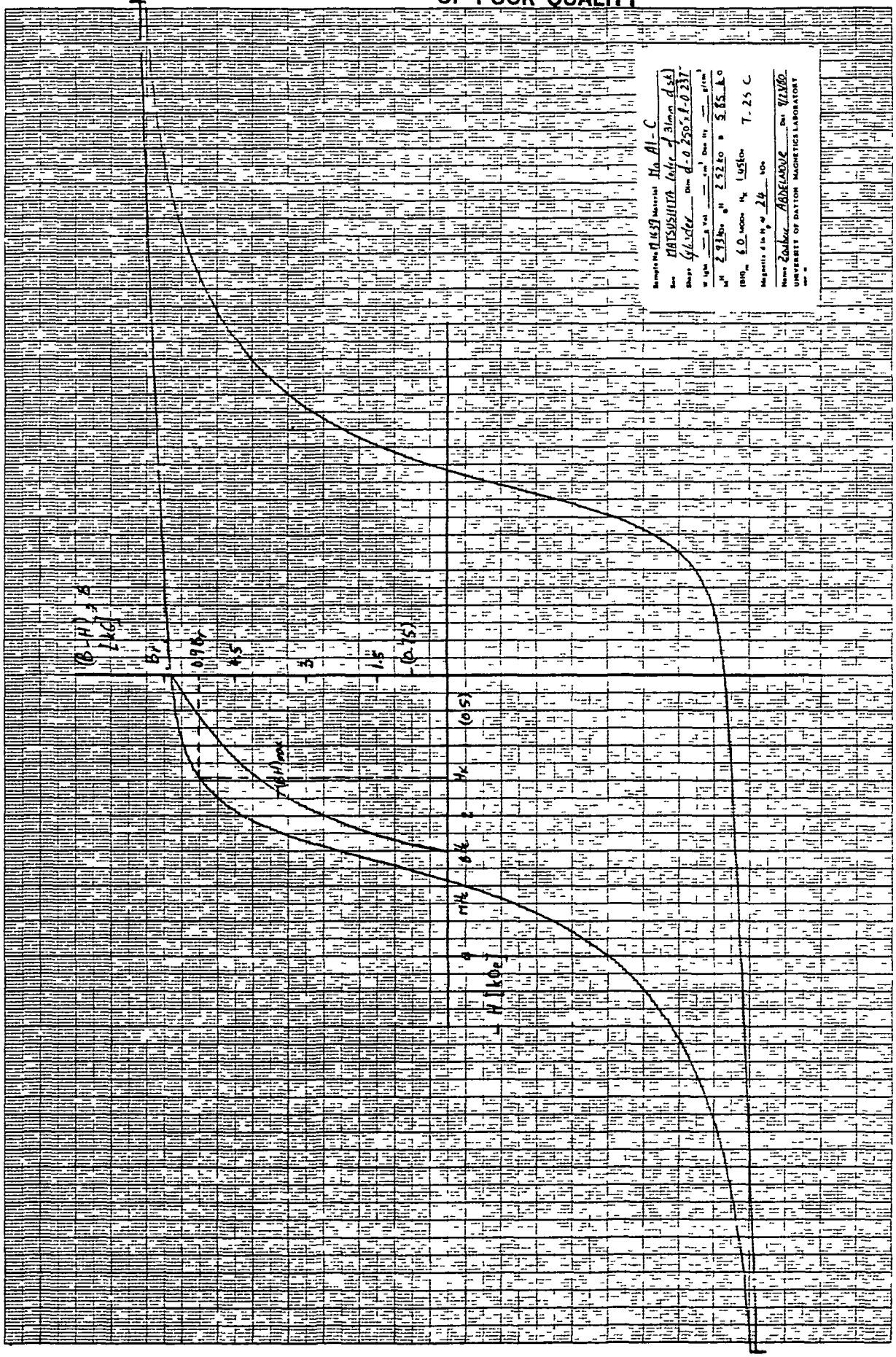

Fig. 8 Major Hysteresis Loops For Cylinder M-1639 at 25°C.

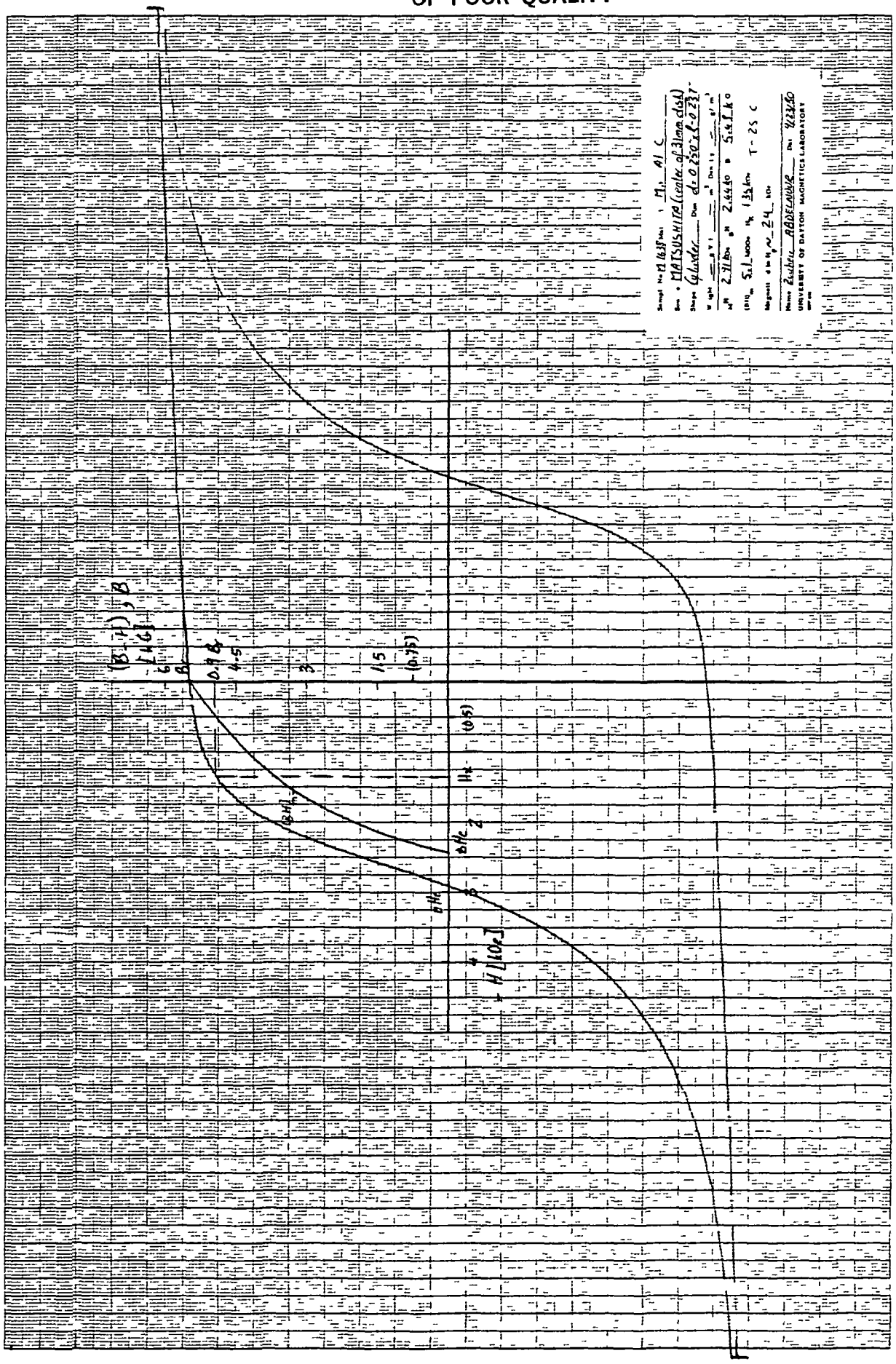

Fig. 9 Major Hysteresis Loops For Cylinder M-1638 at 25°C.

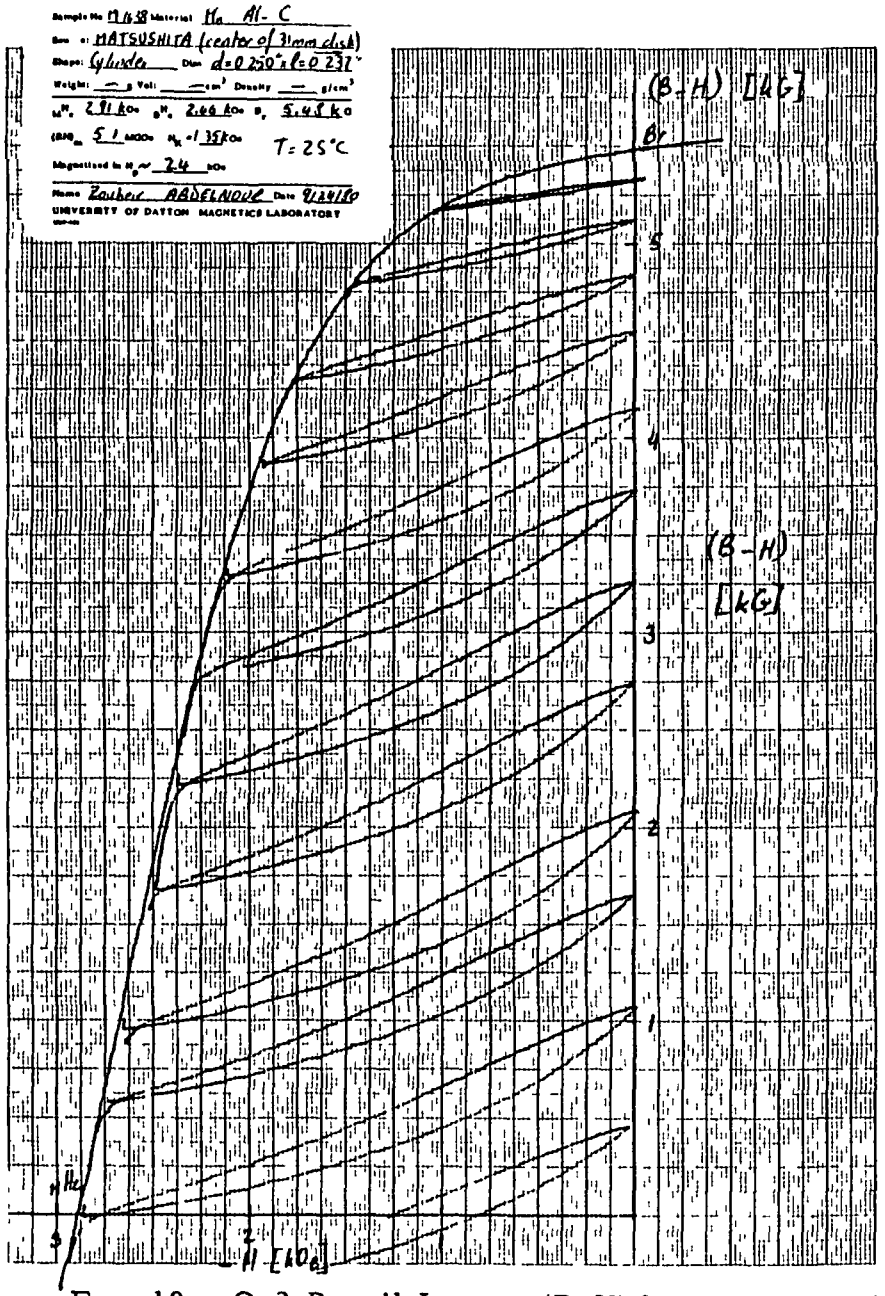

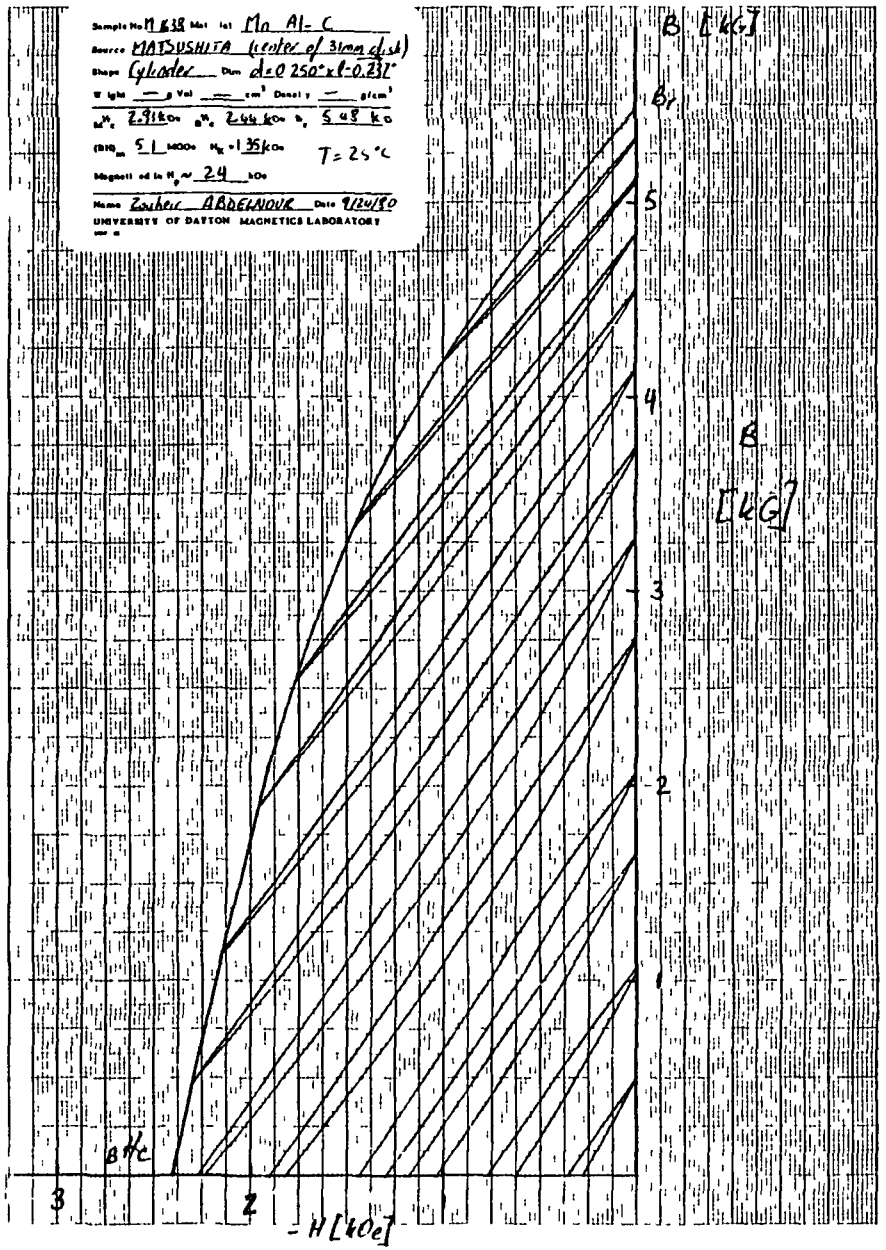

Fig. 10 Q-2 Recoil Loops, (B-H) &B, For Cylinder M-1638 at 25°C.

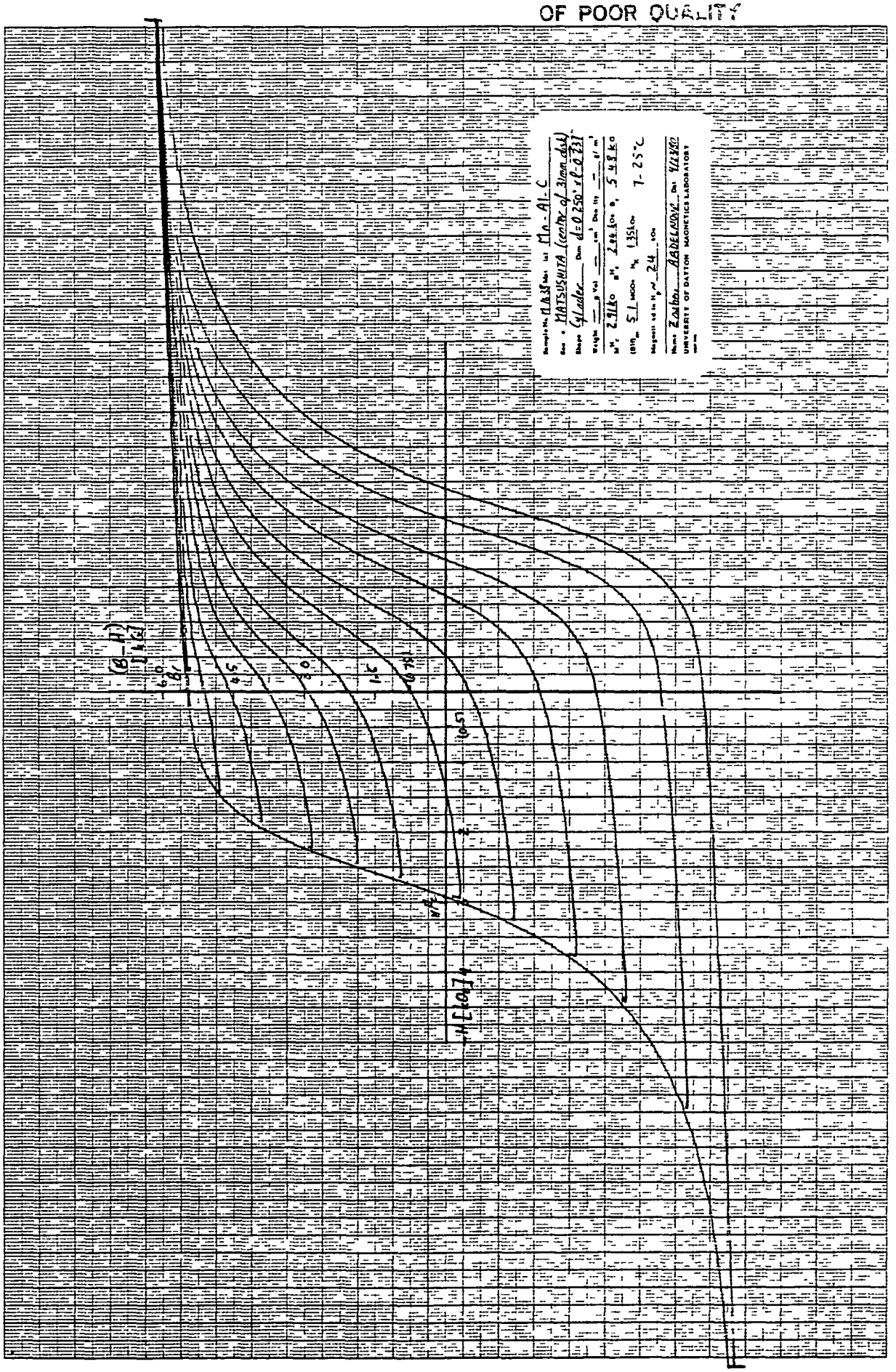

Fig. 11 Full Minor-Loop Field For Cylinder M-1638 at 25°C.

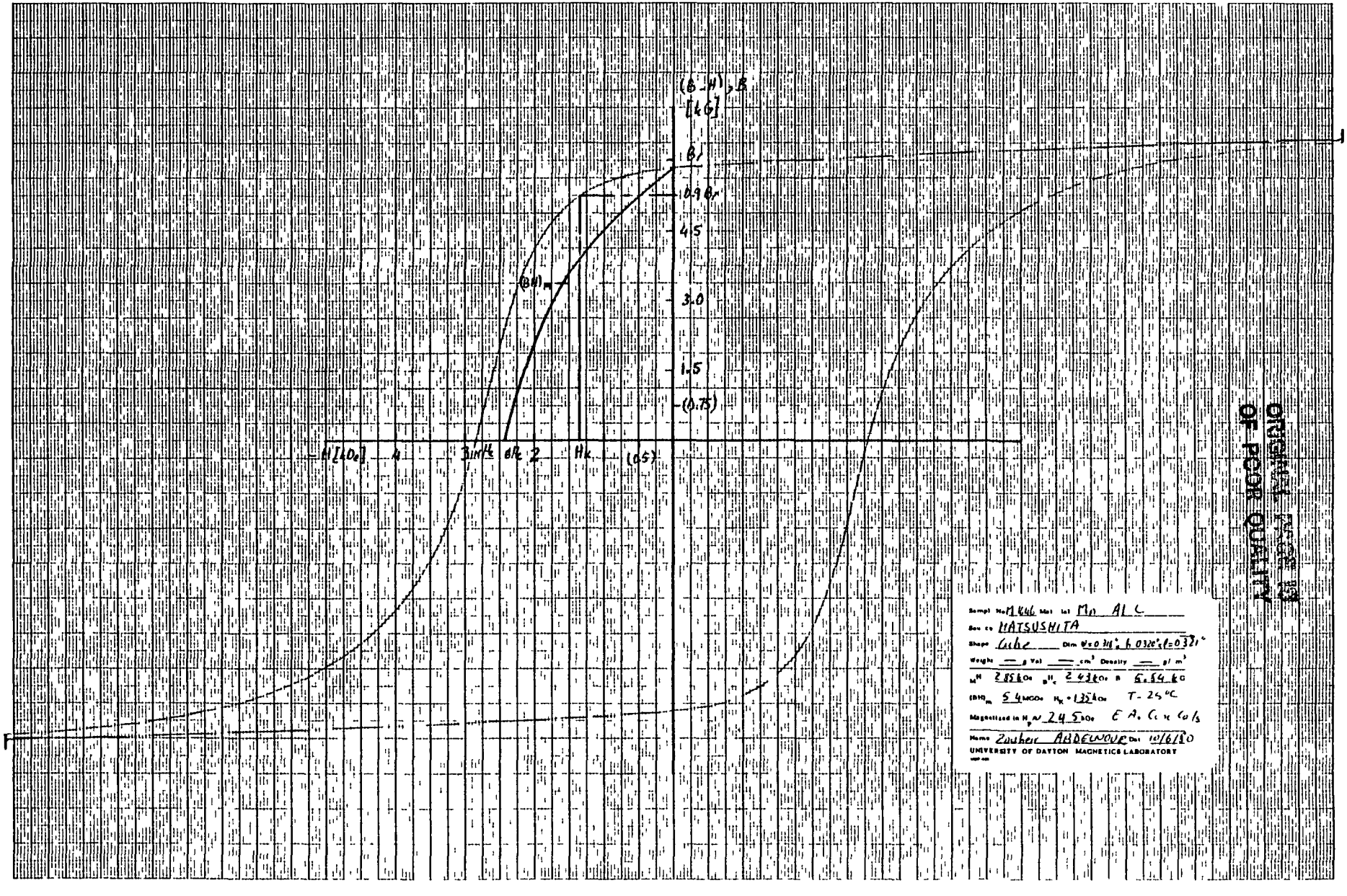

Fig. 12 Major Hysteresis Loops For Cube M-1646 at 25°C. (Using Conc. Coils)

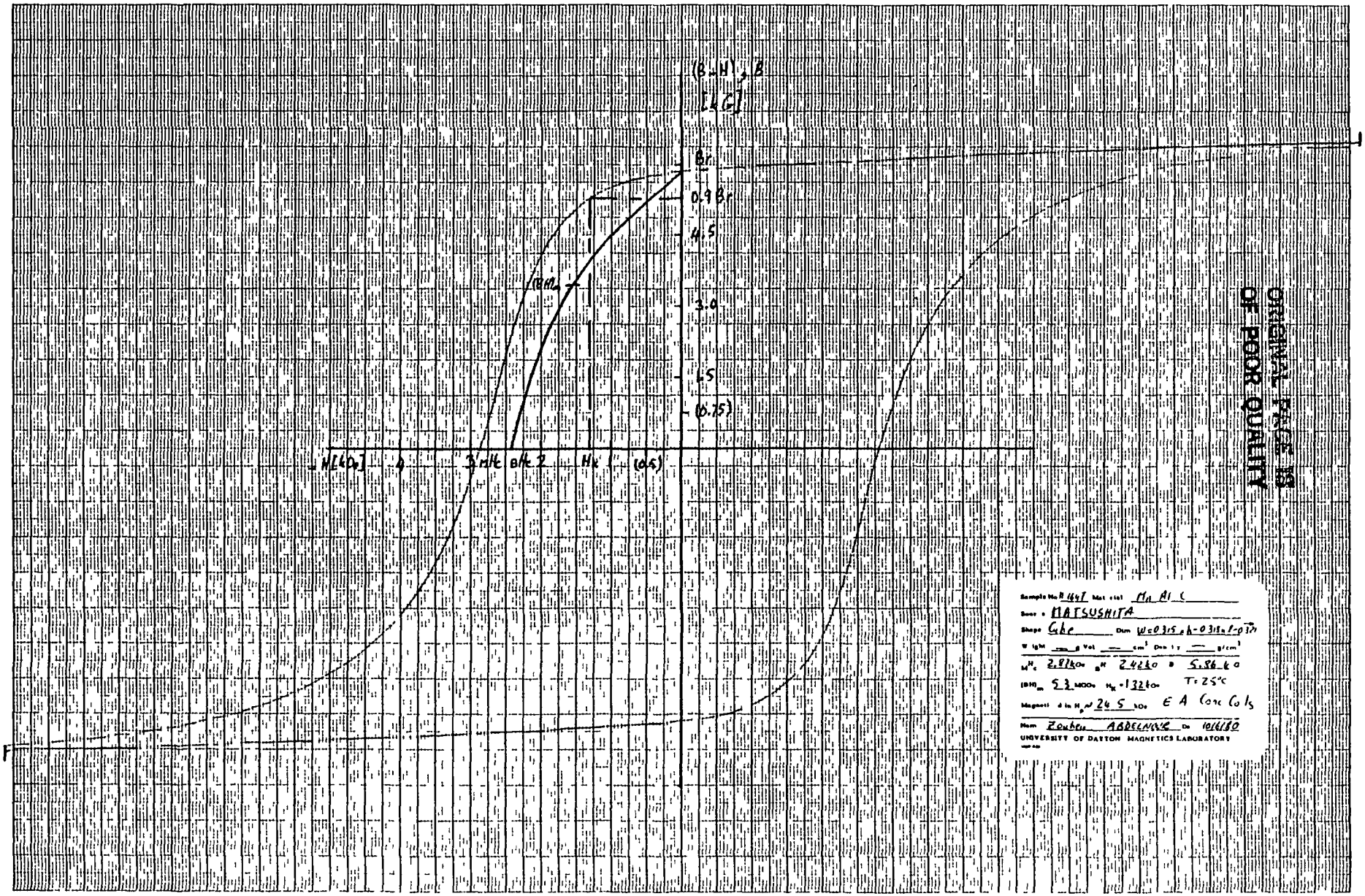

Fig. 13 Major Hysteresis Loops For Cube M-1647 at 25°C. (Using Conc. Coils)

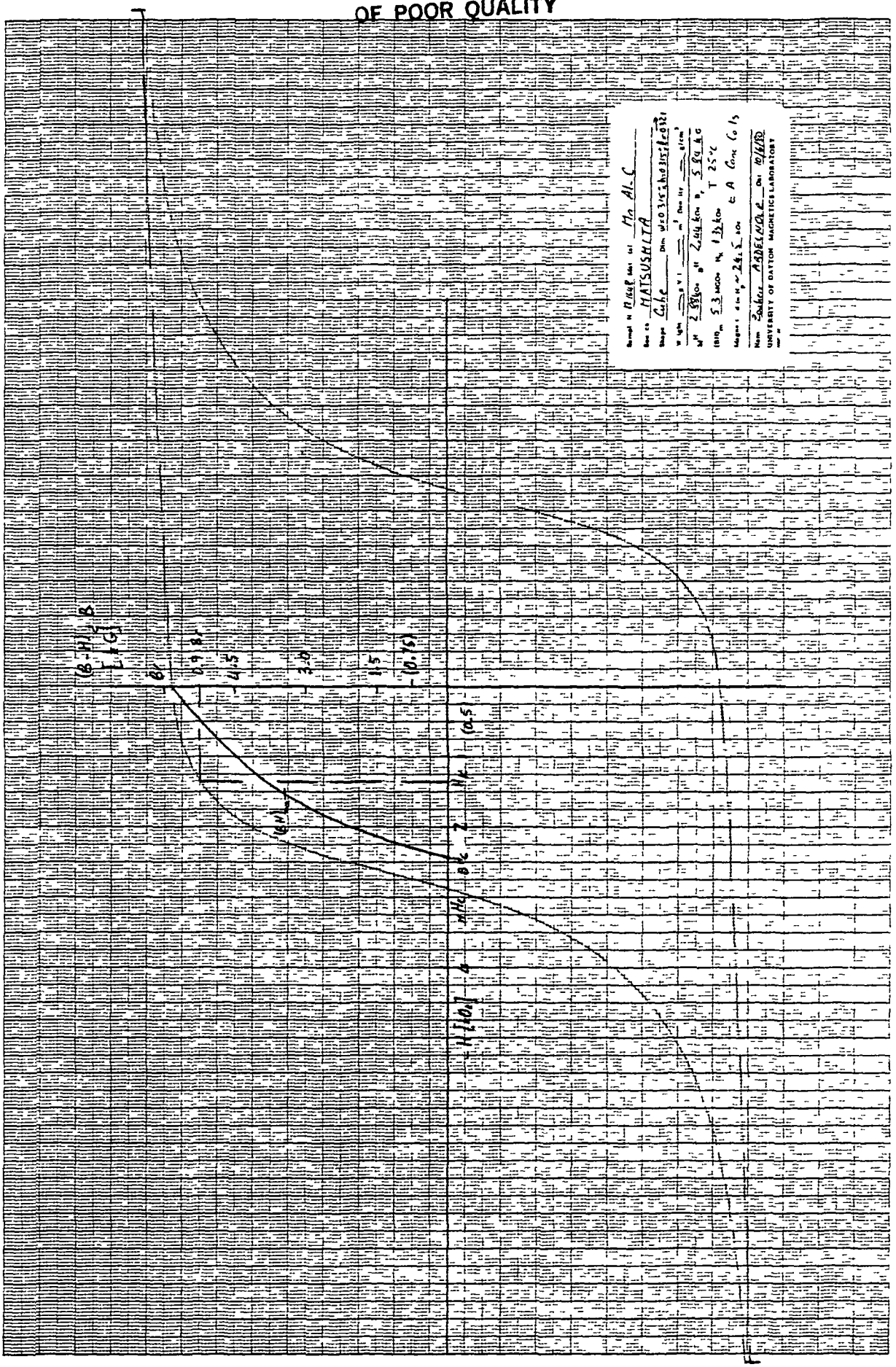

Fig. 14 Major Hysteresis Loops For Cube M-1648 at 25°C. (Using Conc. Coils)

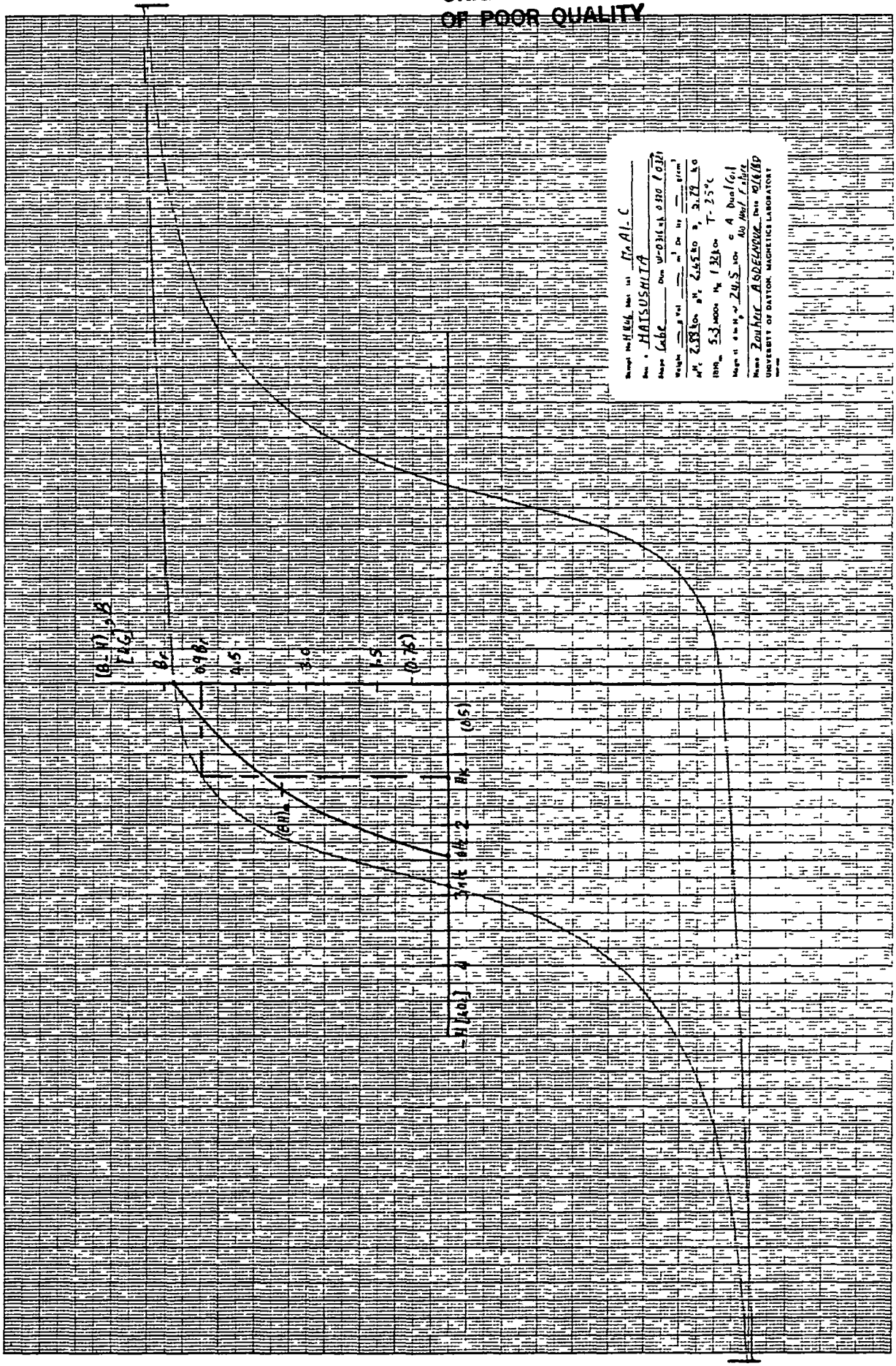

Fig. 15 Major Hysteresis Loops For Cube M-1646 at 25°C. (Using Dual Coils Without H/C Fixture)

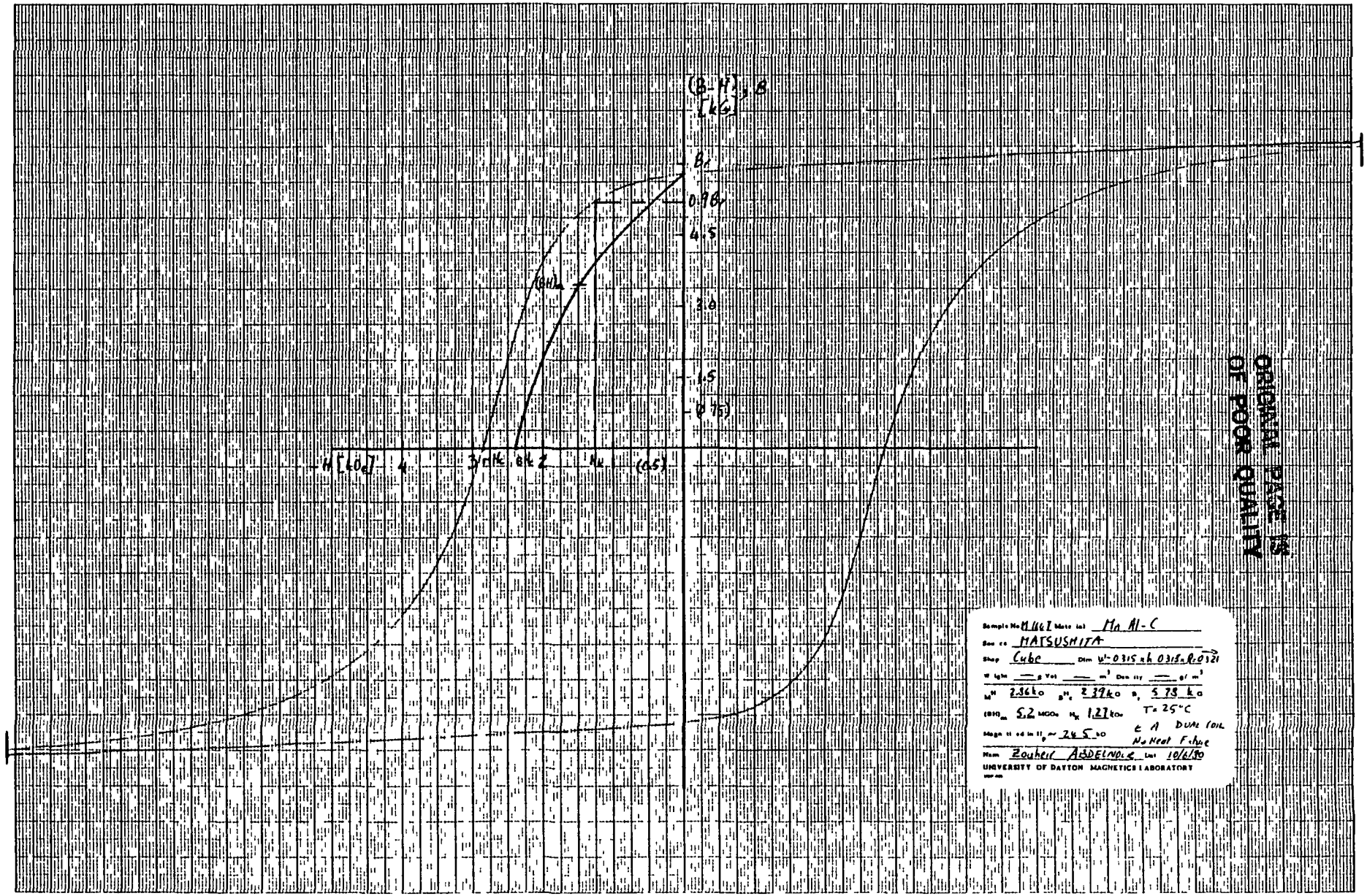

Fig. 16 Major Hysteresis Loops For Cube M-1647 at 25°C (Using Dual Coils Without H/C Fixture)

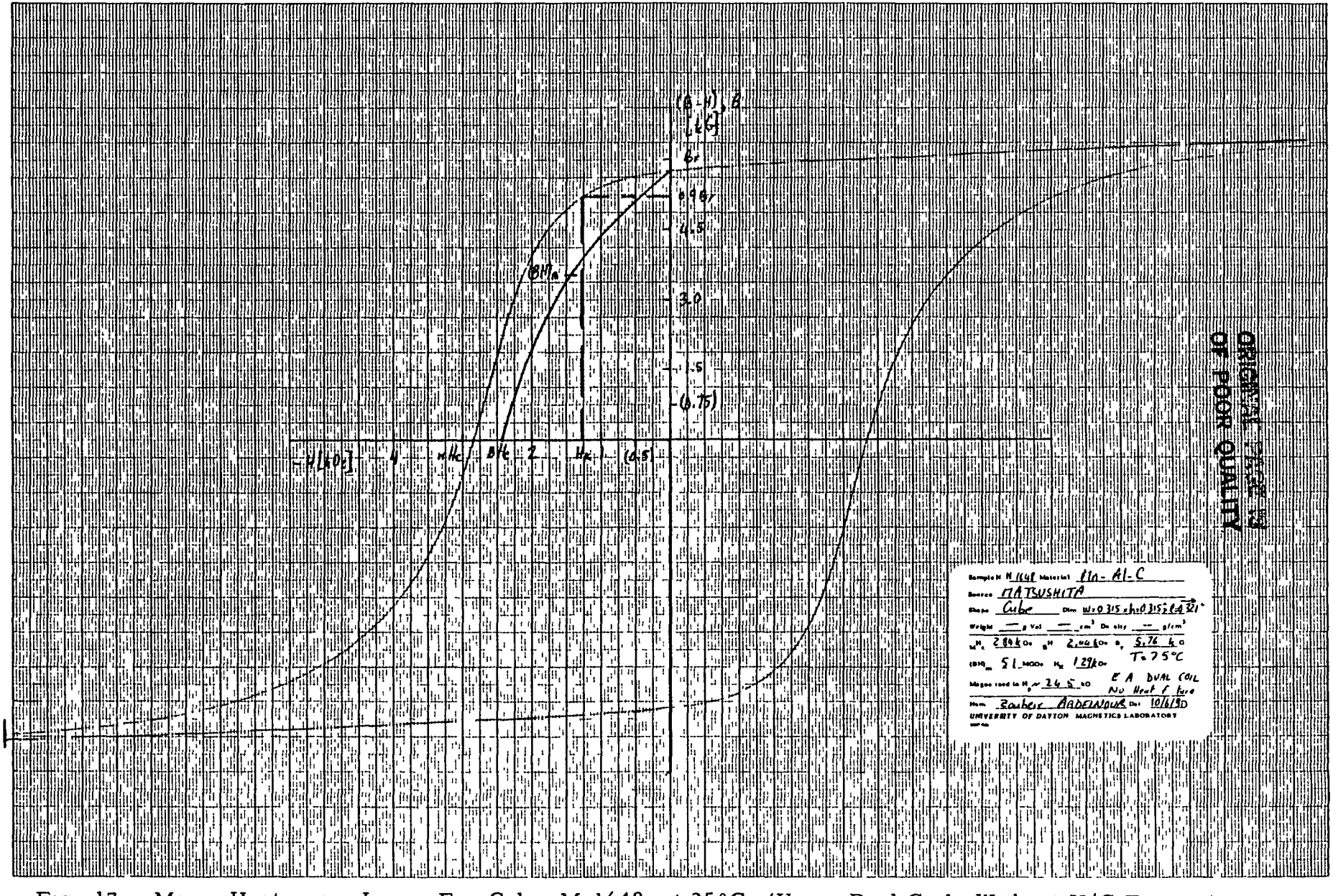

Fig. 17 Major Hysteresis Loops For Cube M-1648 at 25°C. (Using Dual Coils Without H/C Fixture)

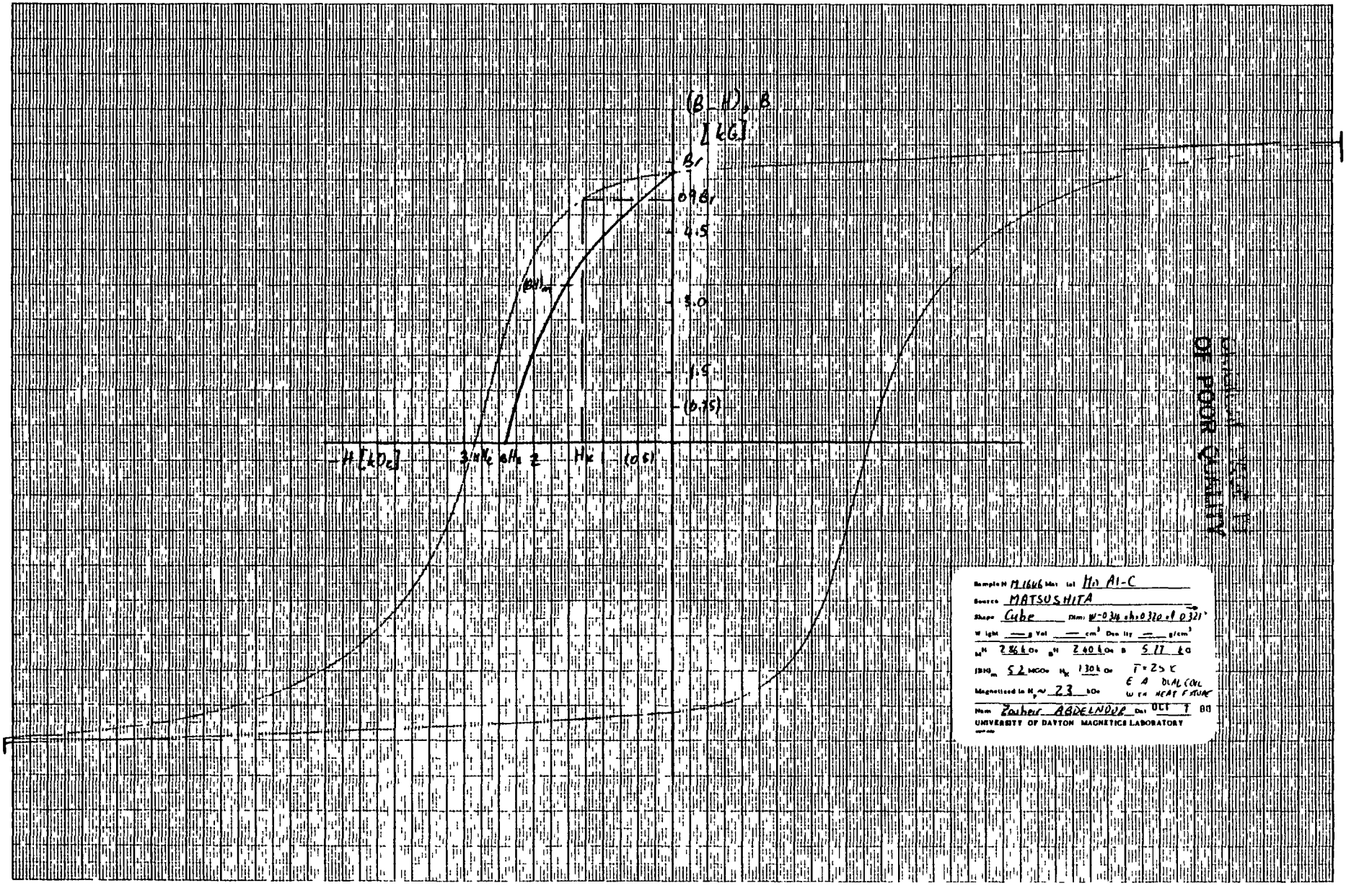

Fig. 18 Major Hysteresis Loops For Cube M-1646 at 25°C (Using Dual Coils With H/C Fixture)

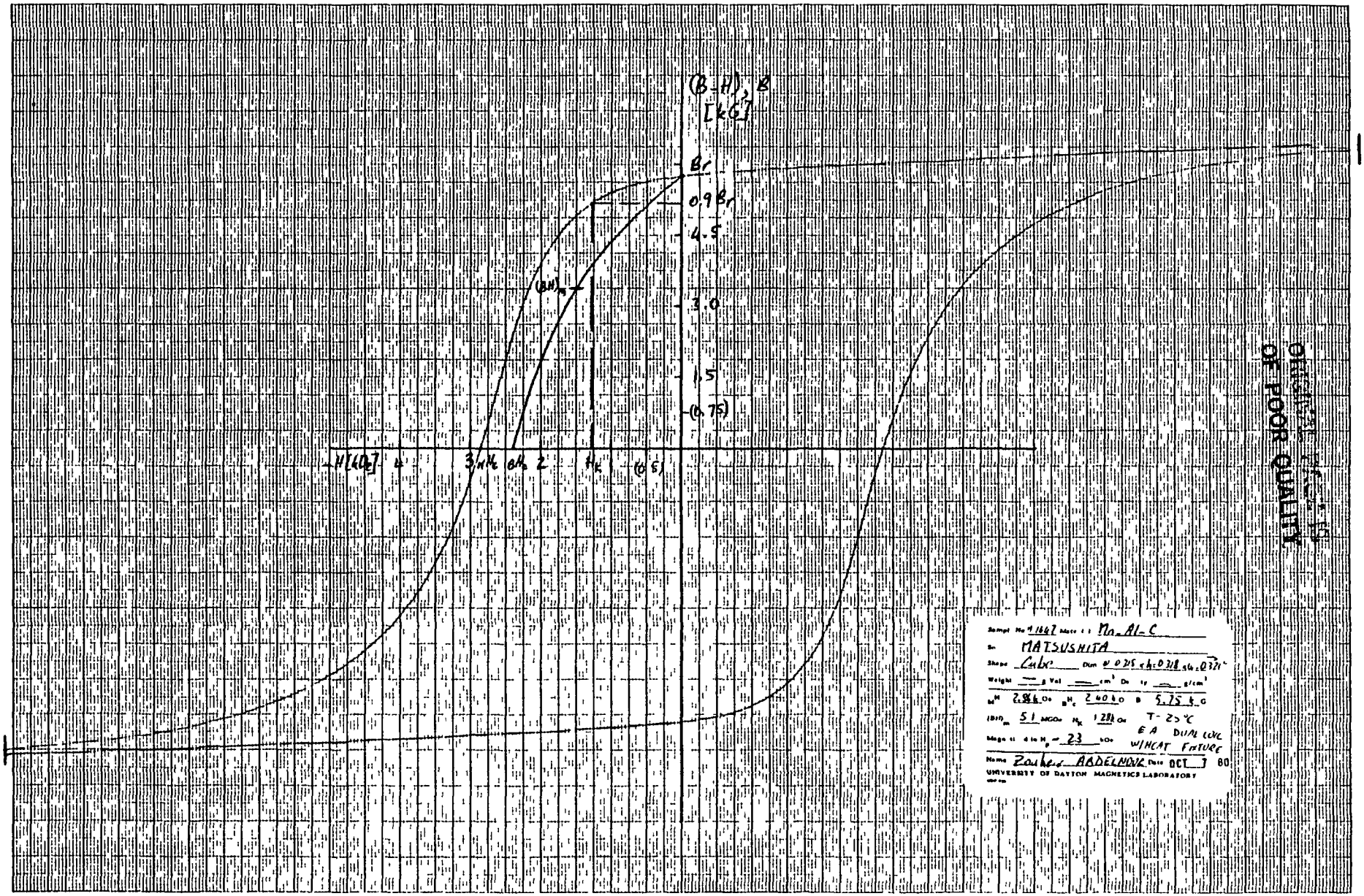

Fig. 19 Major Hysteresis Loops For Cube M-1647 at 25°C. (Using Dual Coils With H/C Fixture)

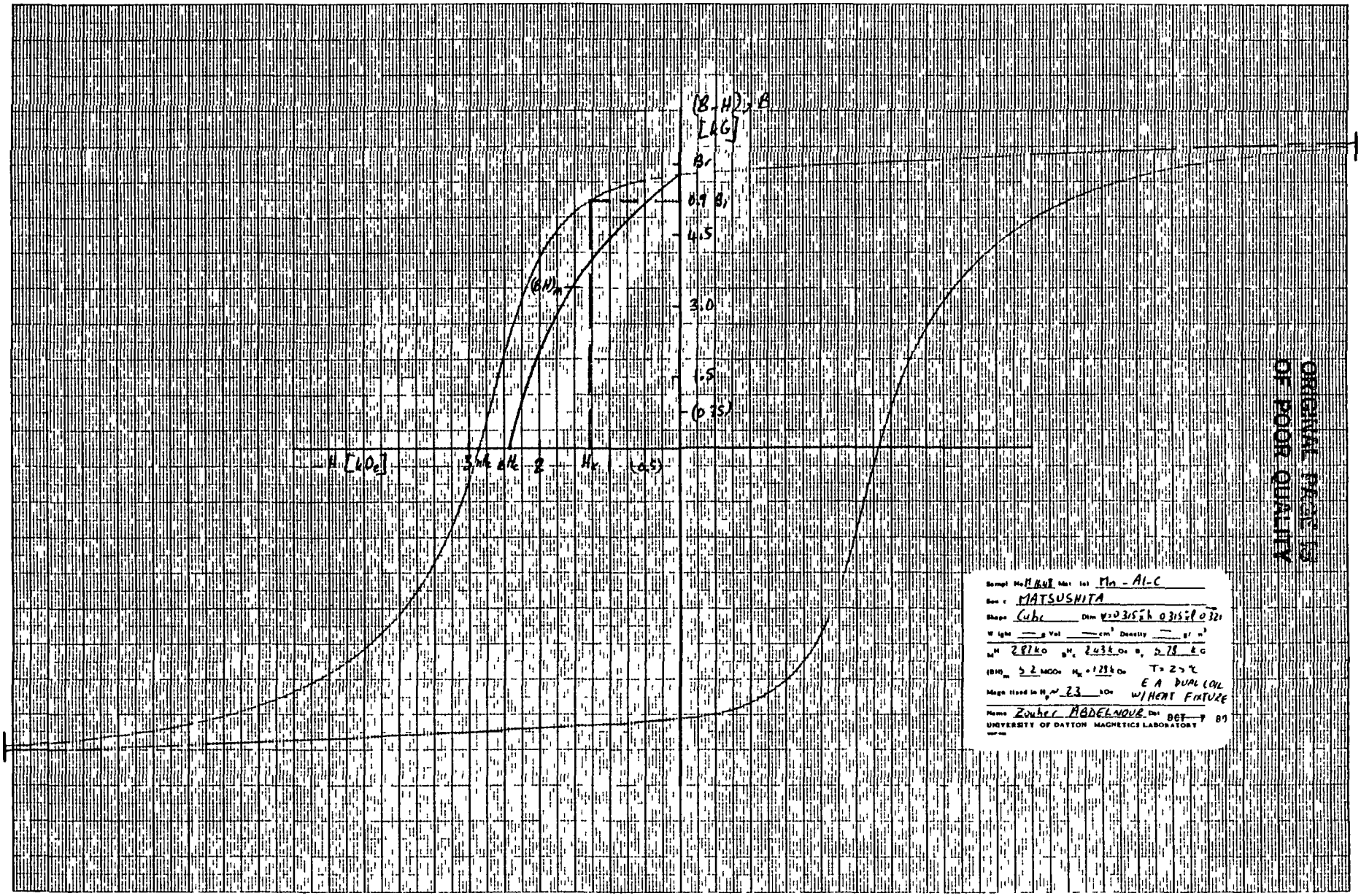

Fig. 20 Major Hysteresis Loops For Cube M-1648 at 25°C (Using Dual Coils With H/C Fixture)

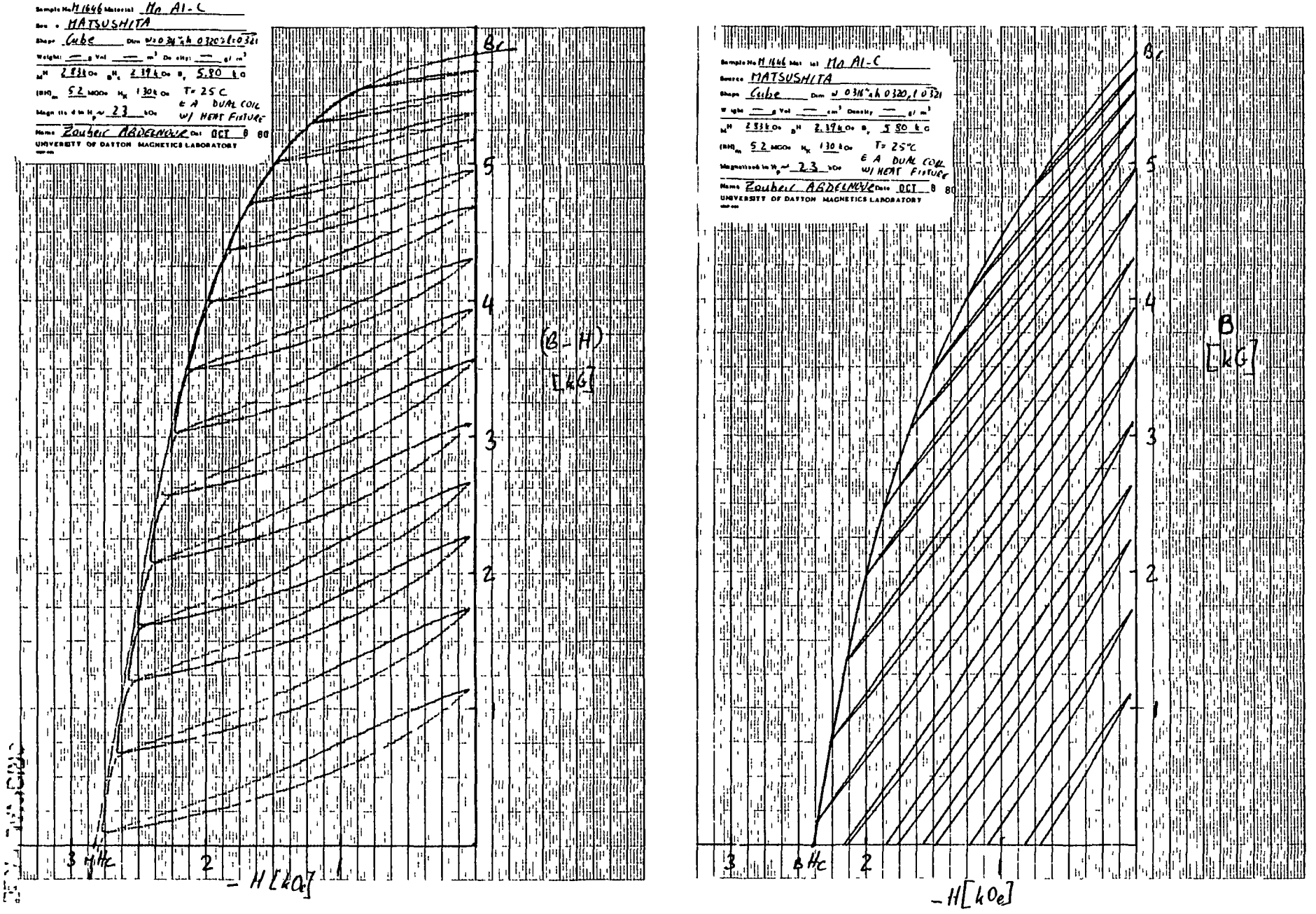

Fig. 21 Q-2 Recoil Loops, (B-H) &B, For Cube M-1646 at 25°C (Using Dual Coils With H/C Fixture)

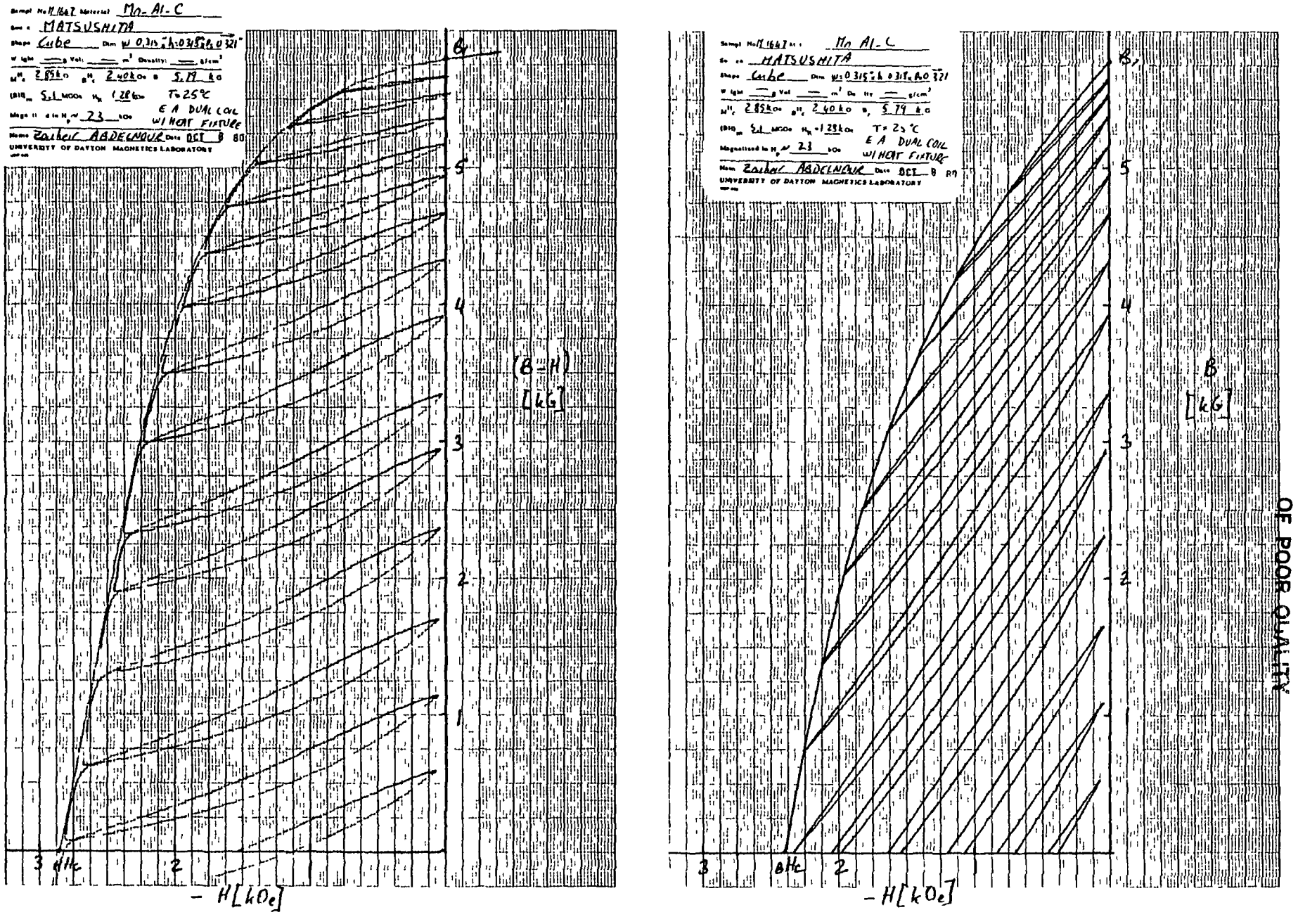

Fig. 22 Q-2 Recoil Loops, (B-H) &B, For Cube M-1647 at 25°C (Using Dual Coils With H/C Fixture)

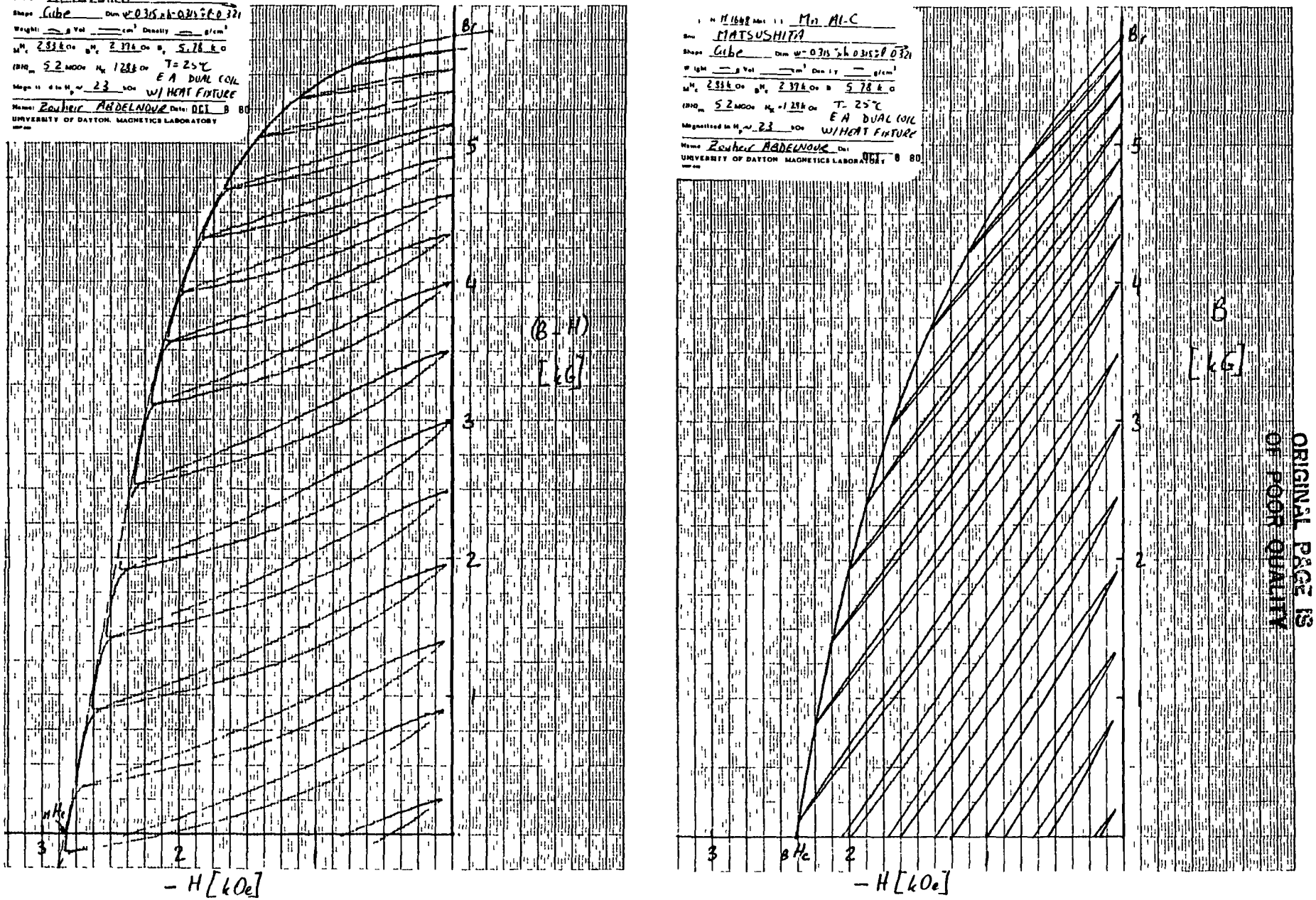

Fig. 23 Q-2 Recoil Loops, (B-H) &B, For Cube M-1648 at 25°C (Using Dual Coils With H/C Fixture)

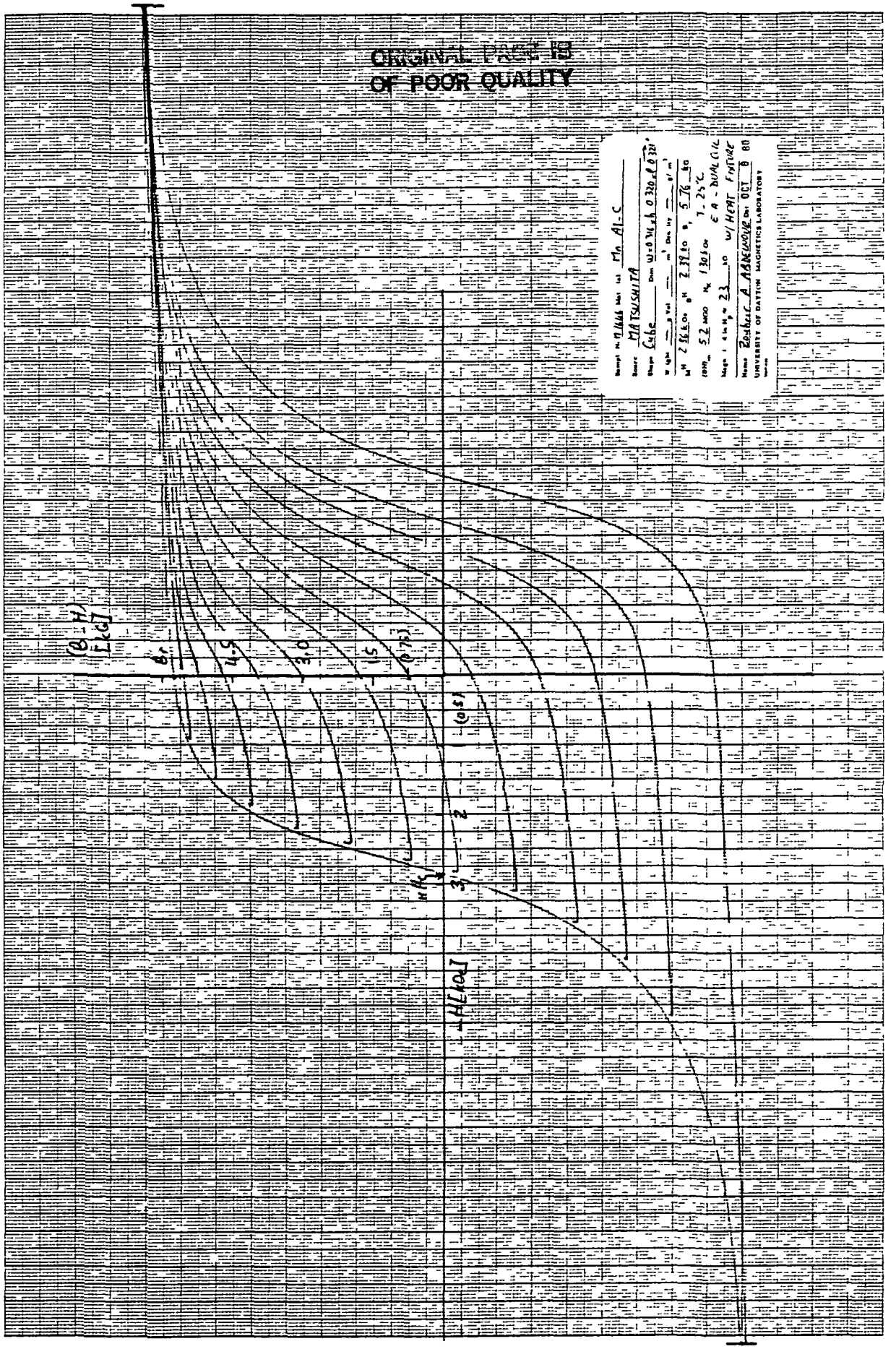

Fig. 24 Full Minor Loop Field For Cube M-1646 at 25°C. (Using Dual Coils With H/C Fixture)

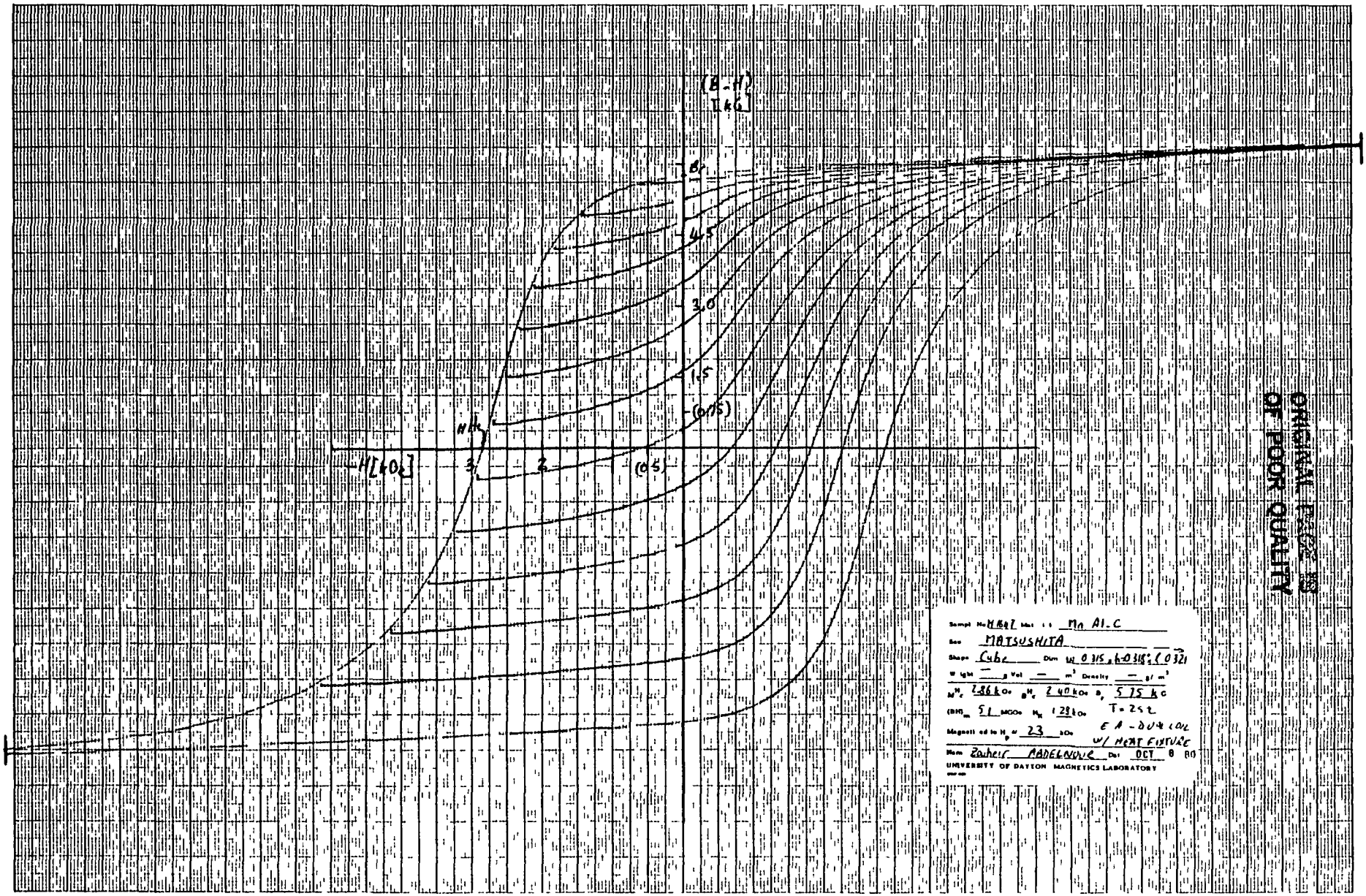

Fig. 25 Full Minor Loop Field For Cube M-1647 at 25°C (Using Dual Coils With H/C Fixture)

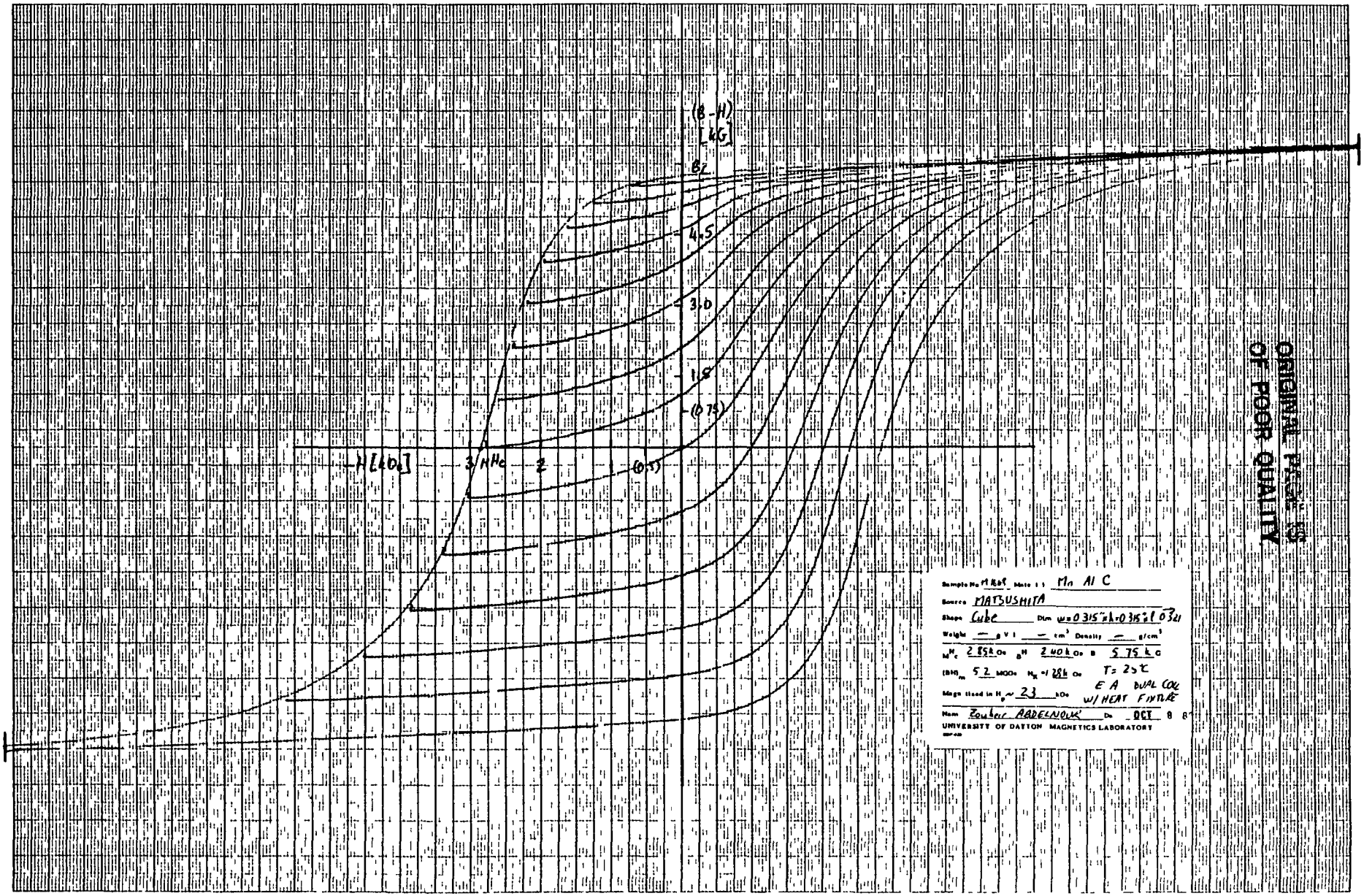

ORIGINAL PAGE IS OF POOR QUALITY

Fig. 26 Full Minor Loop Field For Cube M-1648 at 25°C (Using Dual Coils With H/C Fixture)

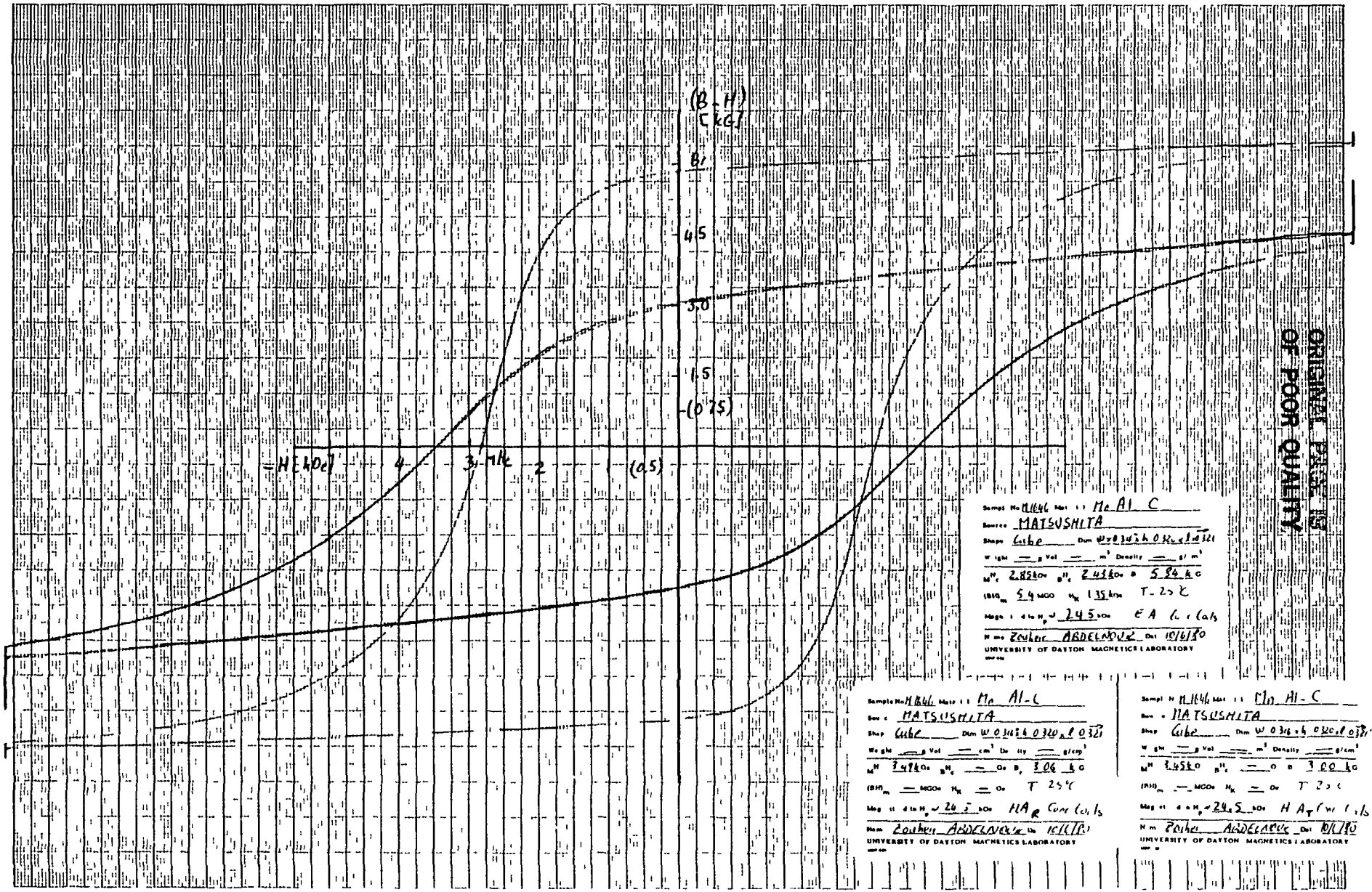

Fig. 27 Major Hysteresis Loops For All Three Cube Axes For M-1646 at 25°C (Using Conc. Coils)

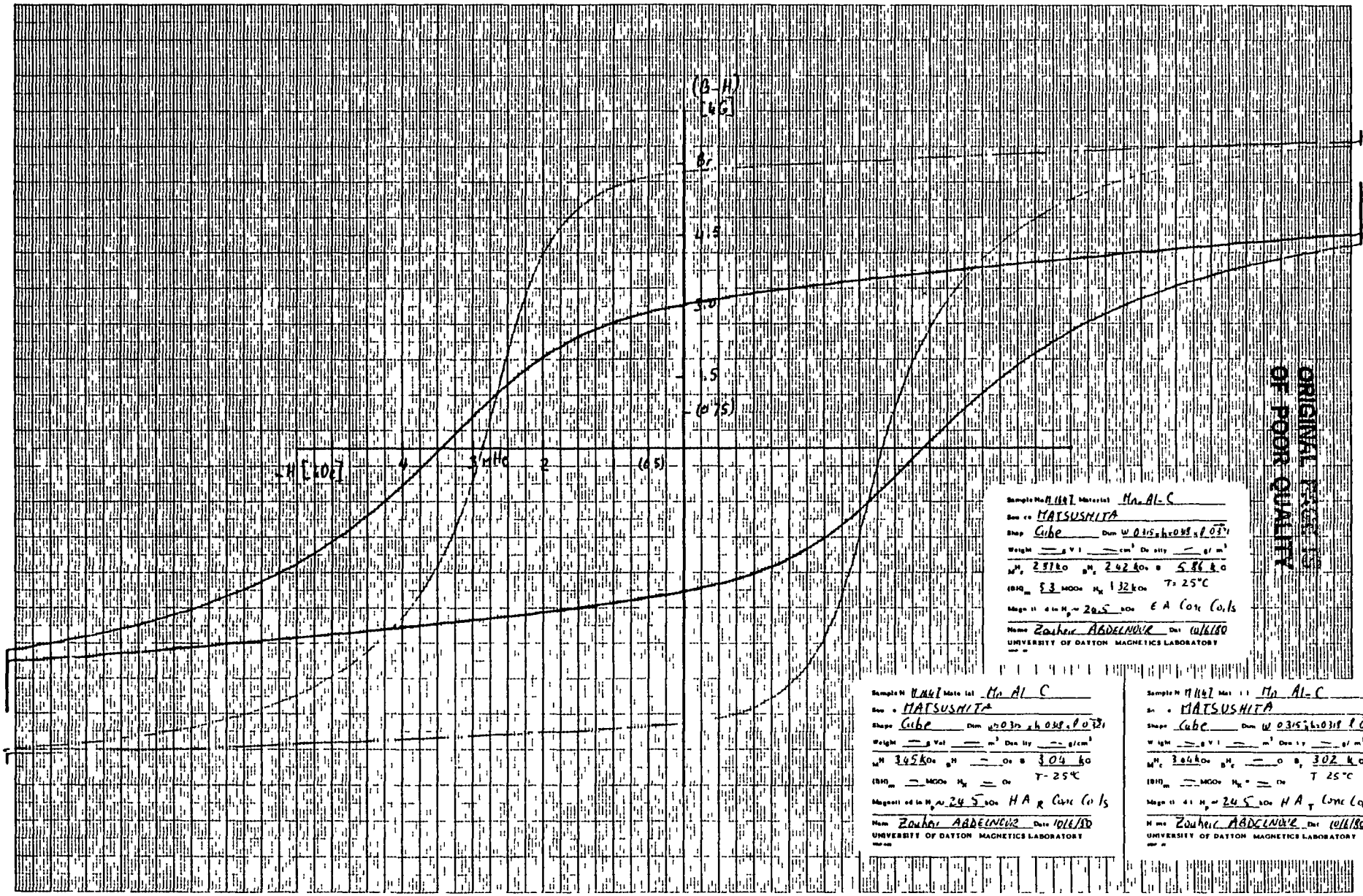

Fig. 28 Major Hysteresis Loops For All Three Cube Axes For M-1647 at 25°C. (Using Conc. Coils)

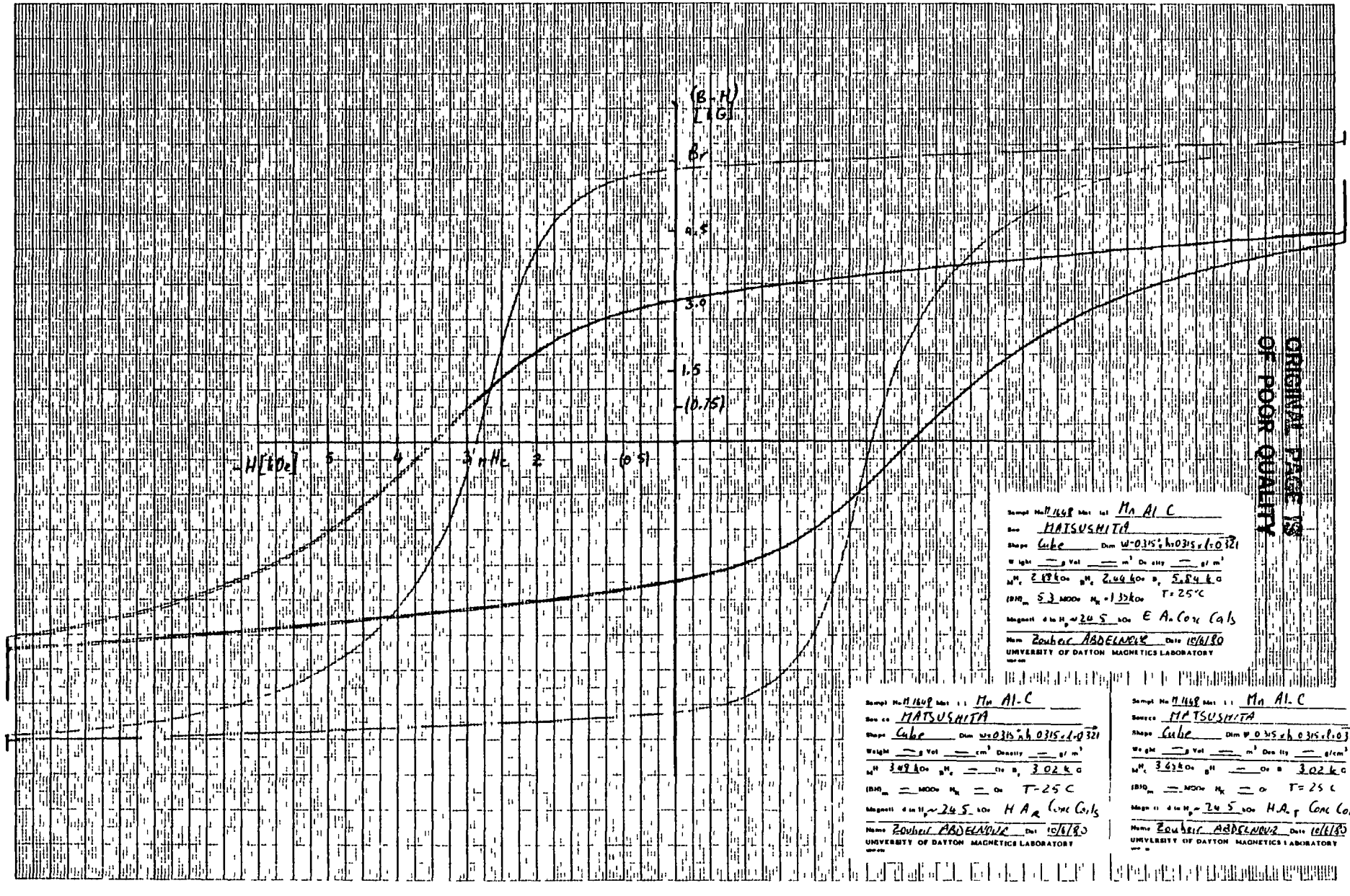

Fig. 29 Major Hysteresis Loops For All Three Cube Axes For M-1648 at 25°C. (Using Conc. Coils)

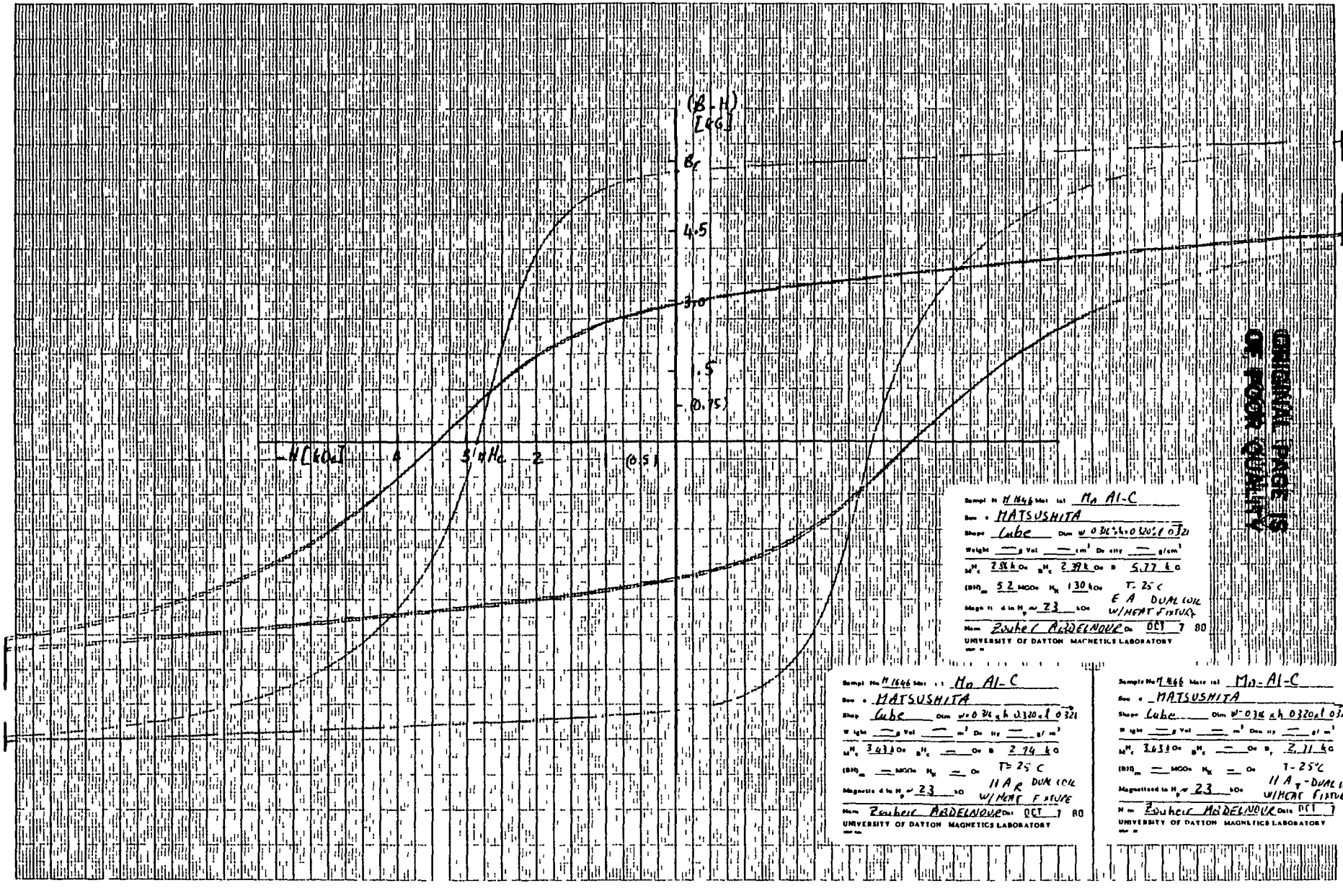

Fig. 30 Major Hysteresis Loops For All Three Cube Axes For M-1646 at 25°C (Using Dual Coils With H/C Fixture)

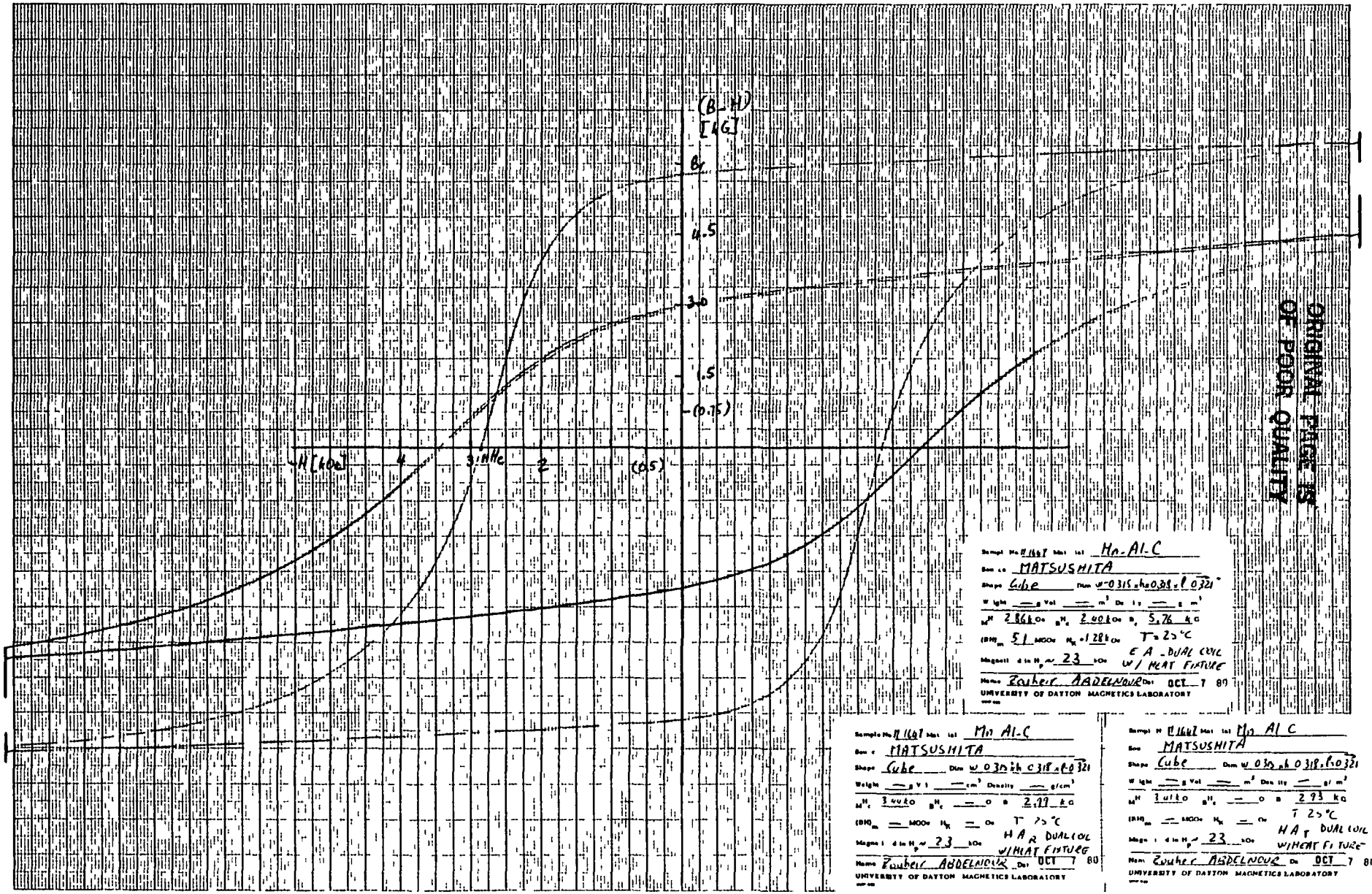

Fig. 31 Major Hysteresis Loops For All Three Cube Axes For M-1647 at 25°C. (Using Dual Coils With H/C Fixture)

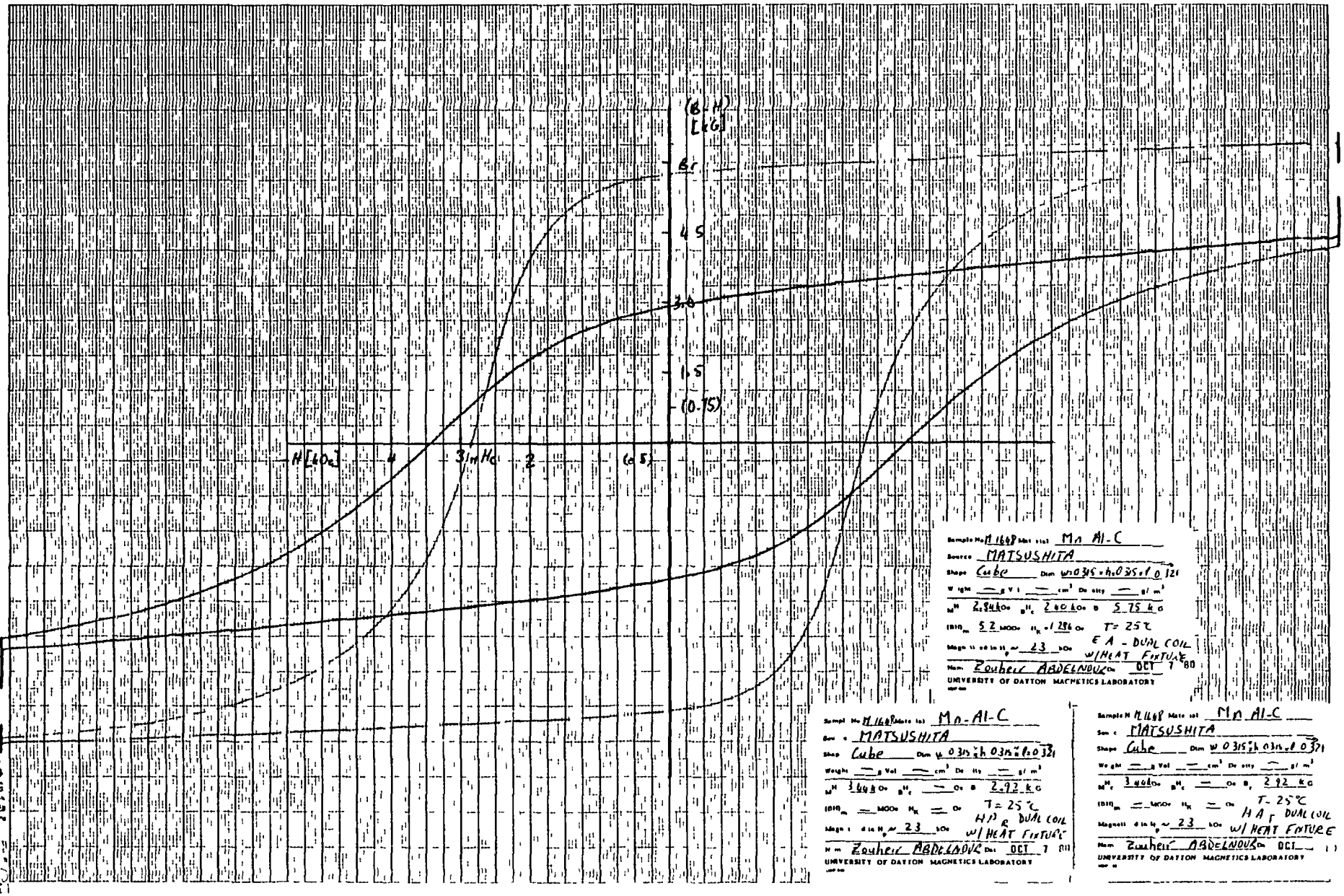

Fig. 32 Major Hysteresis Loops For All Three Cube Axes For M-1648 at 25°C. (Using Dual Coils With H/C Fixture)

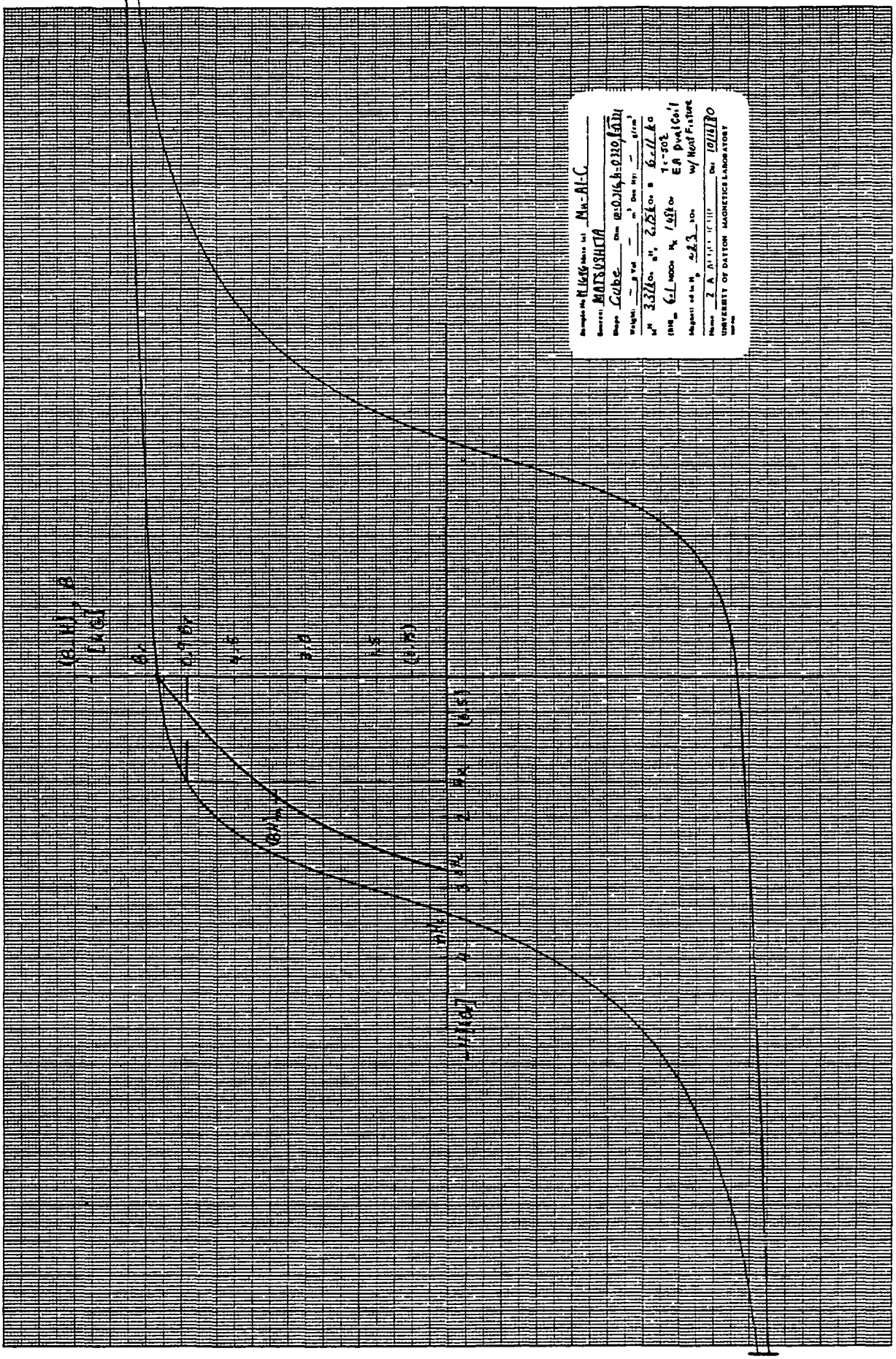

Fig. 33 Major Hysteresis Loops for Cube M-1646 at -50°C.

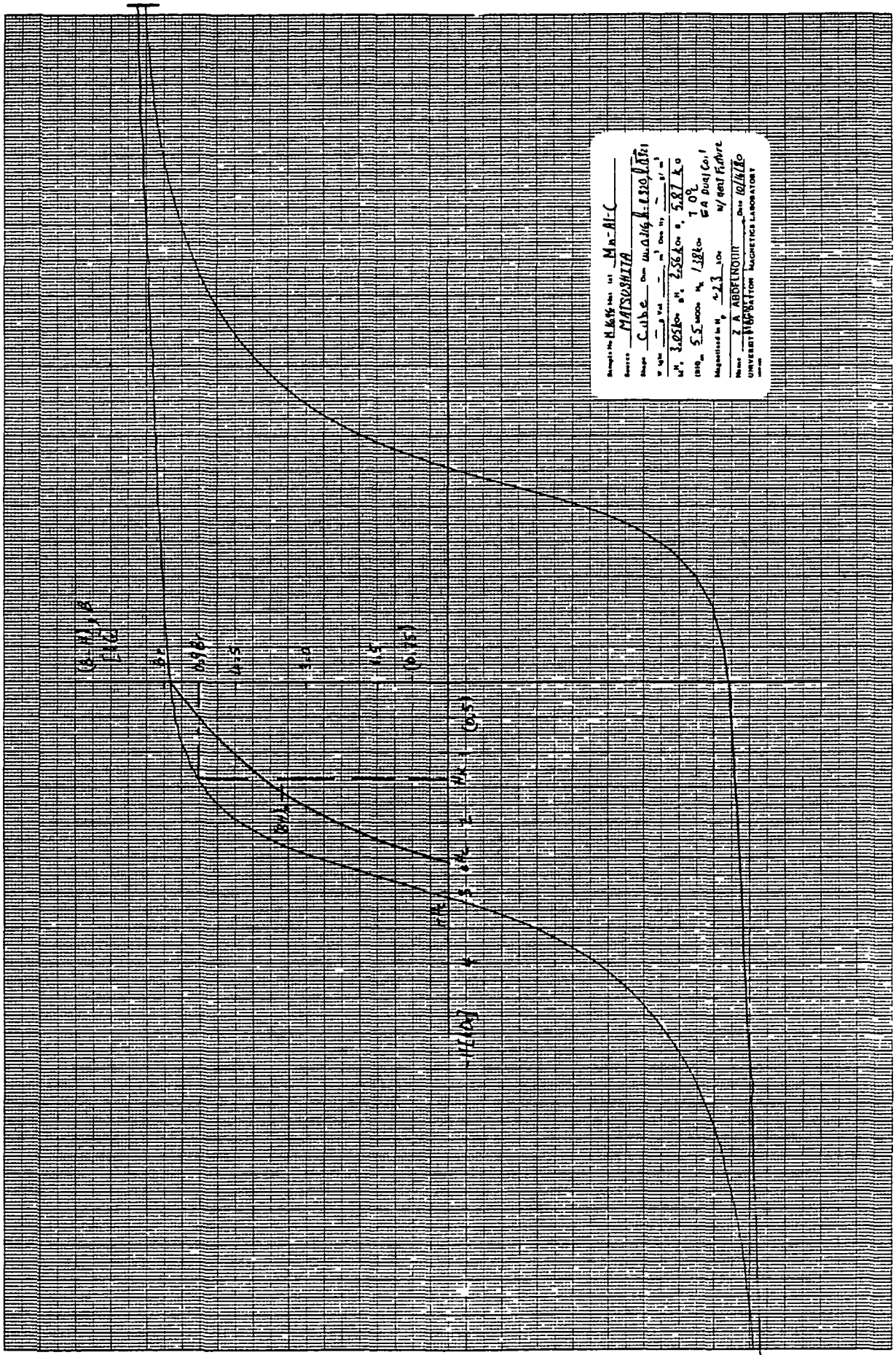

Fig. 34 Major Hysteresis Loops for Cube M-1646 at 0°C.

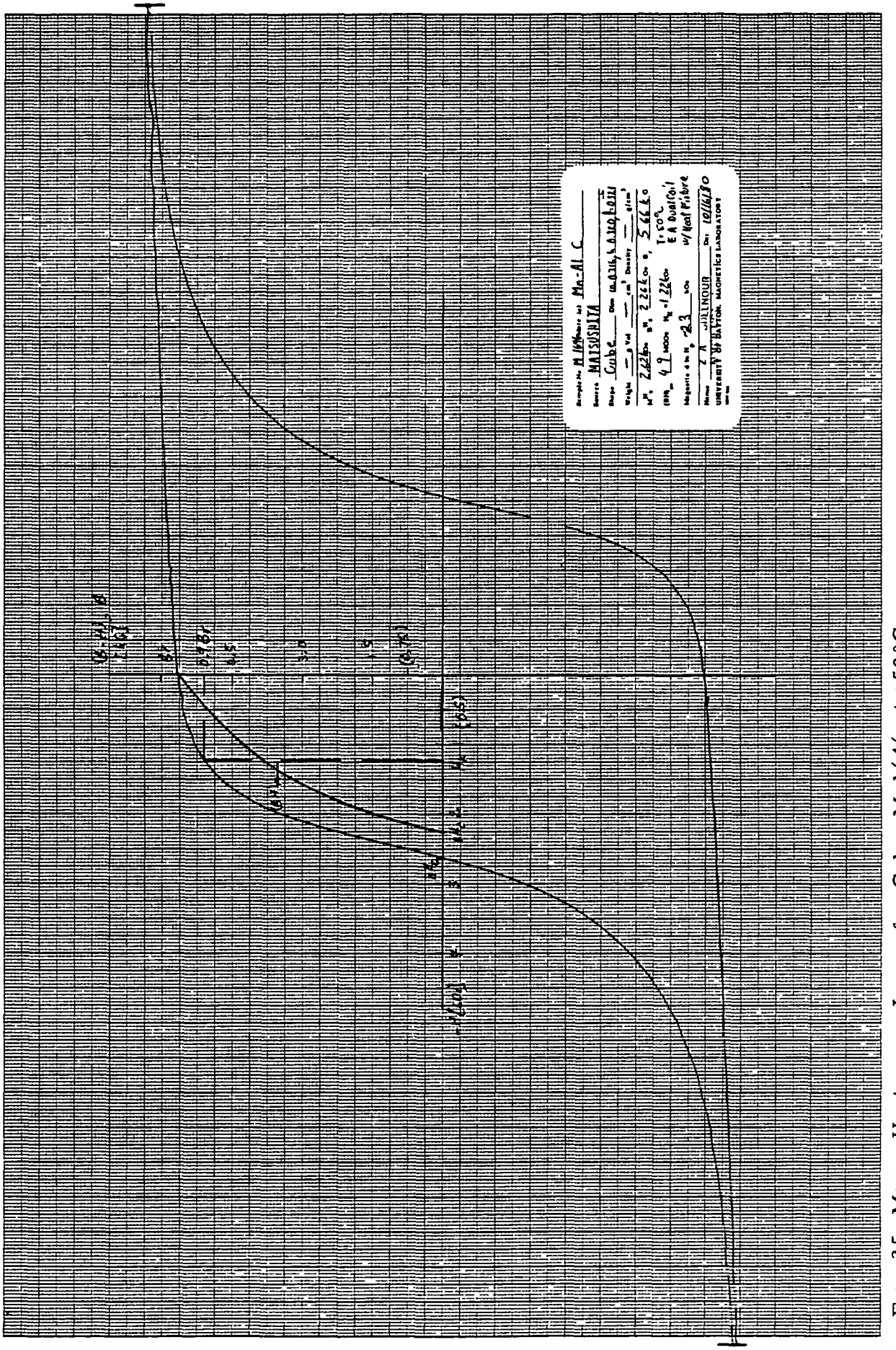

Fig. 35 Major Hysteresis Loops for Cube M-1646 at +50°C.

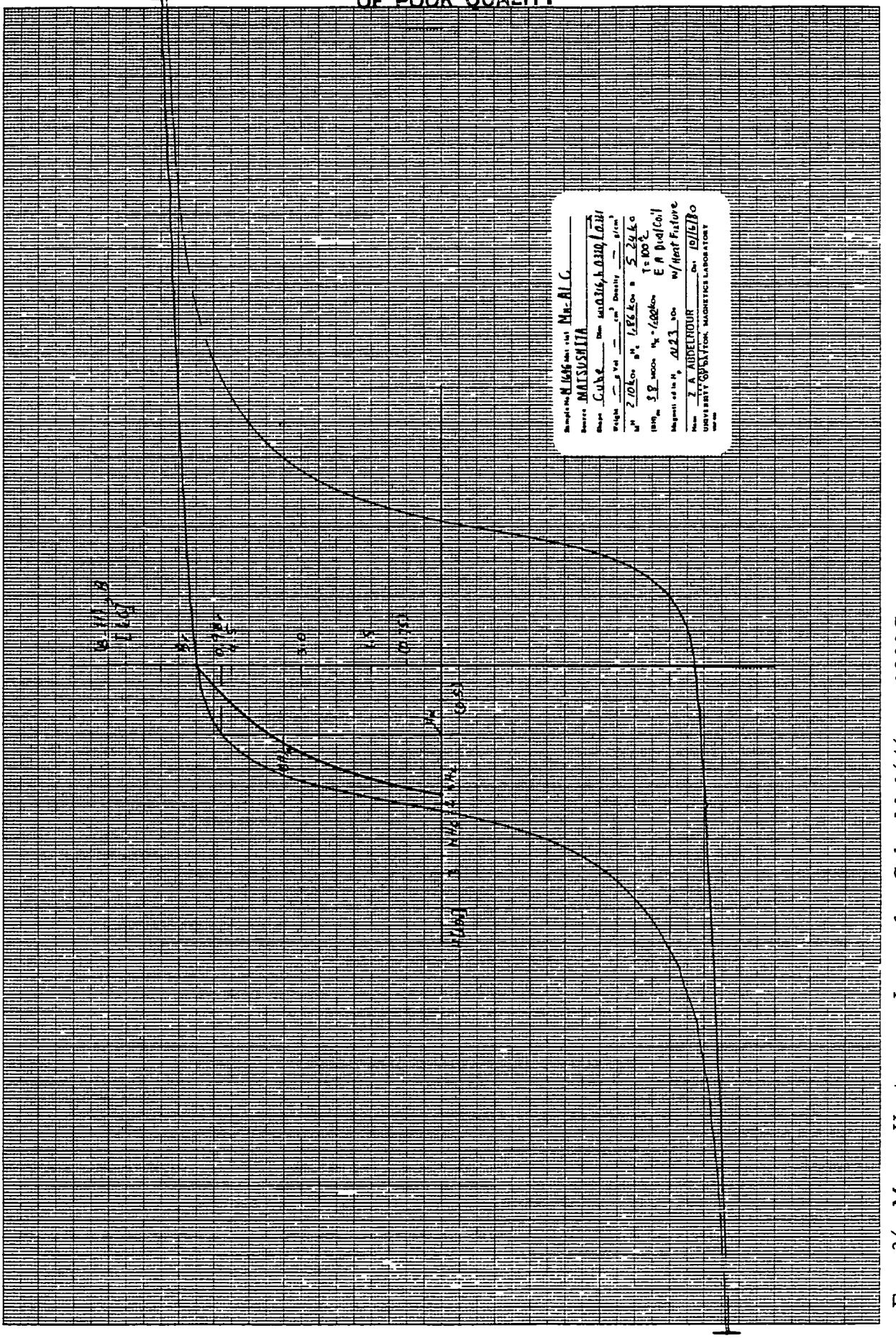

Fig. 36 Major Hysteresis Loops for Cube M-1646 at +100°C.

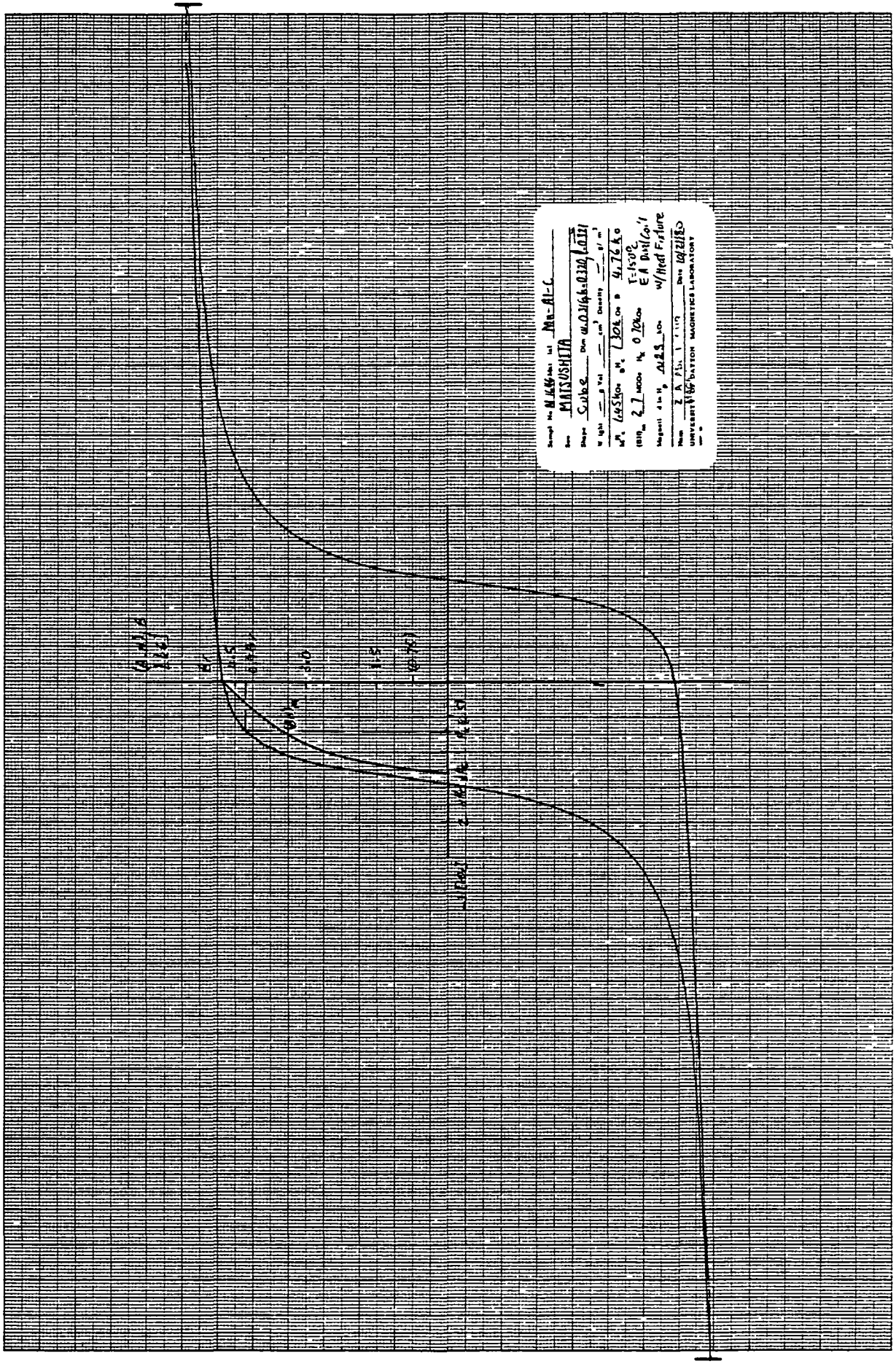

Fig. 37 Major Hysteresis Loops for Cube M-1646 at +150°C.

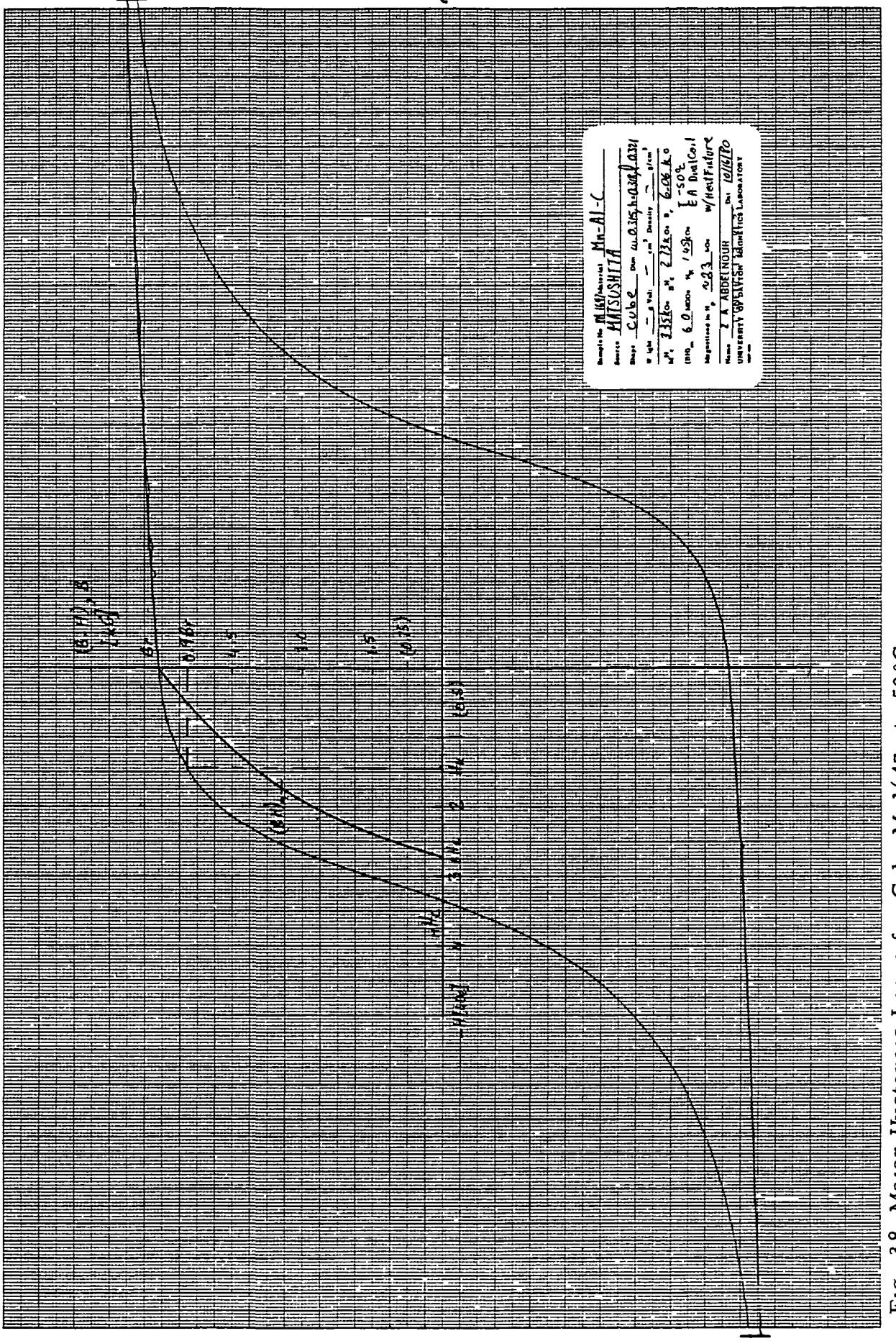

Fig. 38 Major Hystereis Loops for Cube M-1647 at -50°C.

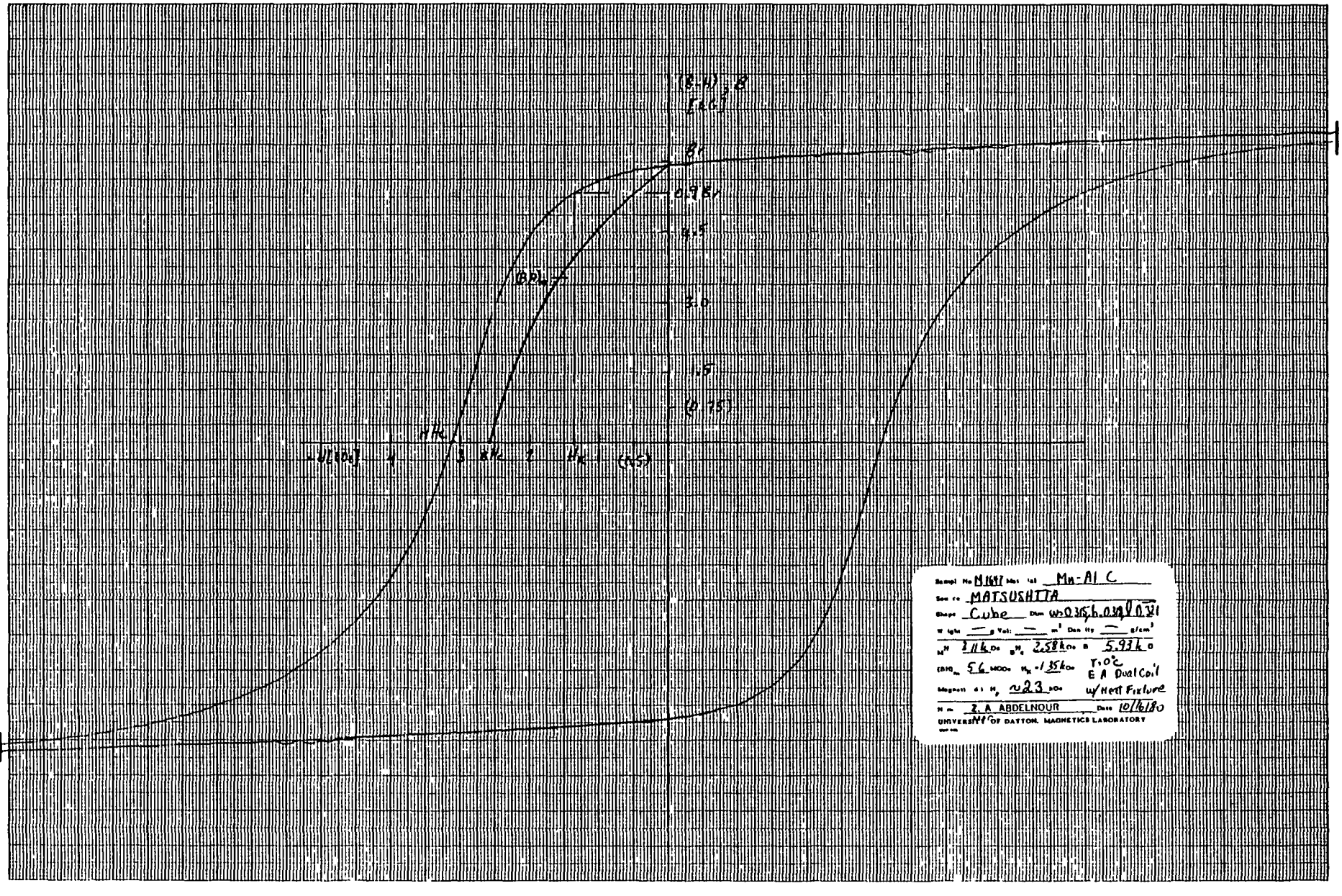

Fig. 39 Major Hysteresis Loops For Cube M-1647 at 0°C.

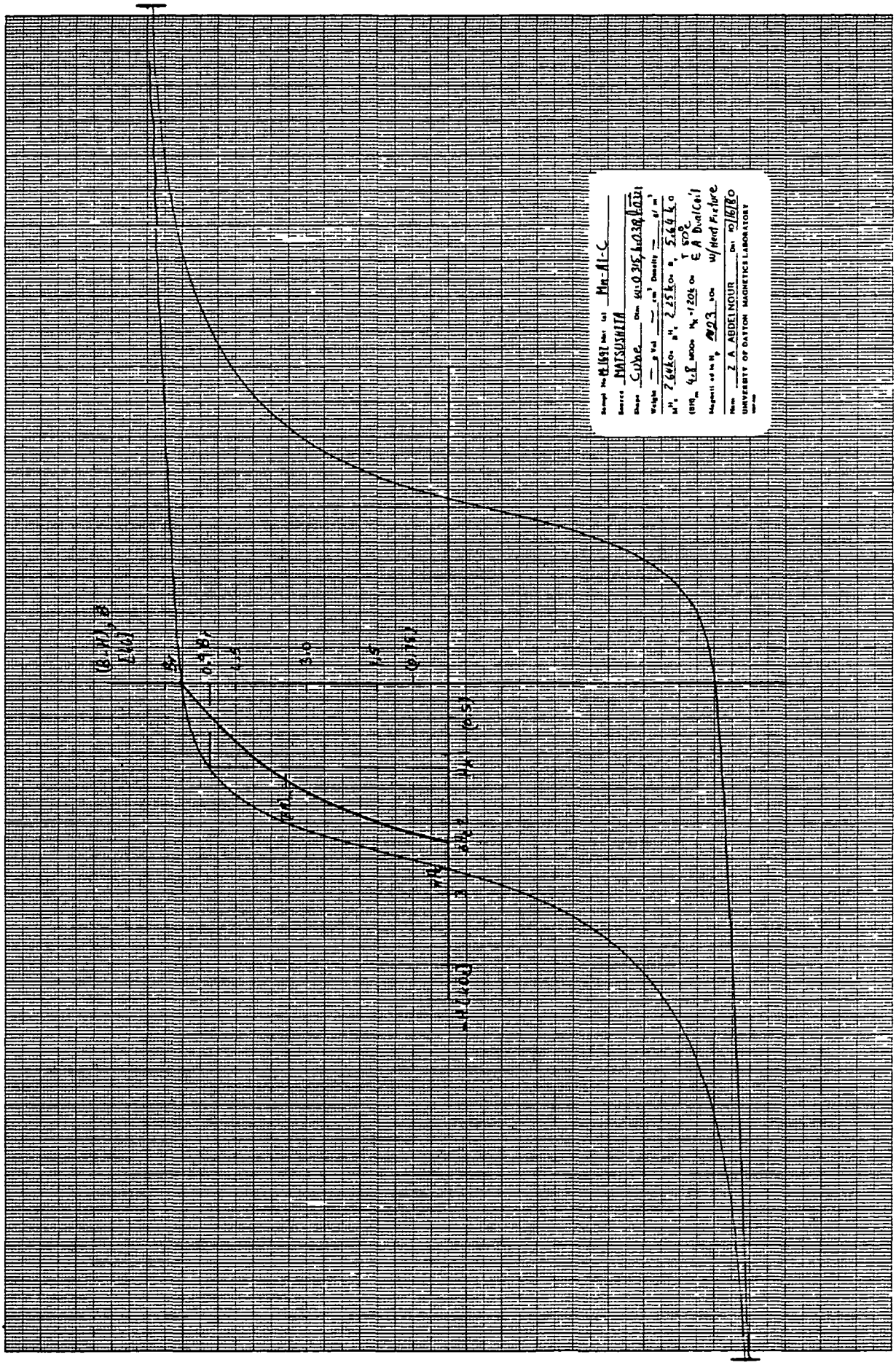

Fig. 40 Major Hysteresis Loops for Cube M-1647 at +50°C.

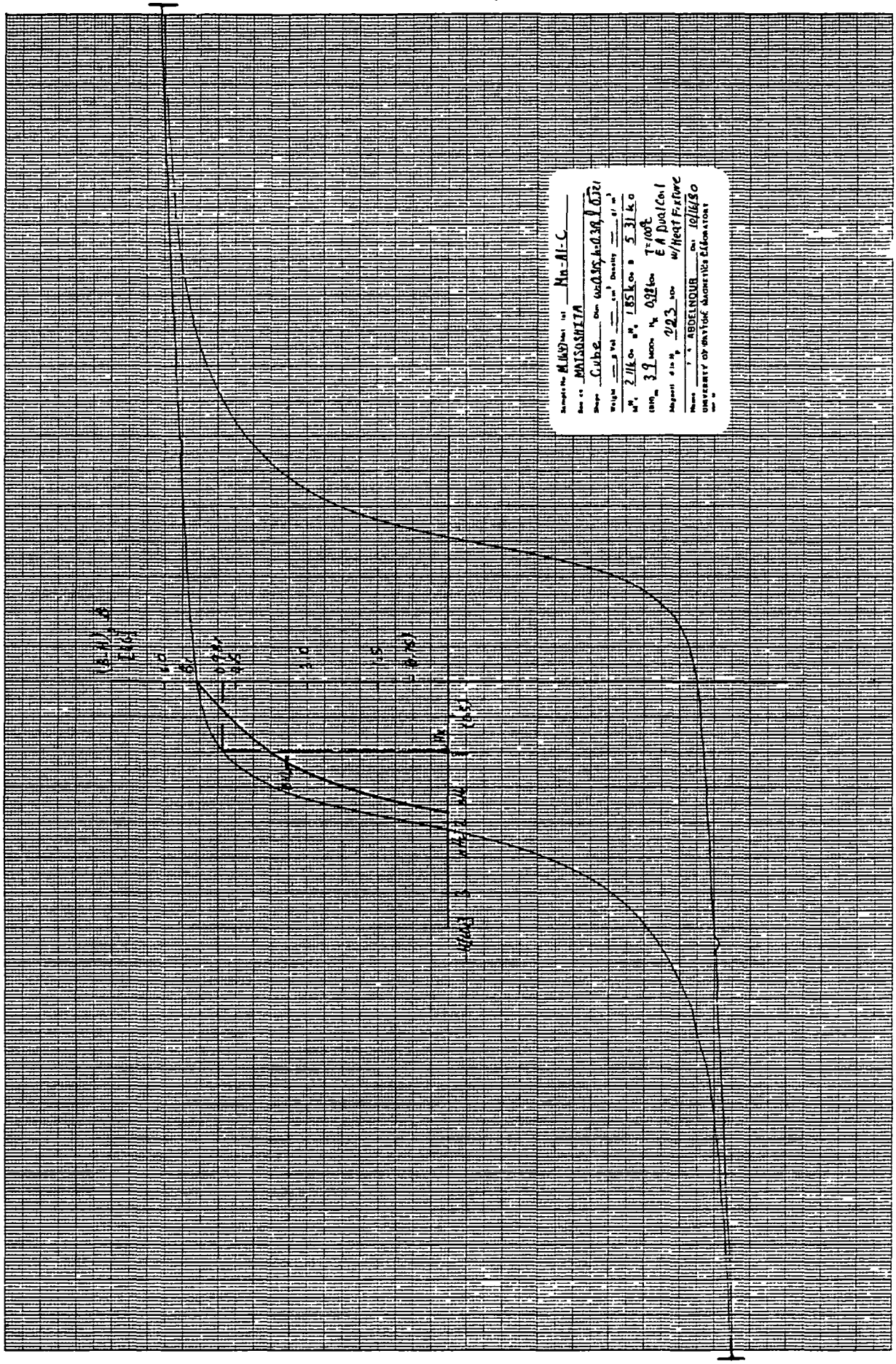

Fig. 41 Major Hysteresis Loops for Cube M-1647 at +100°C.

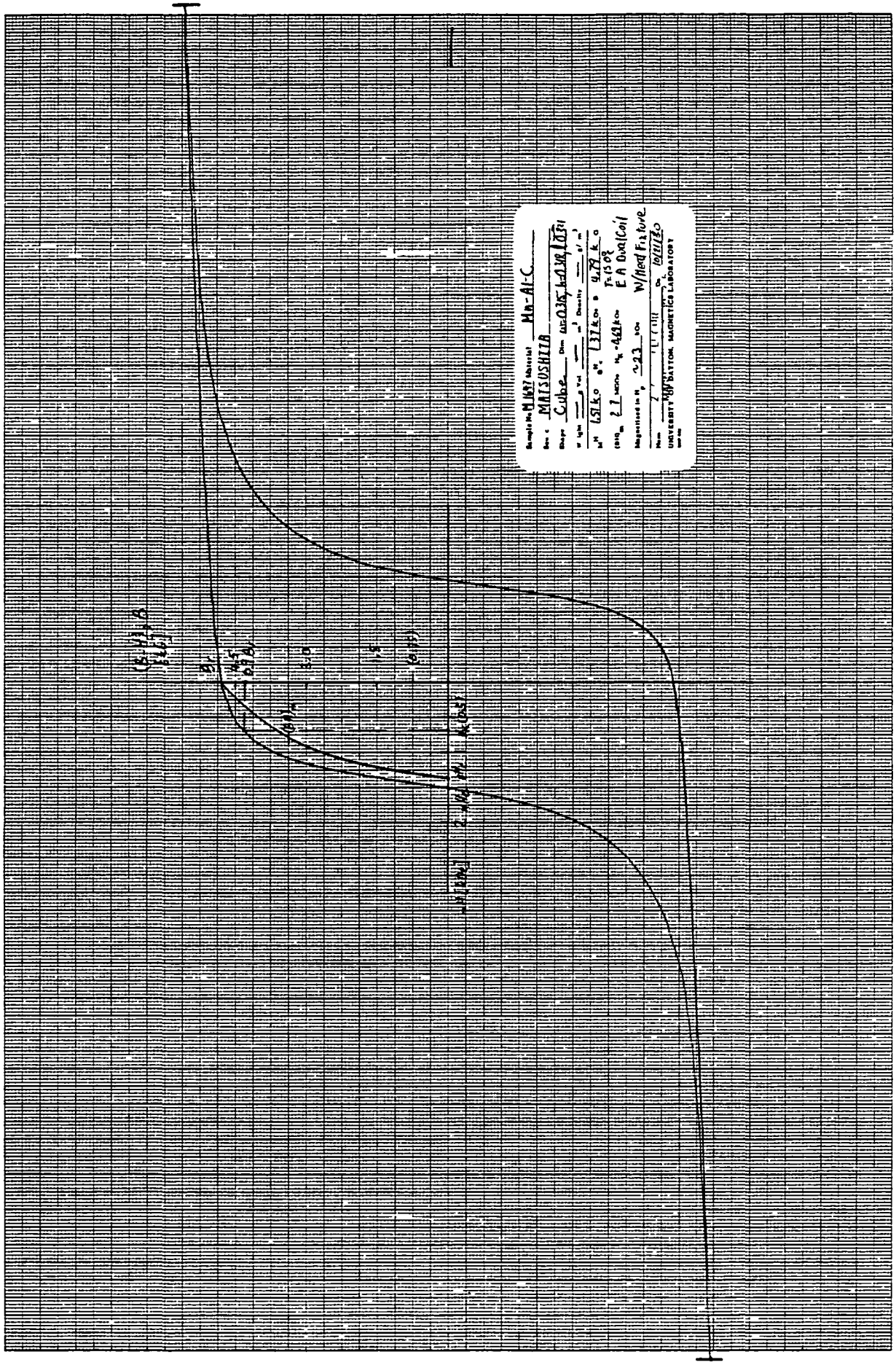

Fig. 42 Major Hysteresis Loops for Cube M-1647 at +150°C.

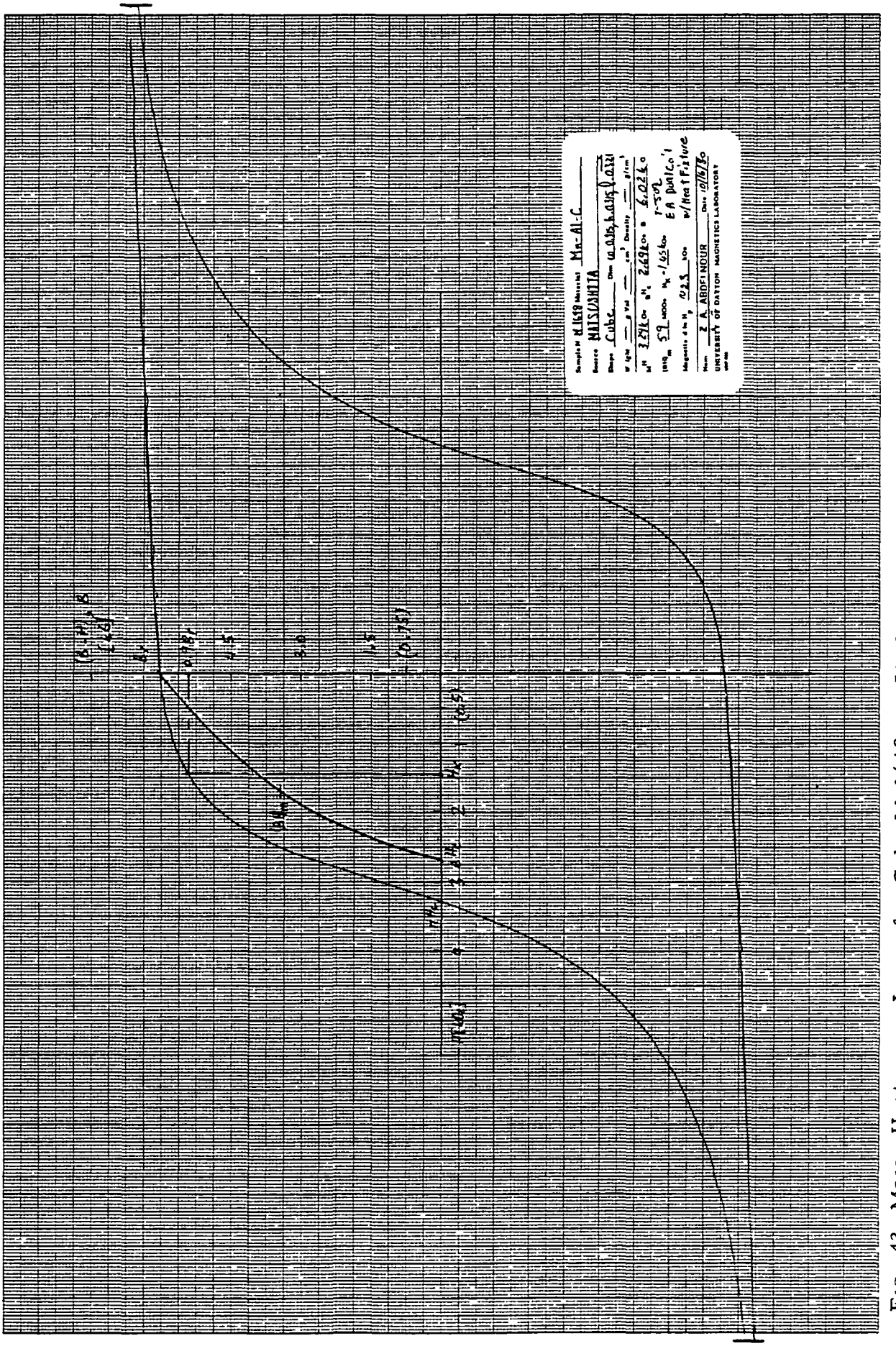

Fig. 43 Majoy Hysteresis Loops for Cube M-1648 at -50°C.

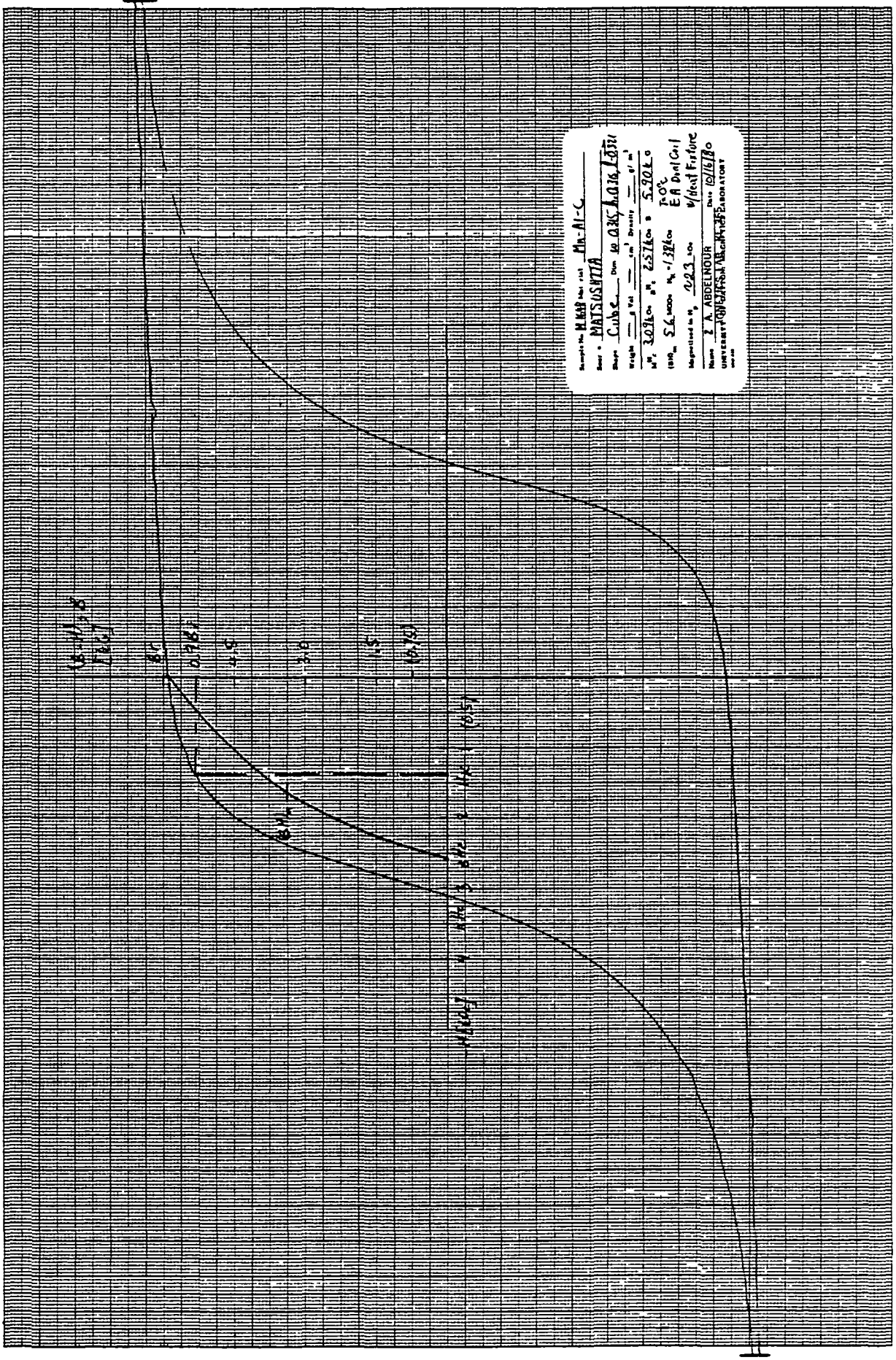

Fig. 44 Major Hysteresis Loops for Cube M-1648 at 0°C.

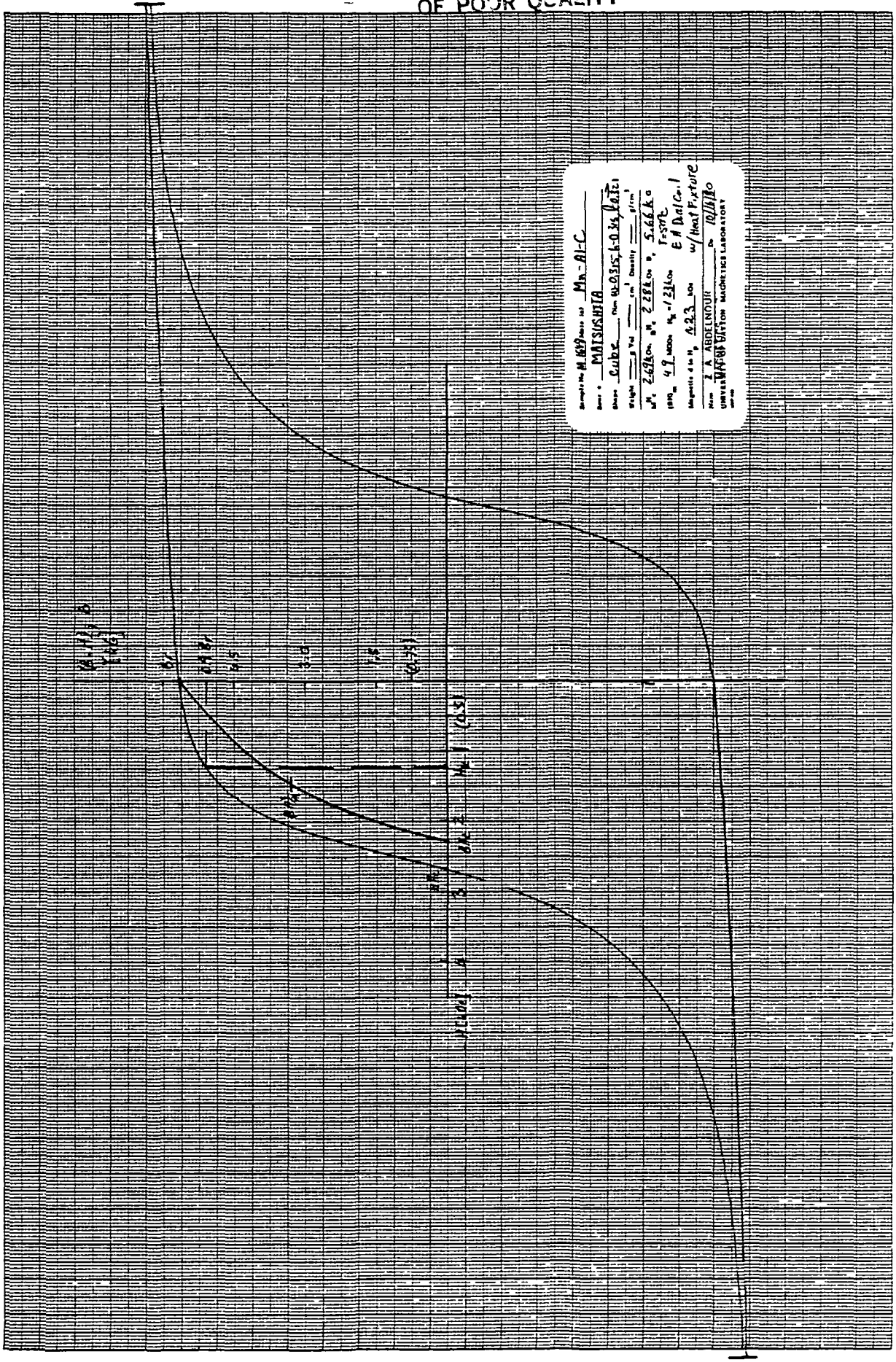

Fig. 45 Major Hysteresis Loops for Cube M-1648 at +50°C.

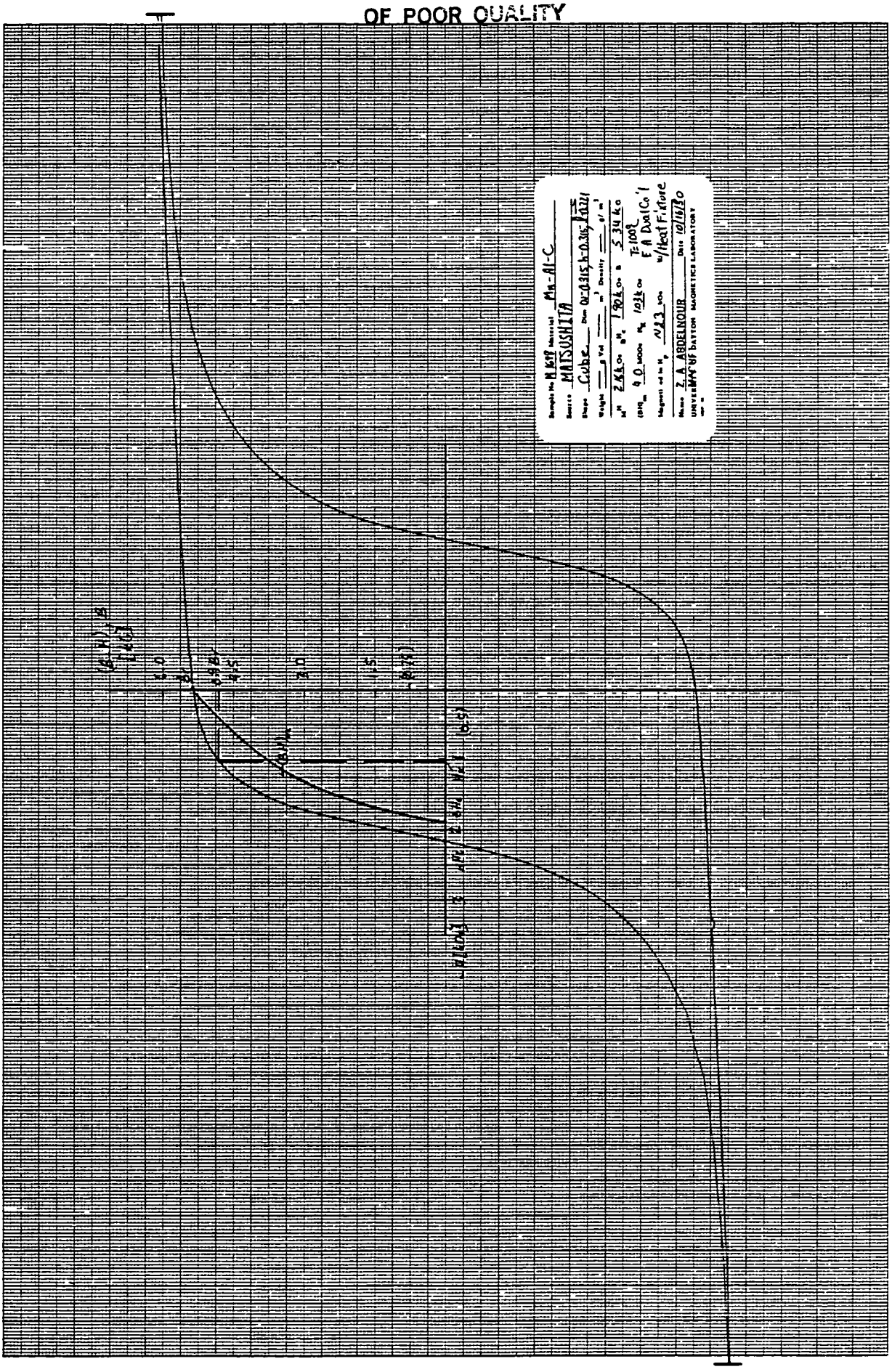

Fig. 46. Major Hysteresis Loops for Cube M-1648 at +100°C.

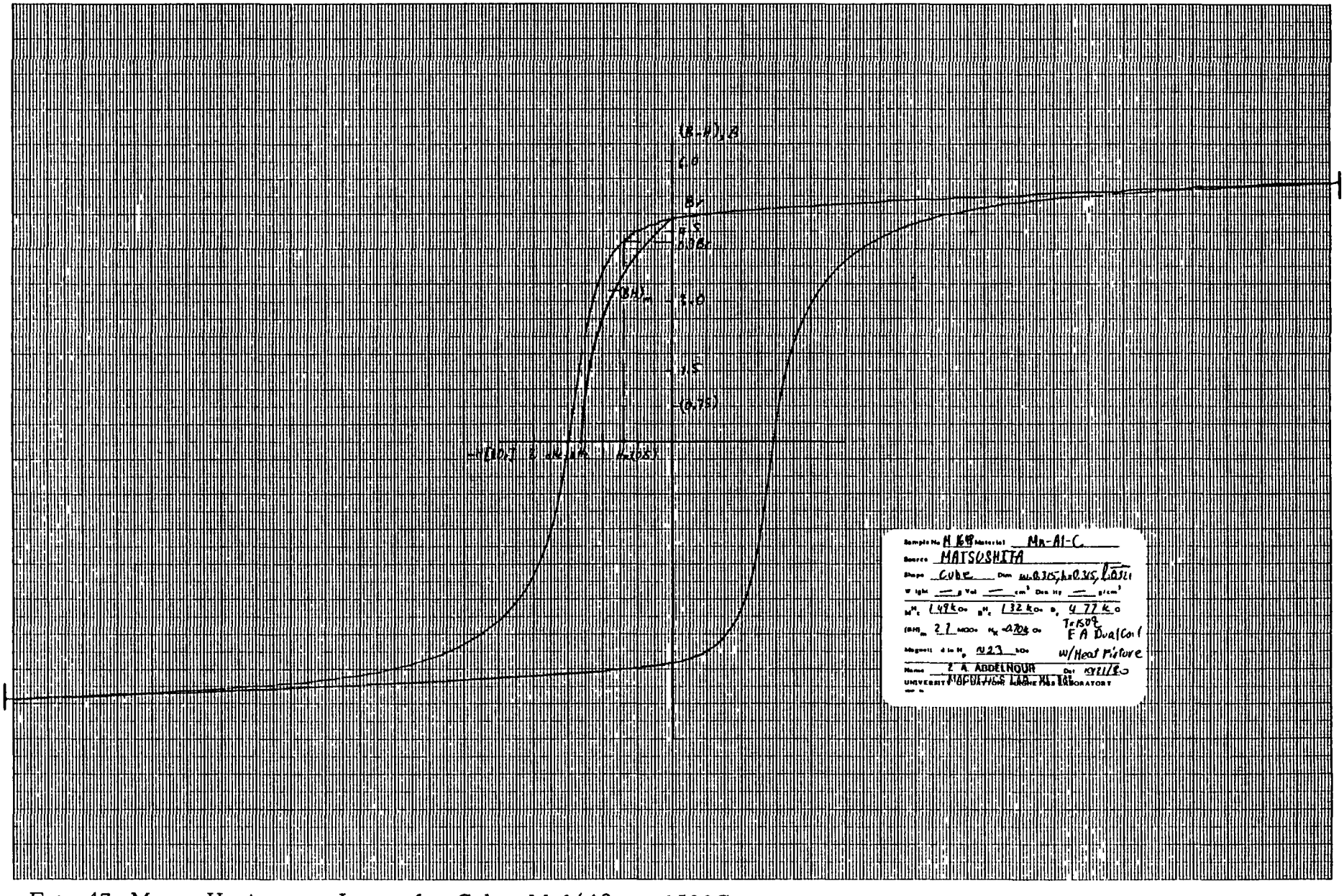

Fig. 47 Major Hysteresis Loops for Cube M-1648 at +150°C.

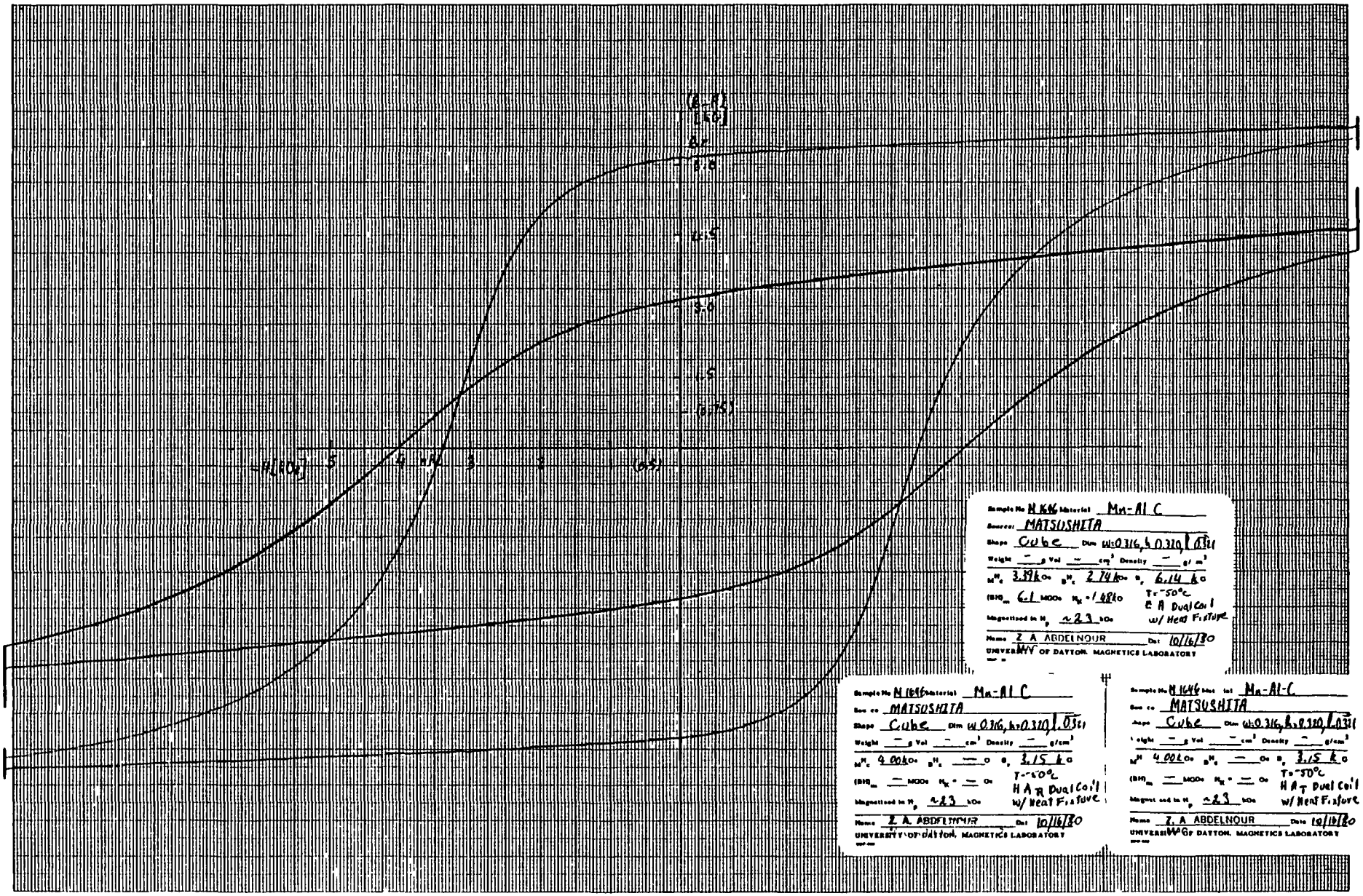

Fig. 48 Major Hysteresis Loops for All Three Cube Axes for M-1646 at -50°C.

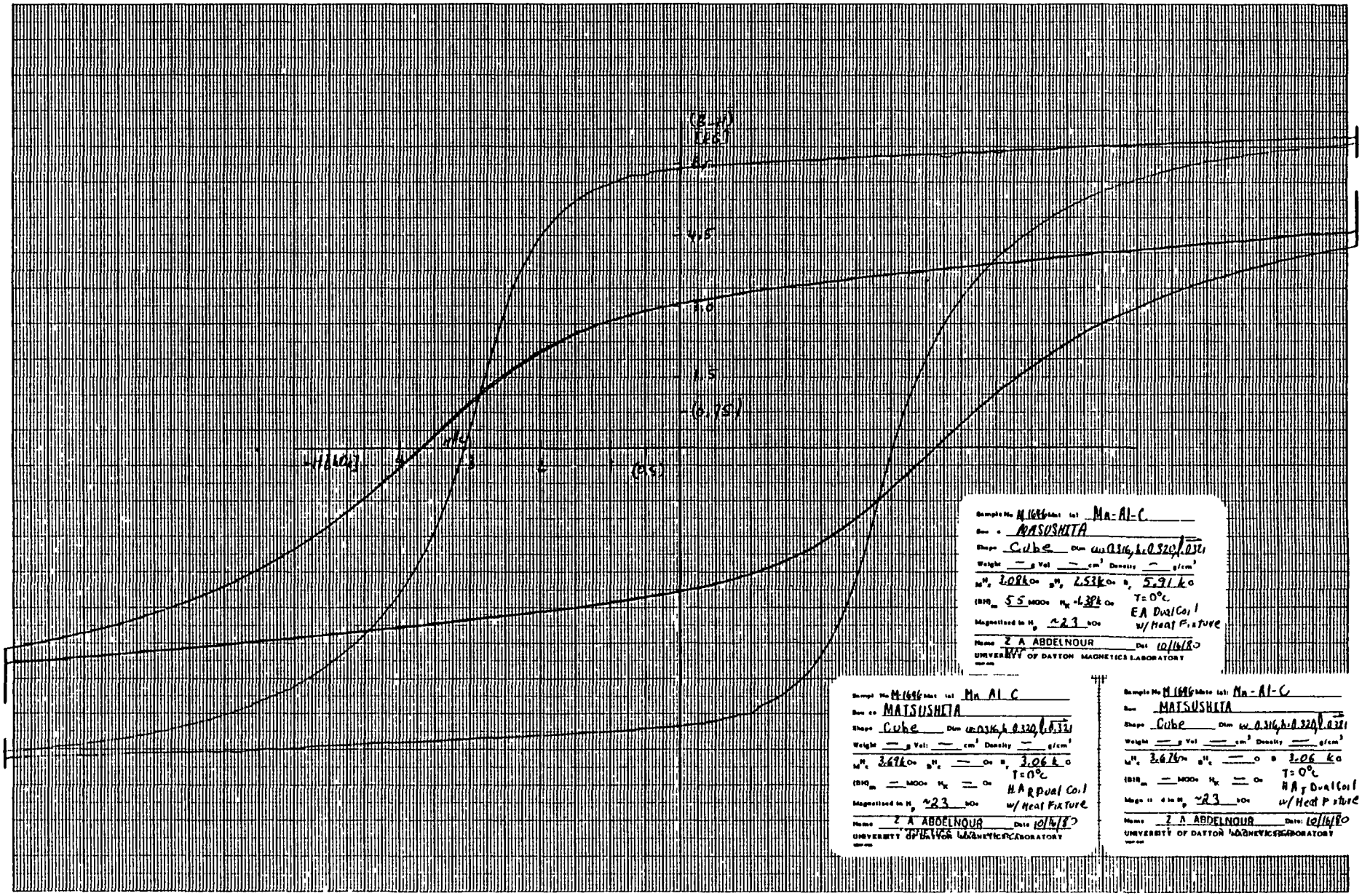

Fig. 49 Major Hysteresis Loops for all Three Cube Axes for M-1646 at 0°C.

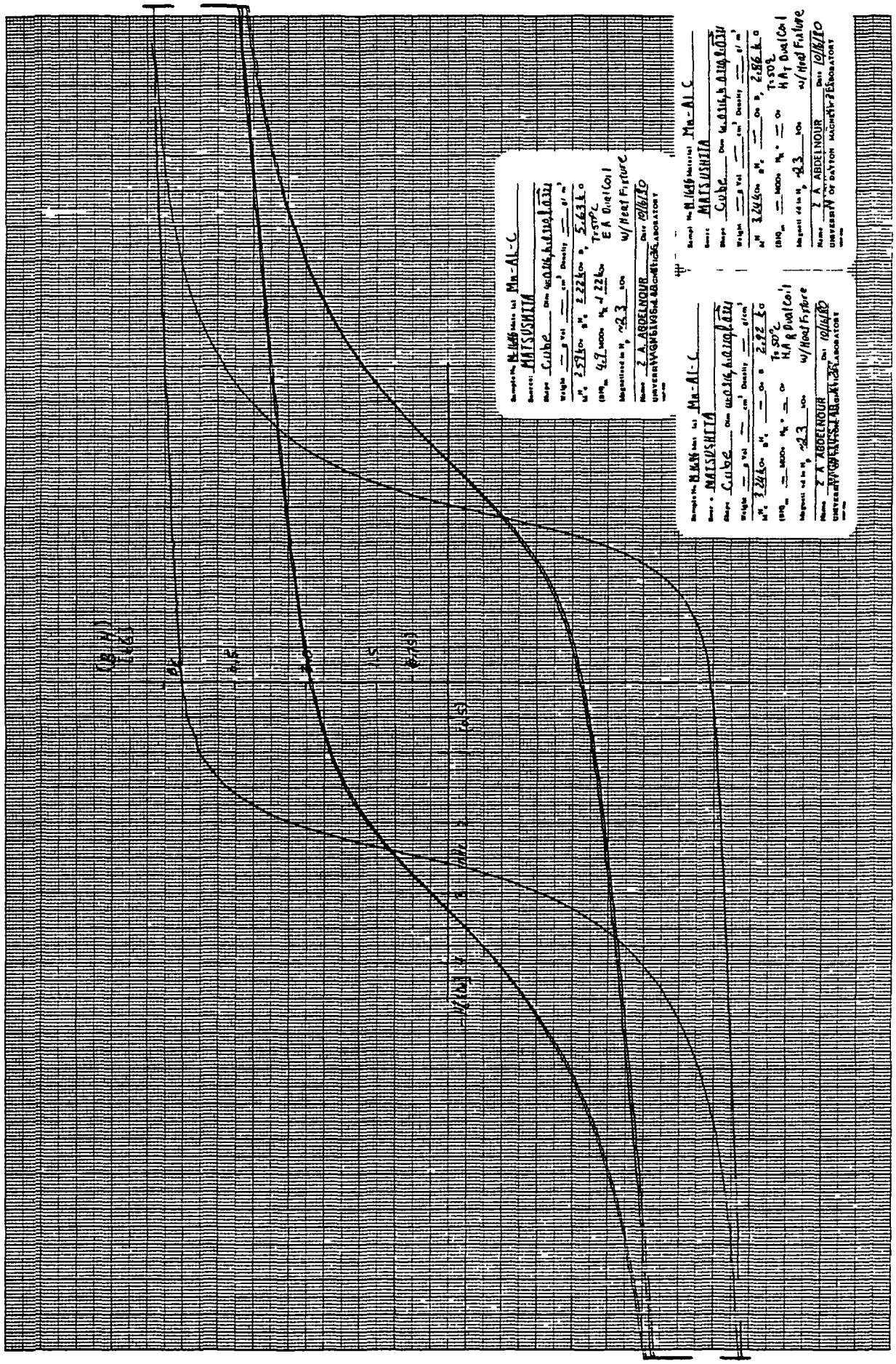

Fig. 50 Major Hysteresis Loops for all Three Cube Axes for M-1646 at +50 °C.

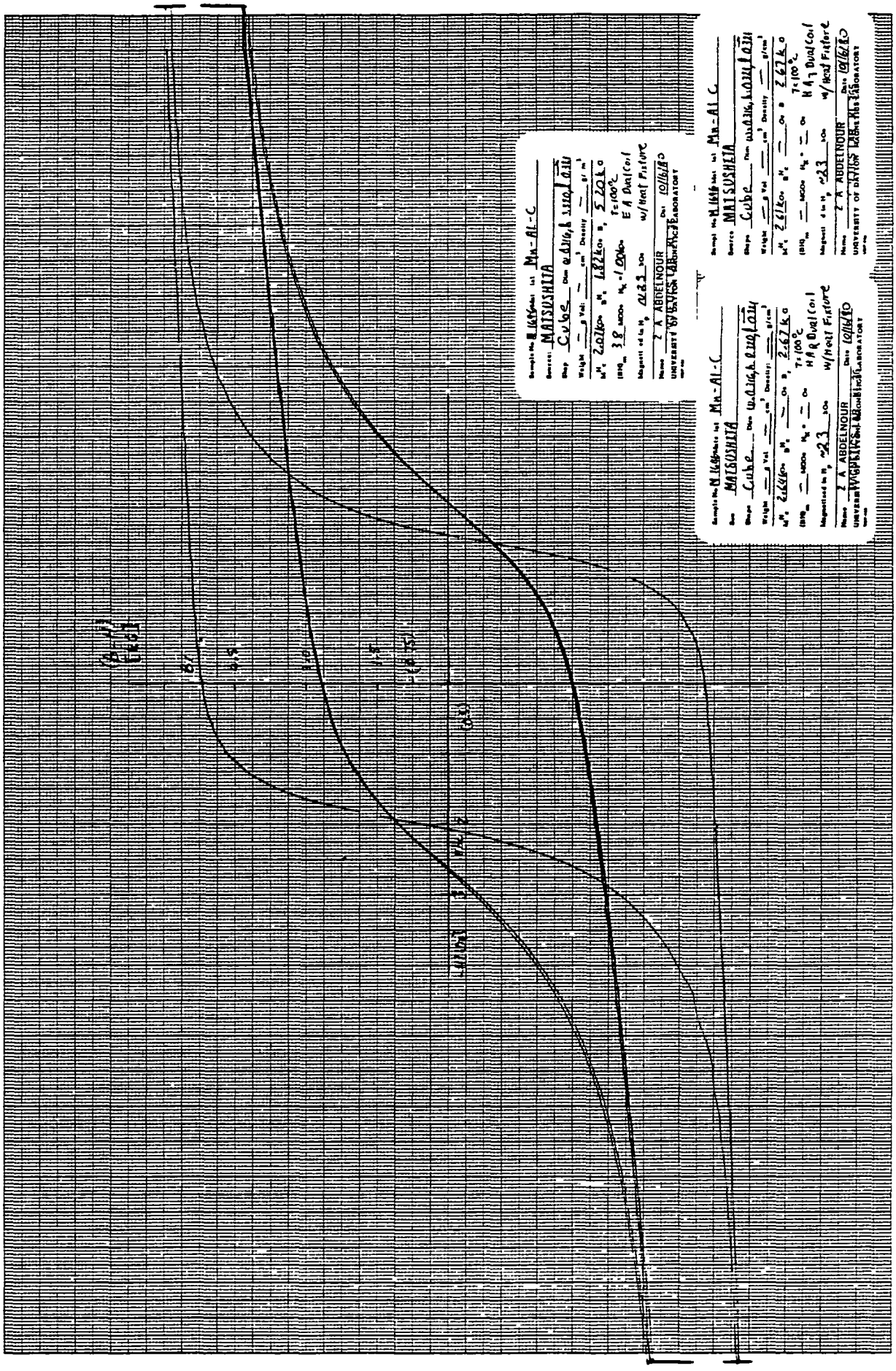

Fig. 51 Major Hysteresis Loops for all Three Cube Axes for M-1646 at +100°C.

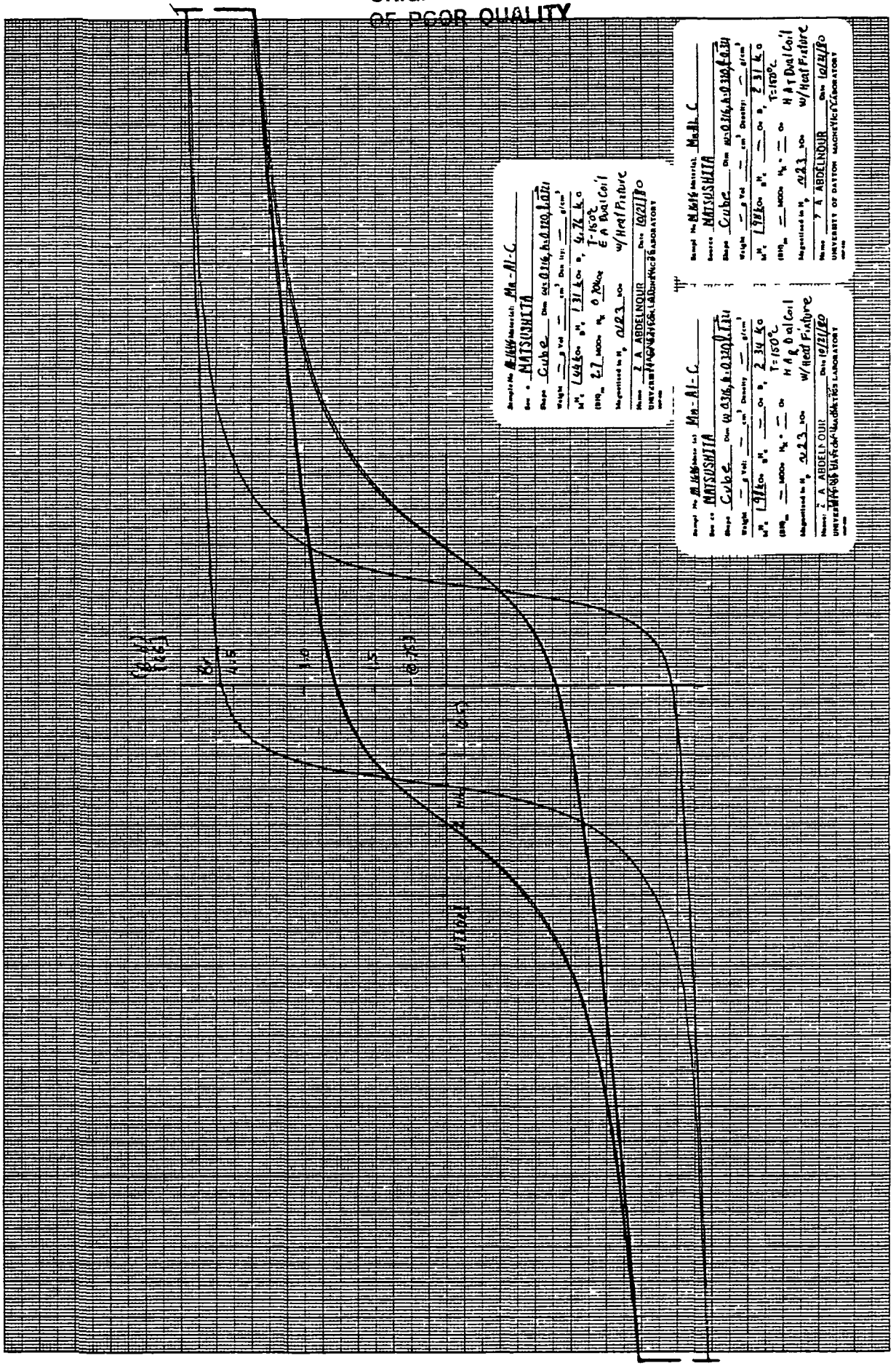

Fig. 52 Major Hysteresis Loops for all Three Cube Axes for M-1646 at +150 °C.

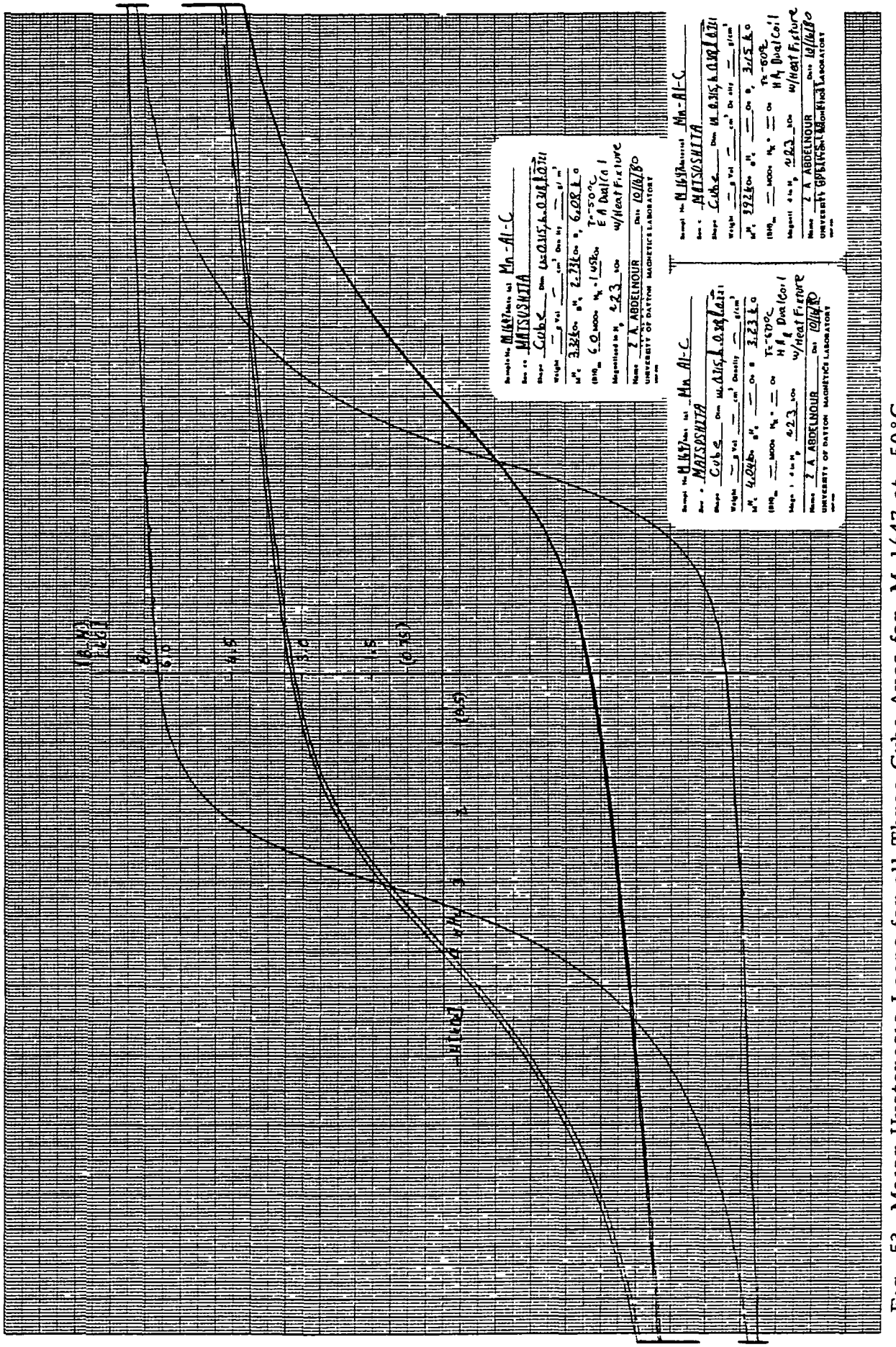

Fig. 53 Major Hysteresis Loops for all Three Cube Axes for M-1647 at -50°C.

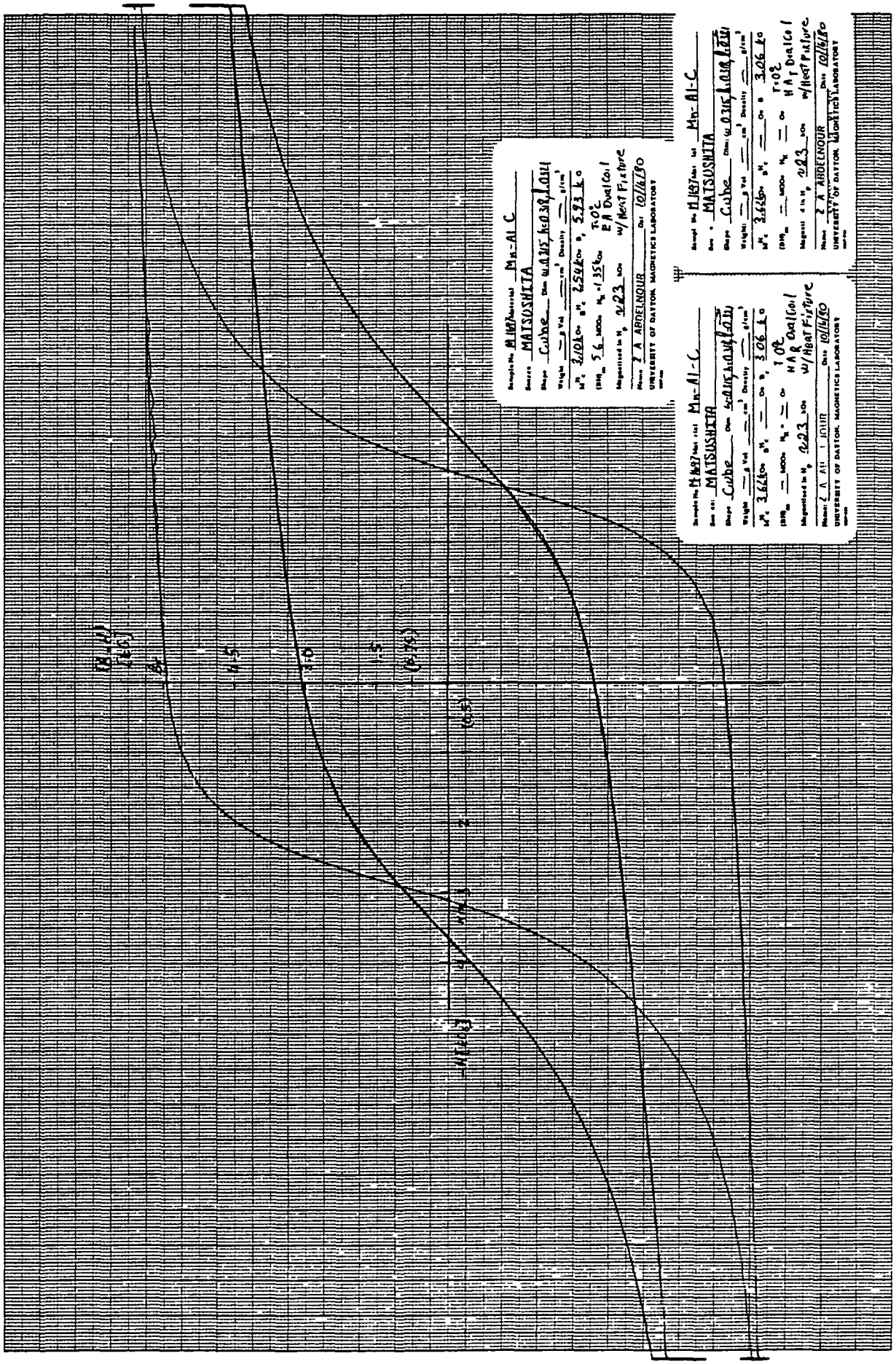

Fig. 54 Major Hysteresis Loops for all Three Cube Axes for M-1647 at 0°C.

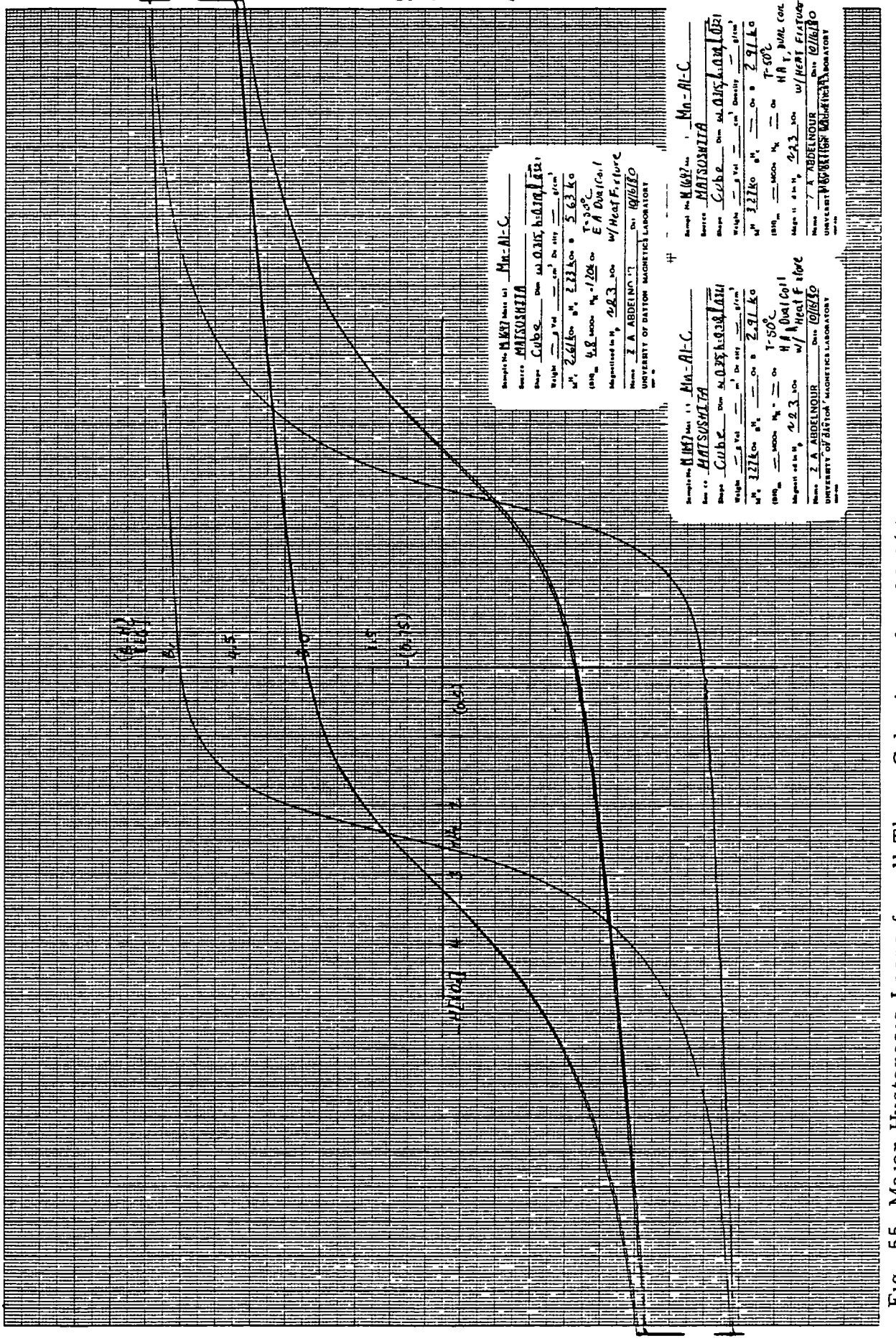

Fig. 55 Major Hysteresis Loops for all Three Cube Axes for M-1647 at +50 °C.

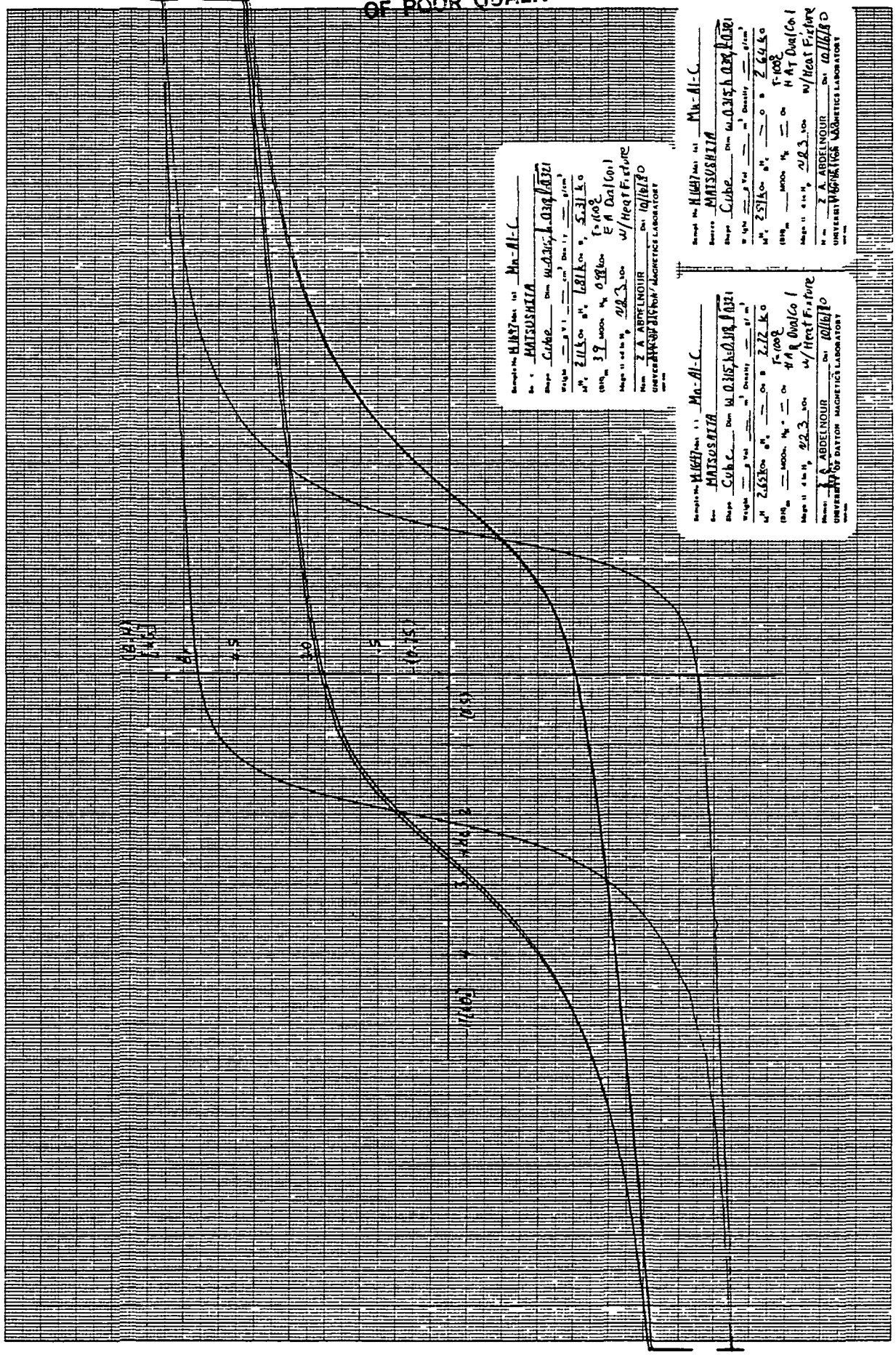

Fig. 56 Major Hysteresis Loops for all Three Cube Axes for M-1647 at +100°C.

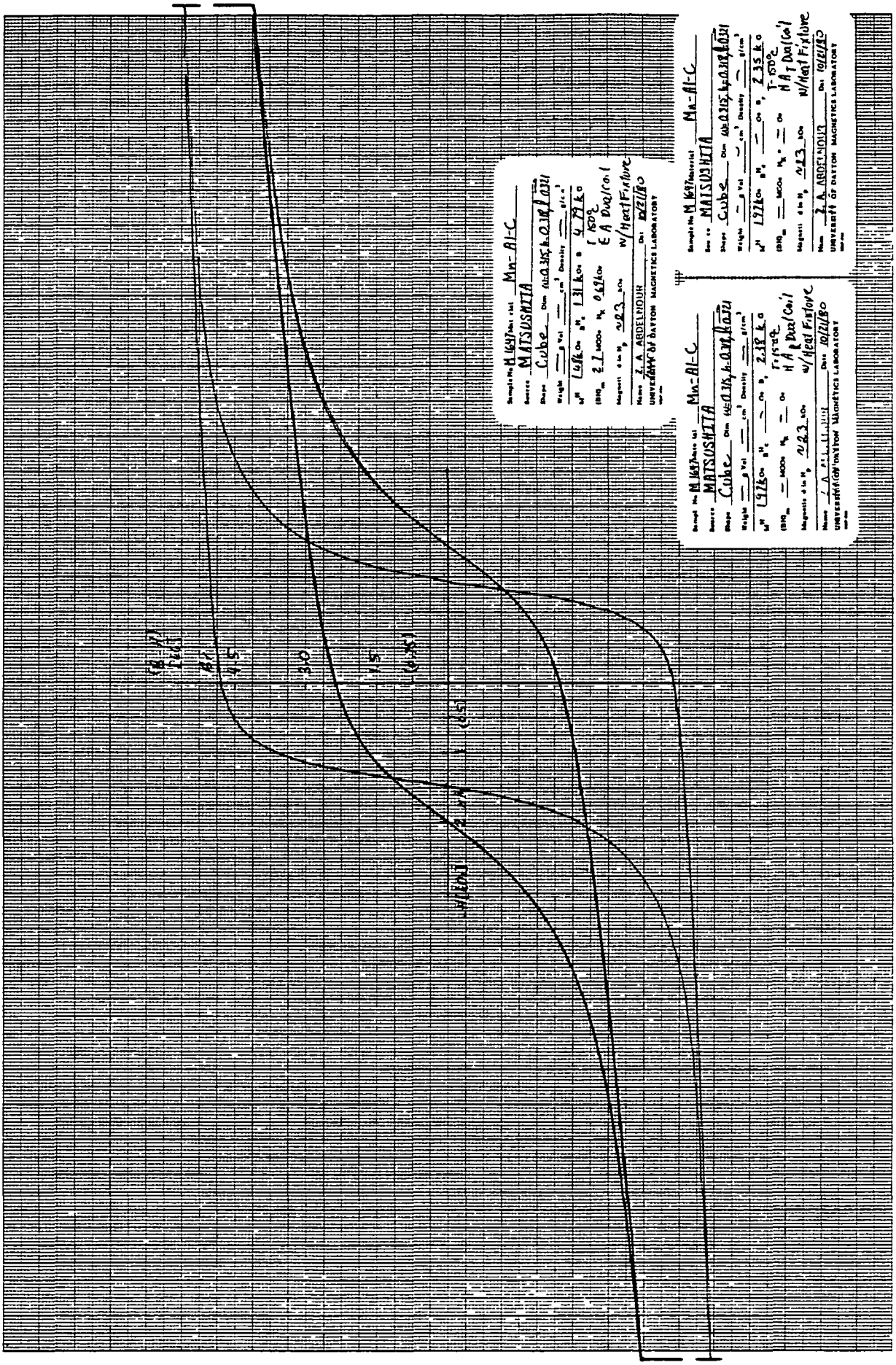

Fig. 57 Major Hysteresis Loops for all Three Cube Axes for M-1647 at +150°C.

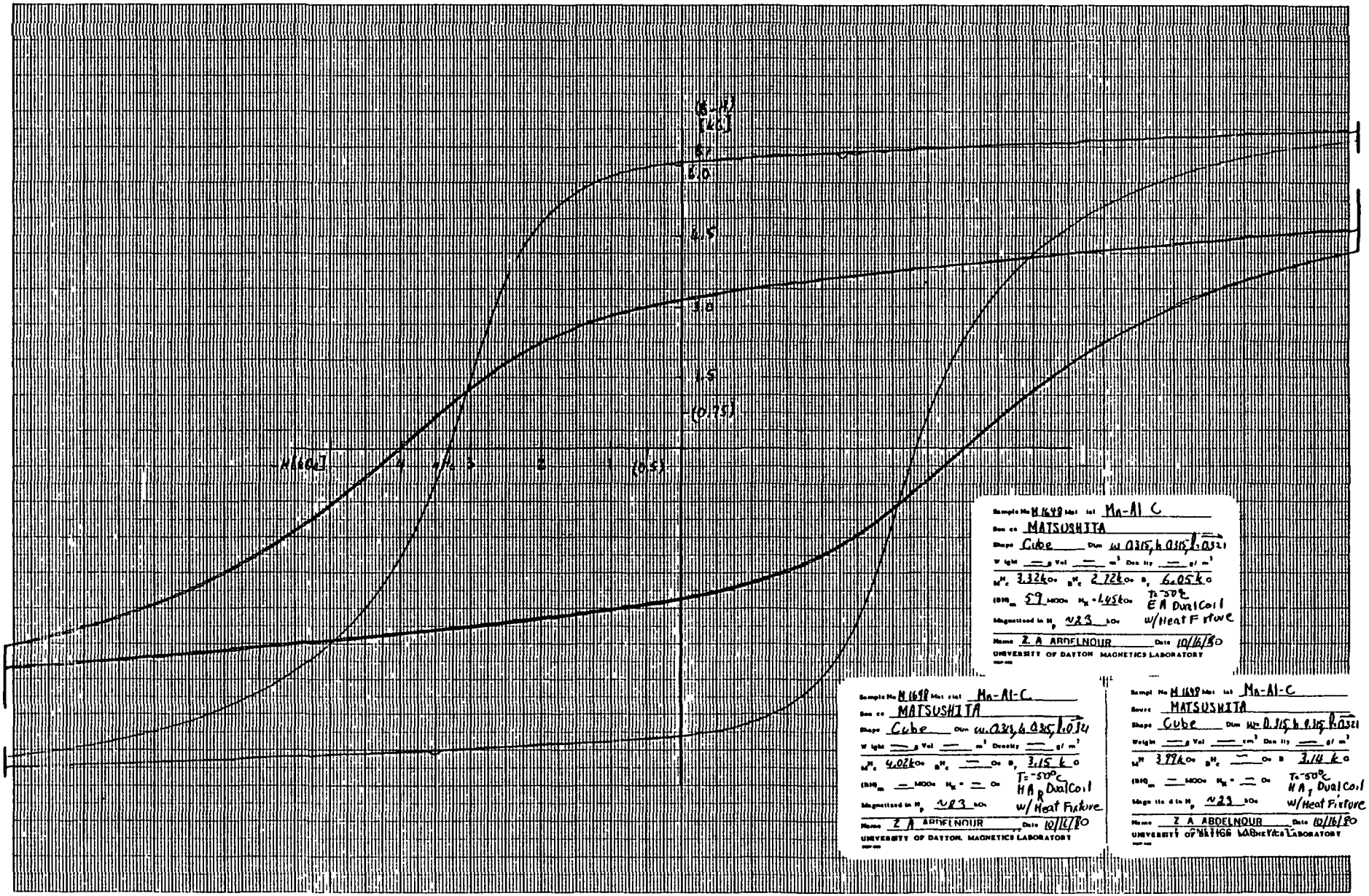

Fig. 58 Major Hysteresis Loops for all Three Cube Axes for M-1648 at -50°C.

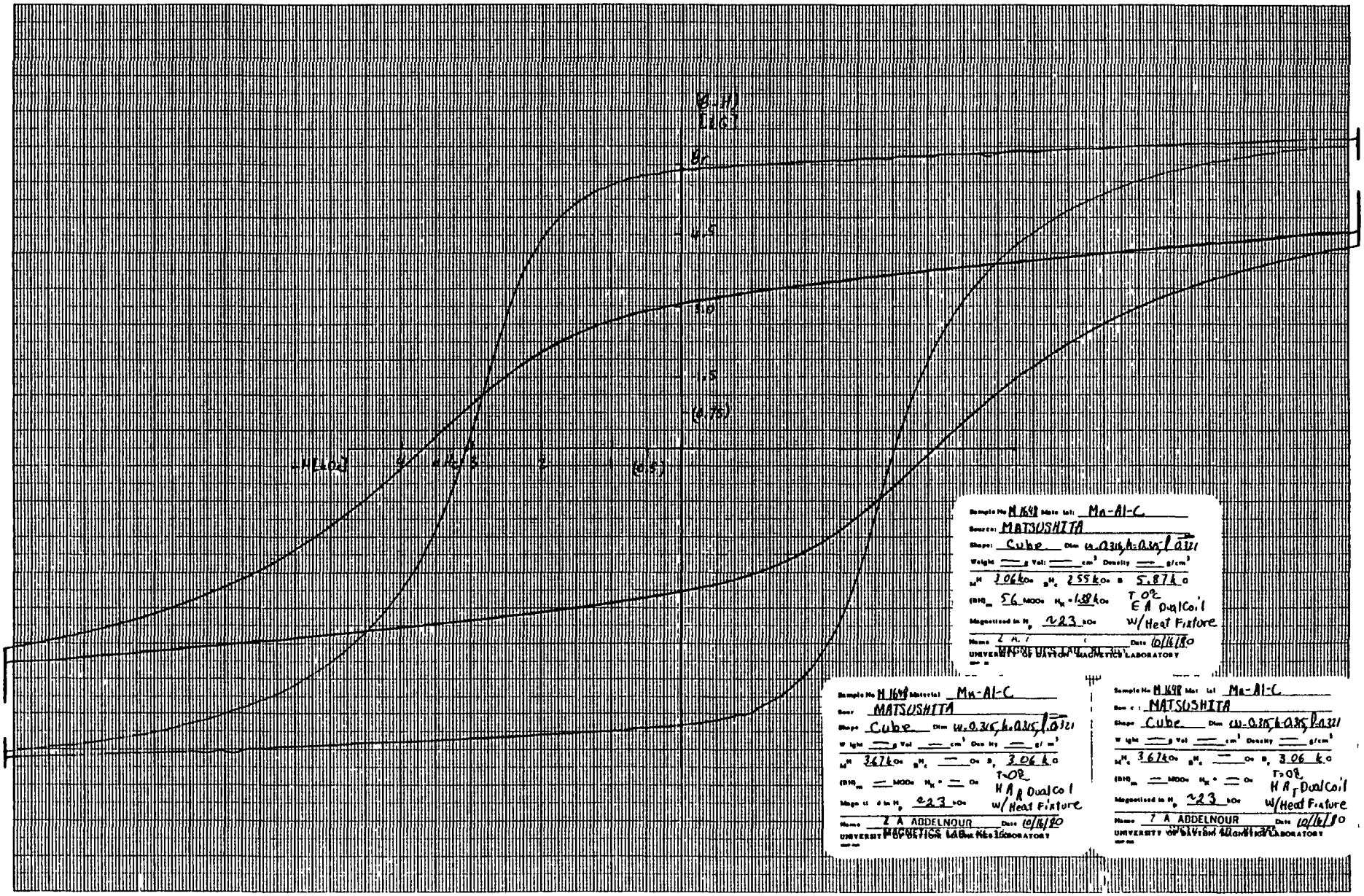

Fig. 59 Major Hysteresis Loops for all Three Cube Axes for M-1648 at 0°C.

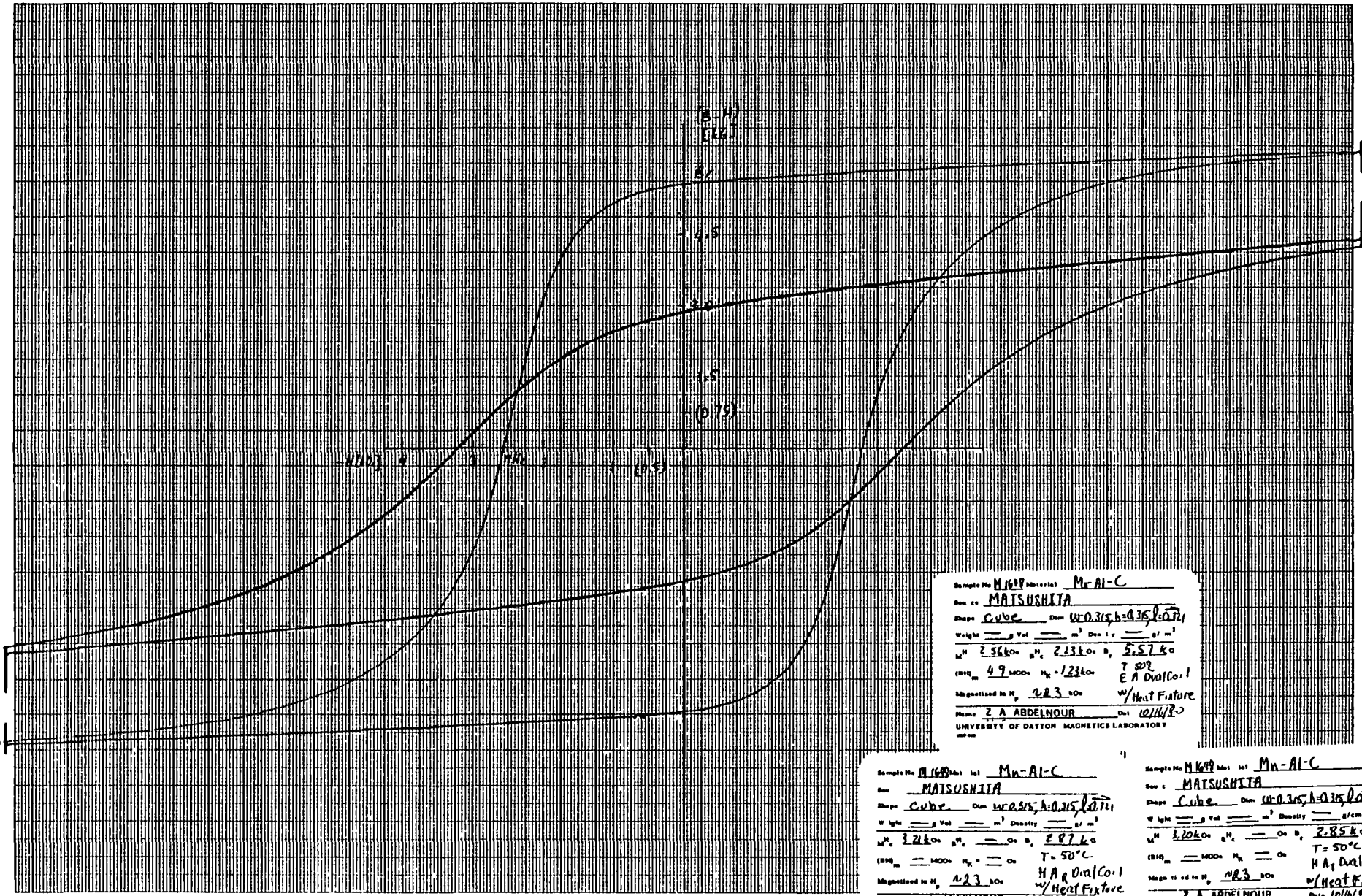

Fig. 60 Major Hysteresis Loops for all Three Cube Axes for M-1648 at +50°C.

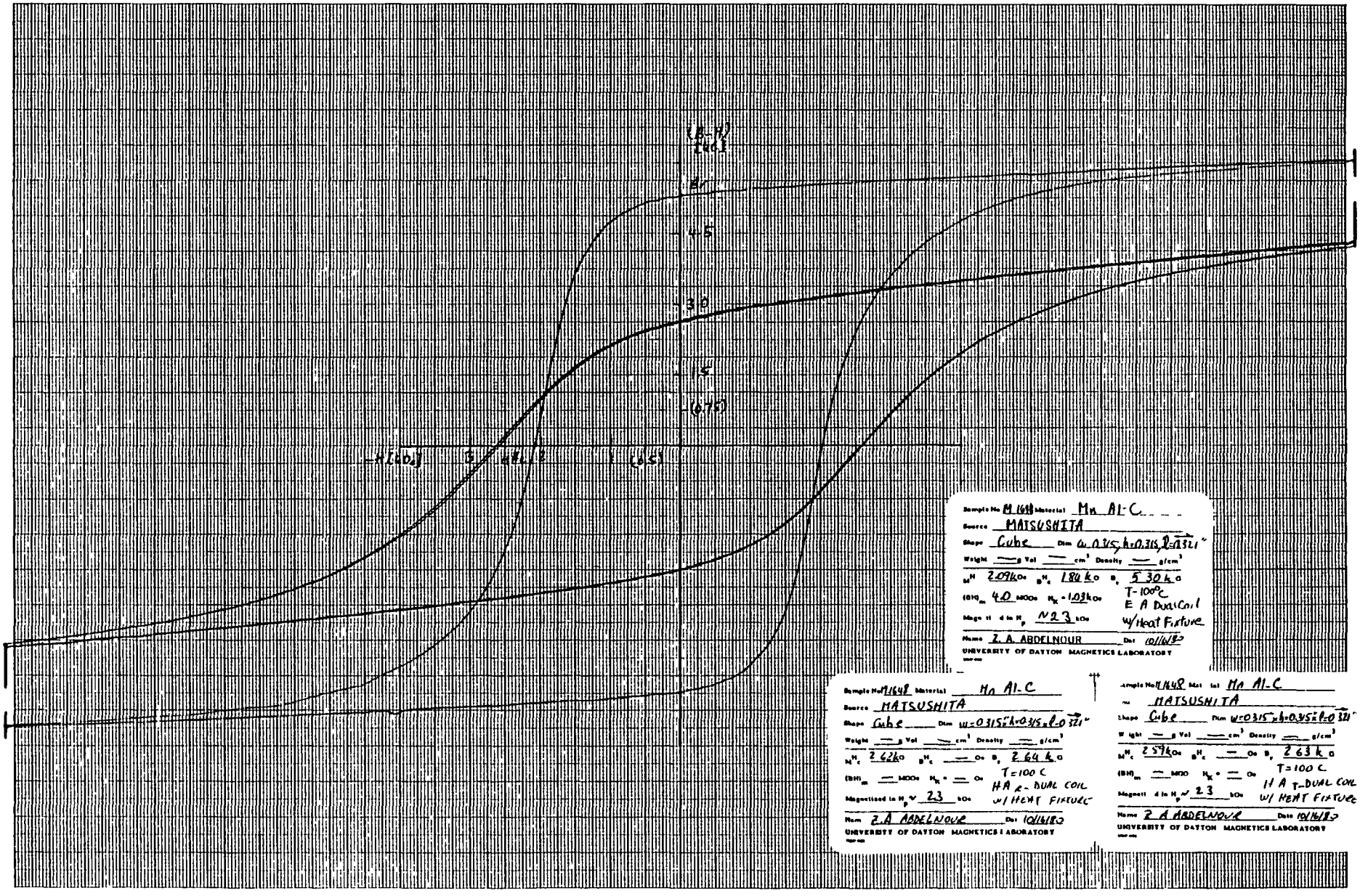

Fig. 61 Major Hysteresis Loops for all Three Cube Axes for M-1648 at +100 °C.

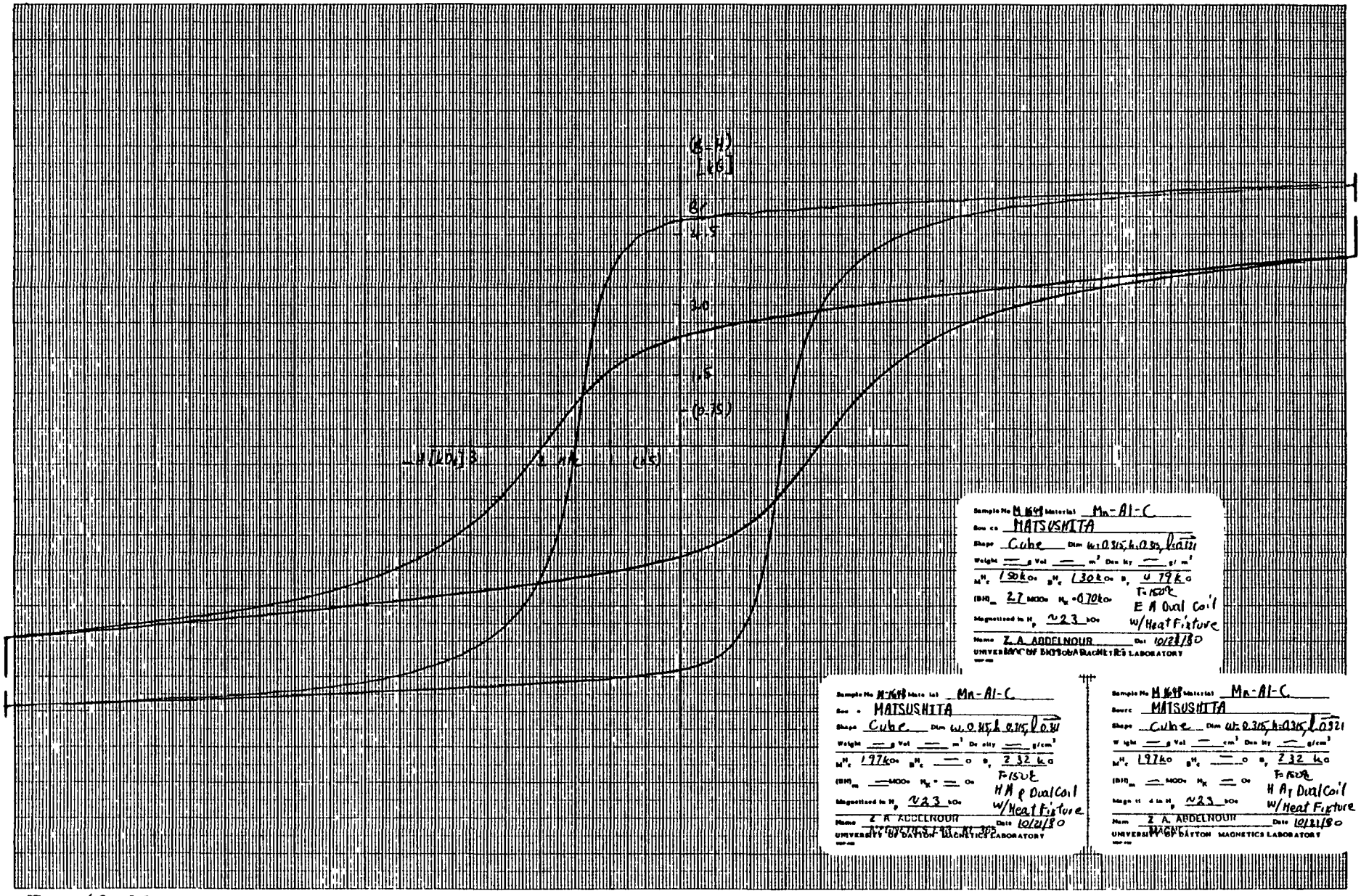

Fig. 62 Major Hysteresis Loops for all Three Cube Axes for M-1648 at +150°C.

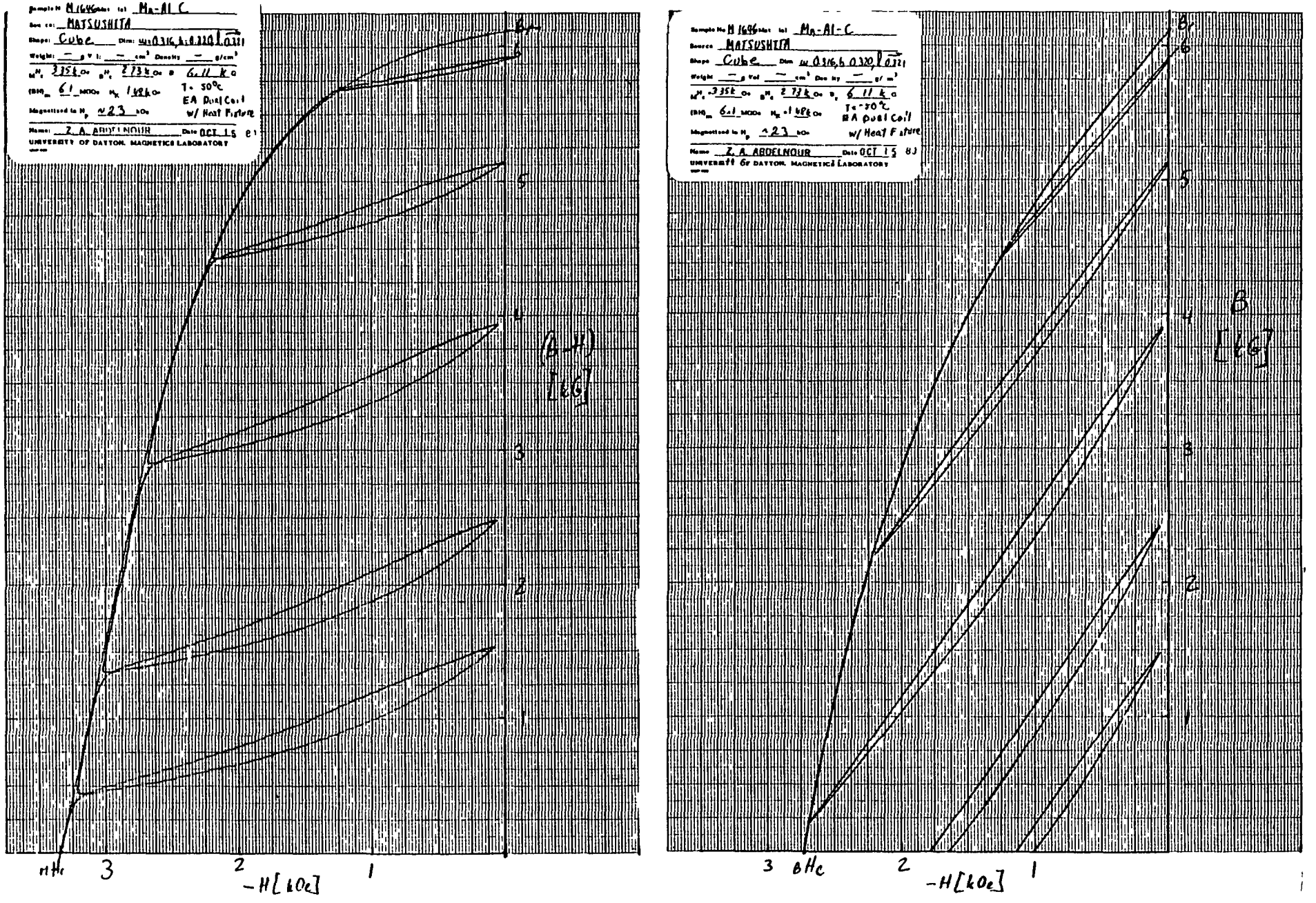

Fig. 63 Q-2 Recoil Loops, (B-H) &B for Cube M-1646 at -50°C.

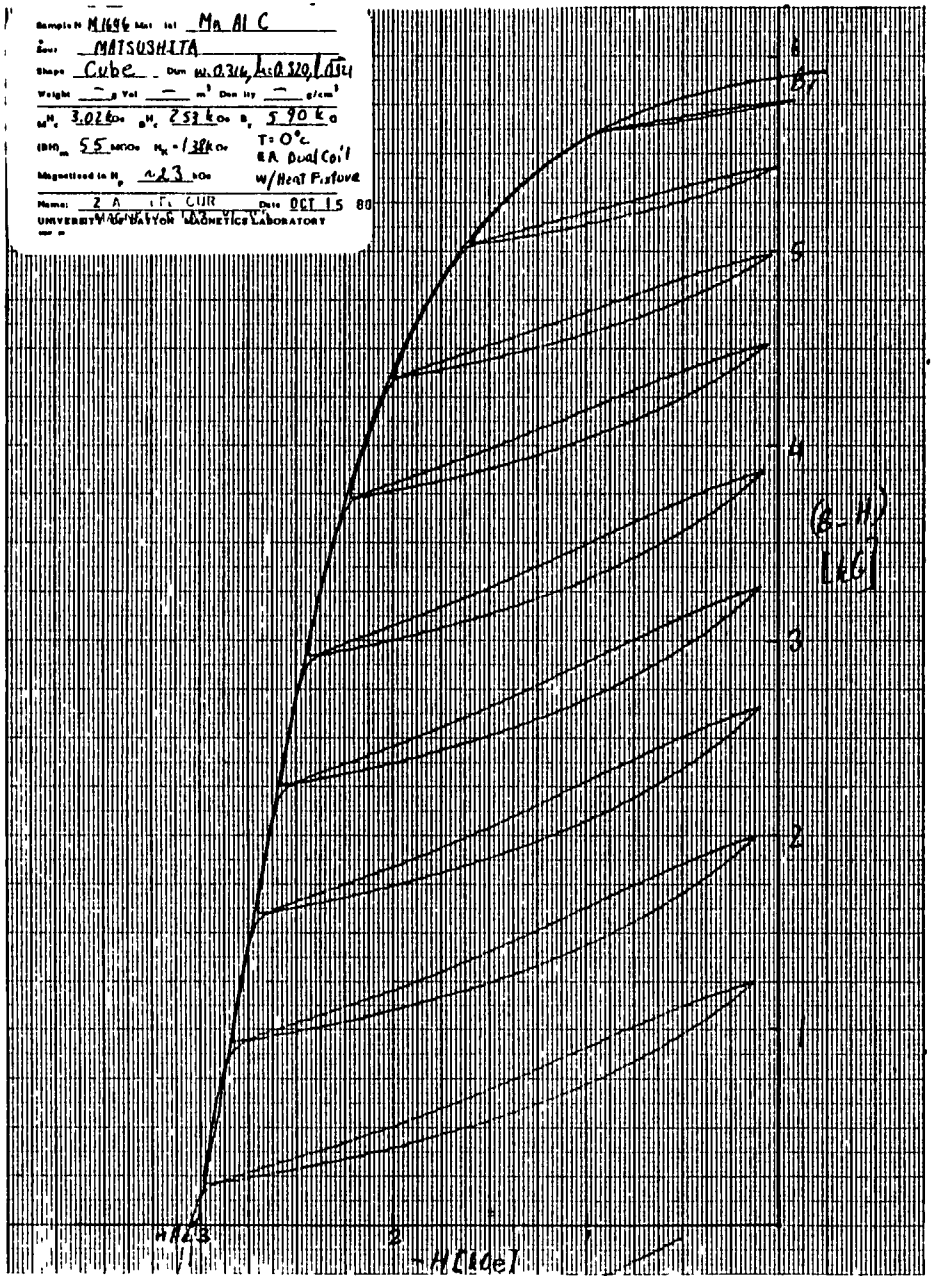

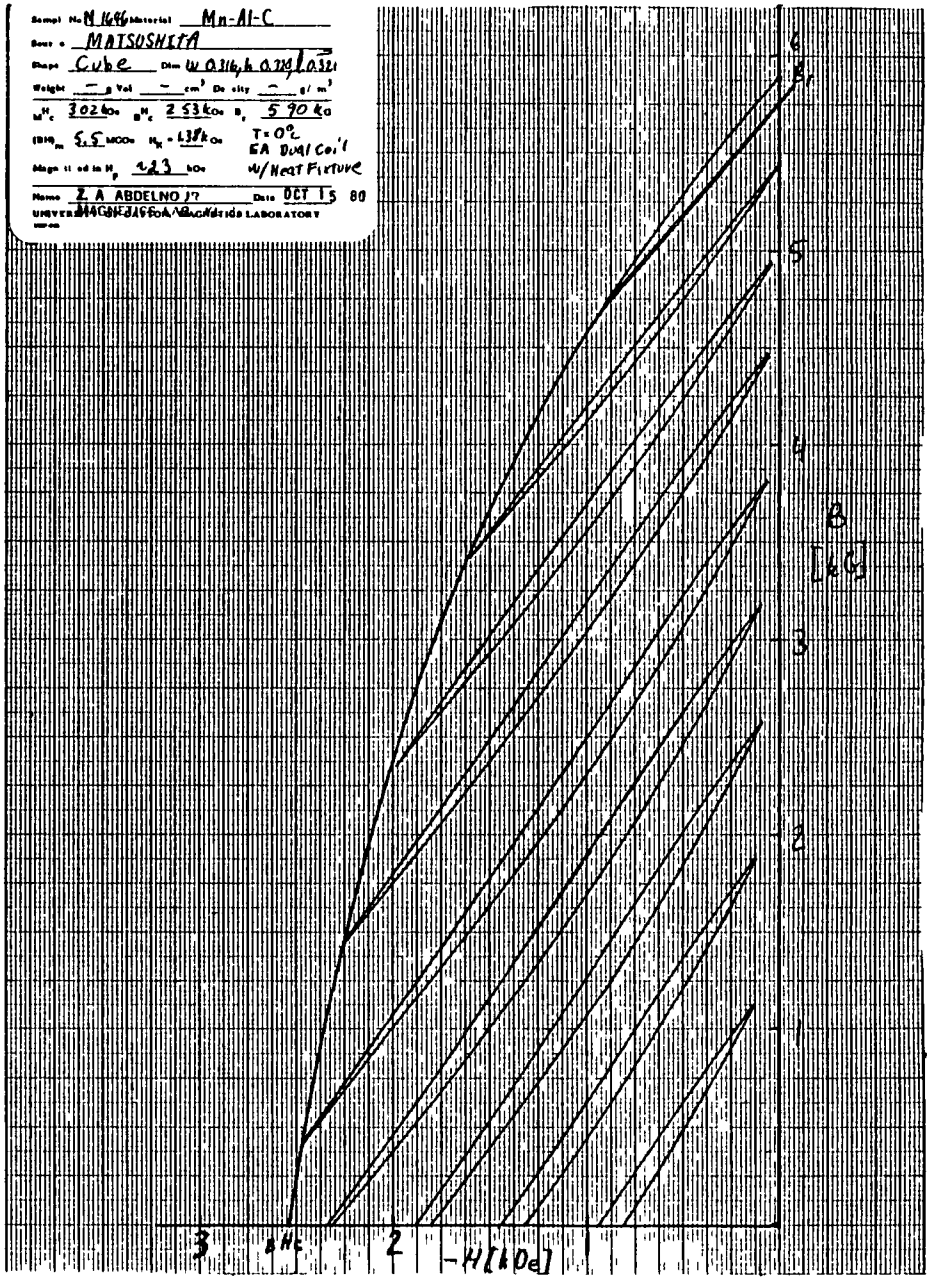

Fig. 64 Q-2 Recoil Loops, (B-H) &B for Cube M-1646 at 0° C.

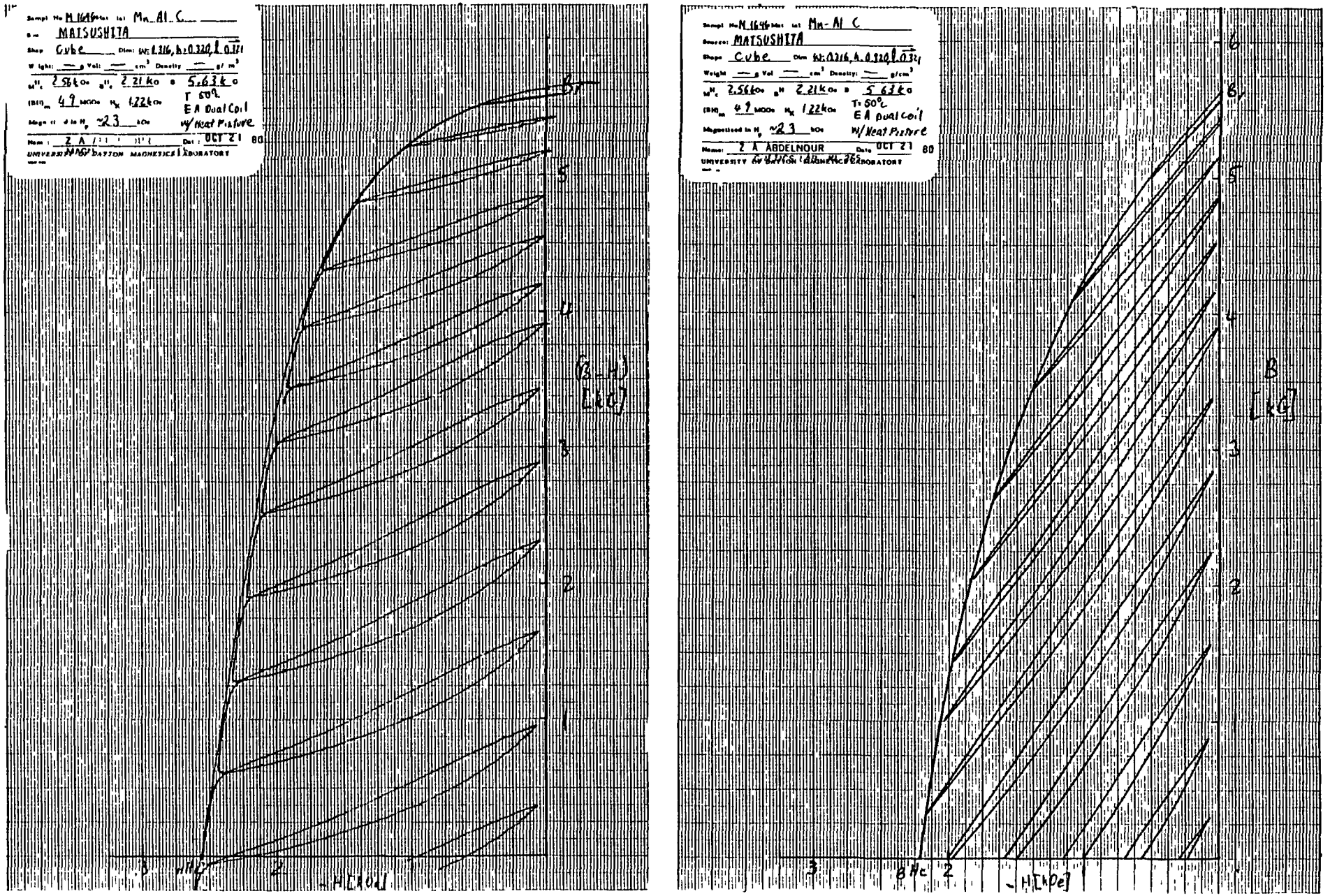

Fig. 65 Q-2 Recoil Loops, (B-H) & B for Cube M-1646 at +50° C.

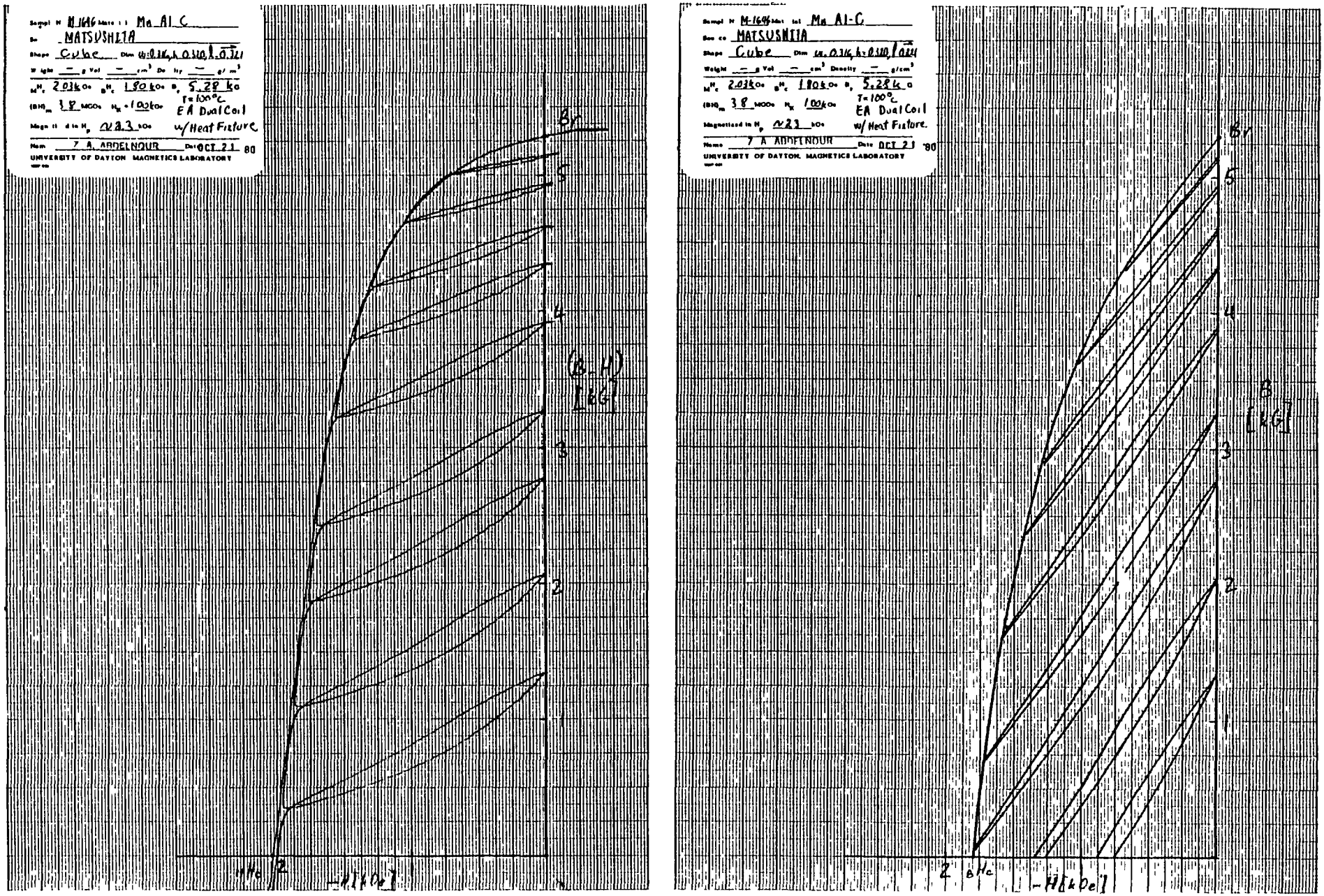

Fig. 66 Q-2 Recoil Loops, (B-H) & B for Cube M-1646 at +100°C.

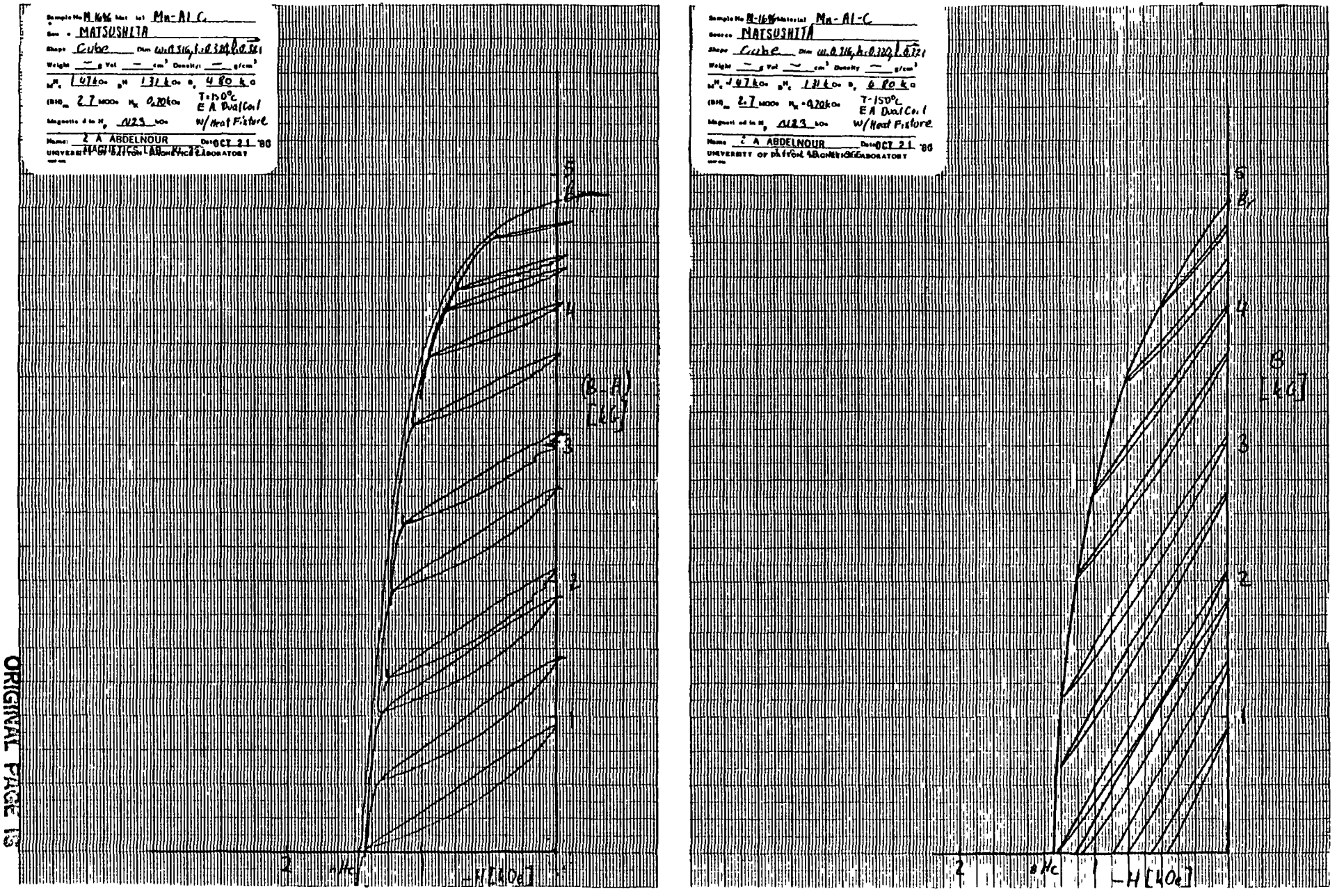

Fig. 67 Q-2 Recoil Loops, (B-H) & B for Cube M-1646 at +150°C

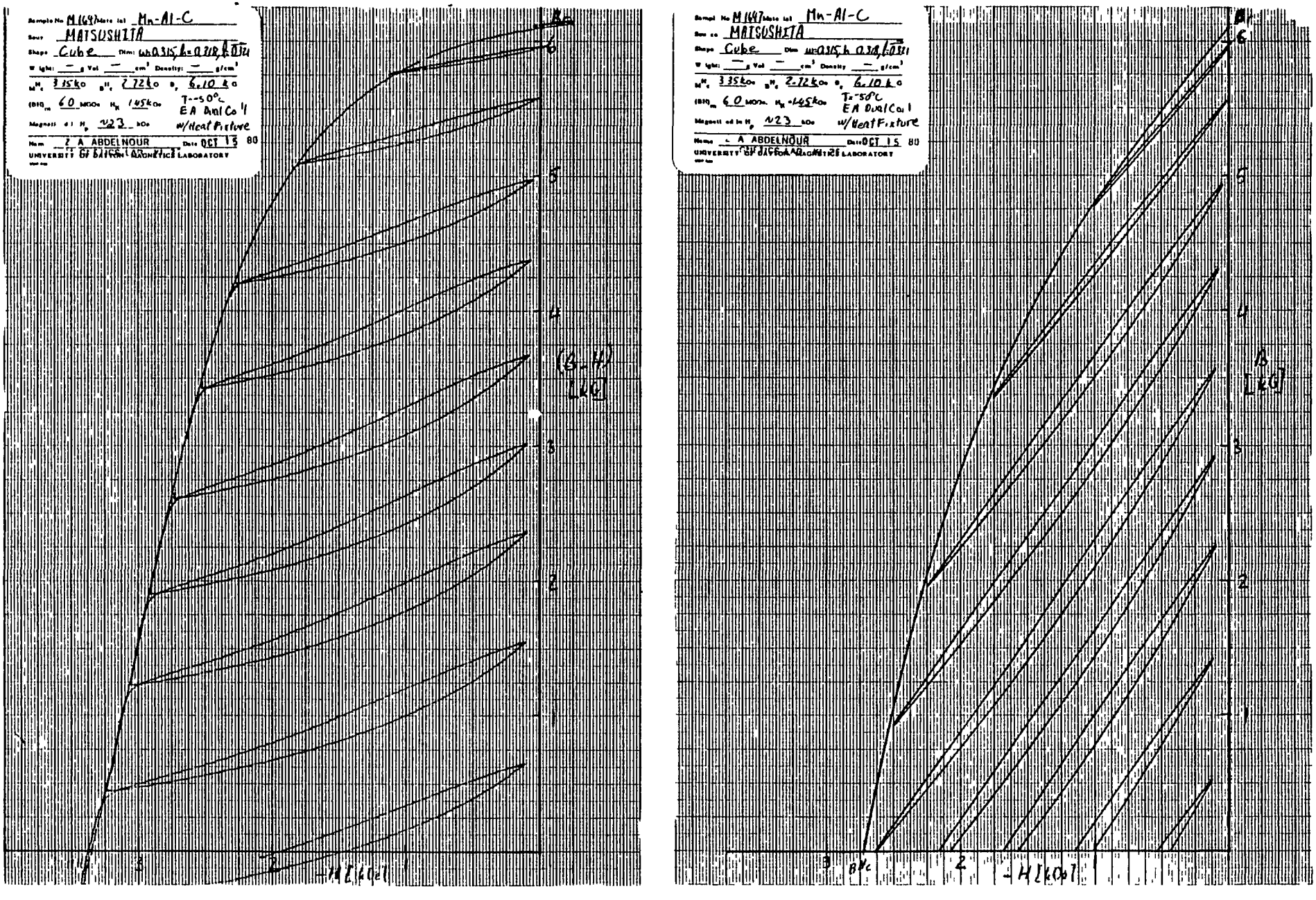

Fig. 68 Q-2 Recoil Loops, (B-H) & B for Cube M-1647 at -50°C.

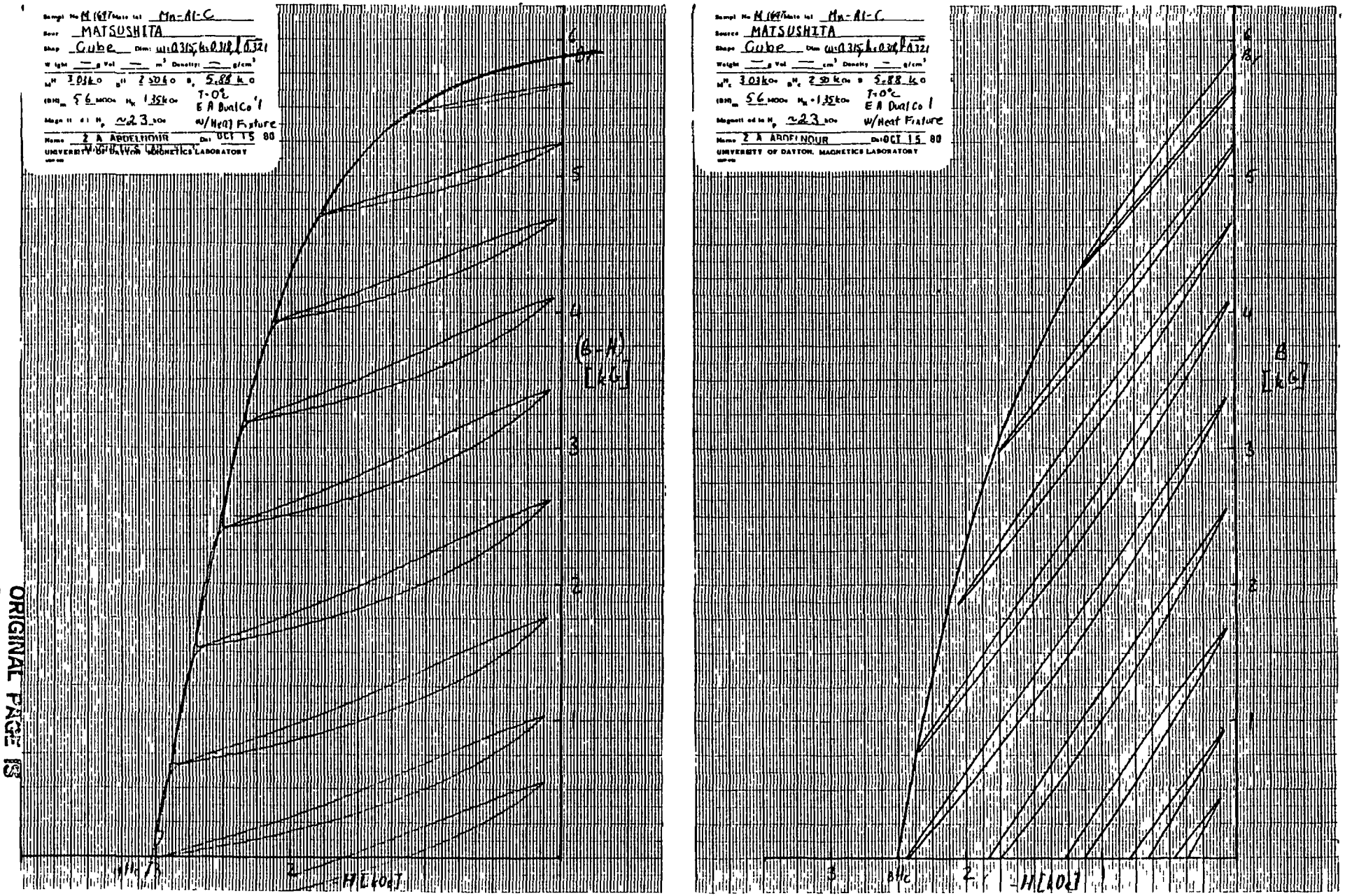

Fig. 69. Q-2 Recoil Loops, (B-H) & B for Cube M-1647 at 0°C.

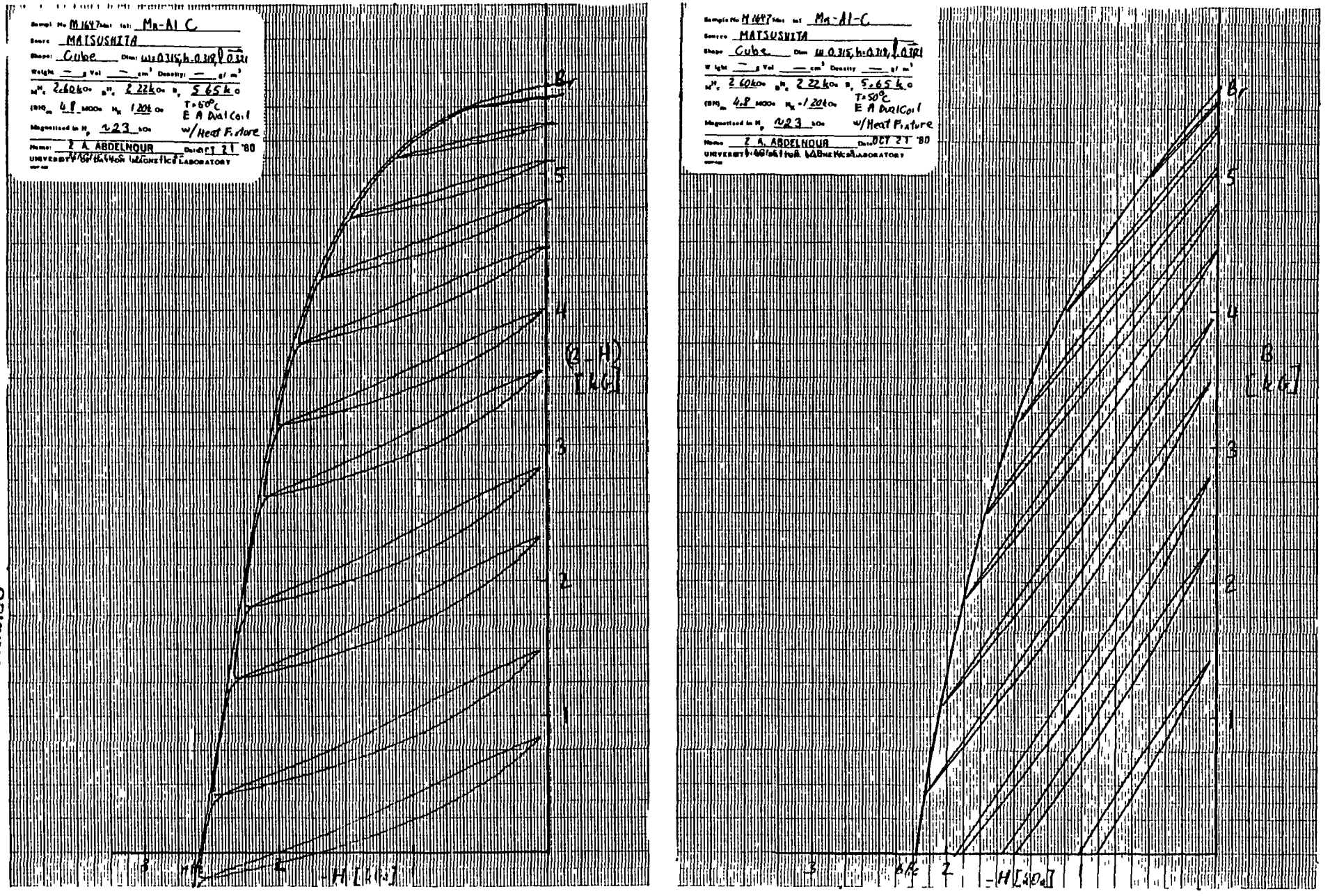

Fig. 70 Q-2 Recoil Loops, (B-H) & B for Cube M-1647 at +50°C.

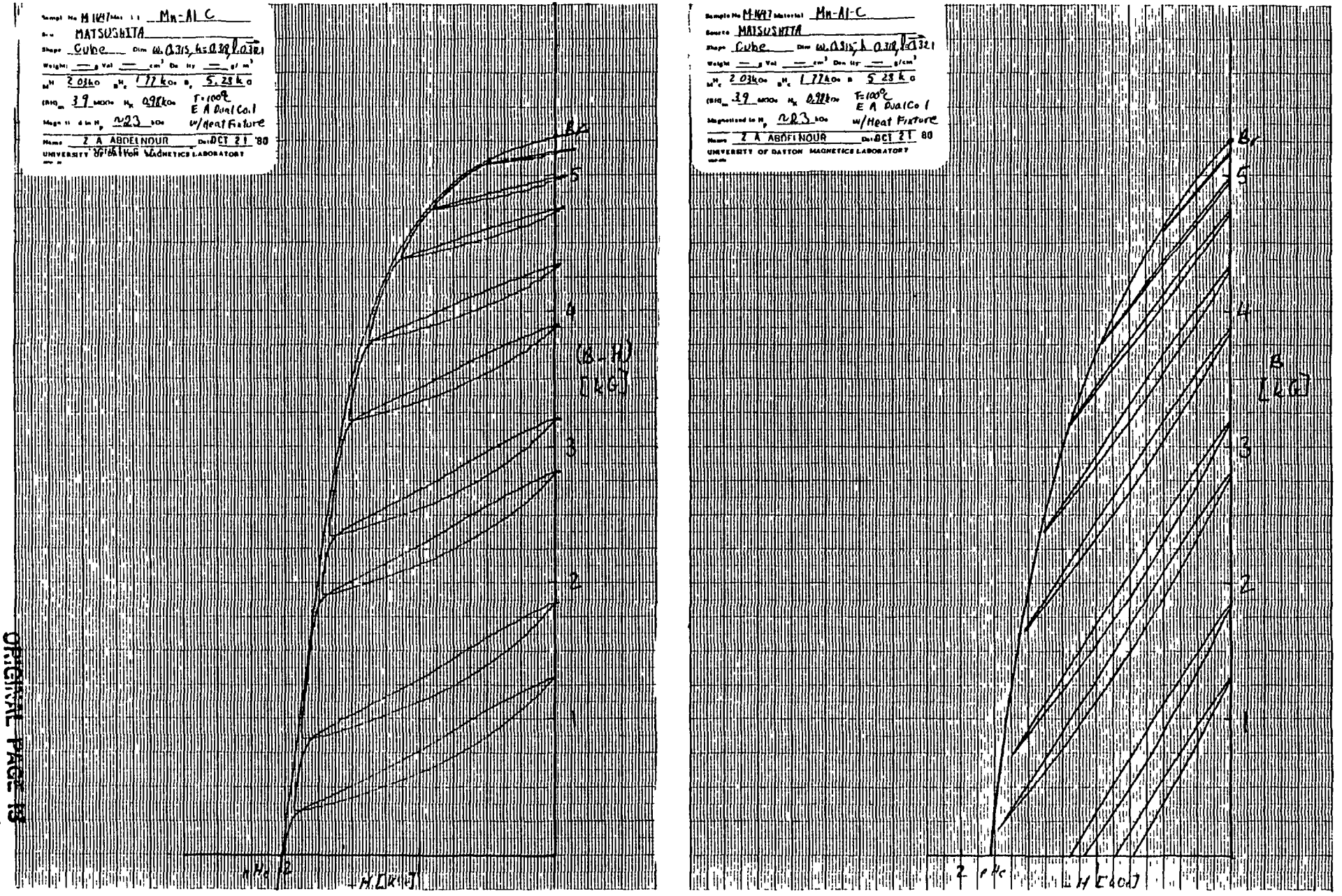

Fig. 71 Q-2 Recoil Loops, (B-H) & B for Cube M-1647 at +100°C.

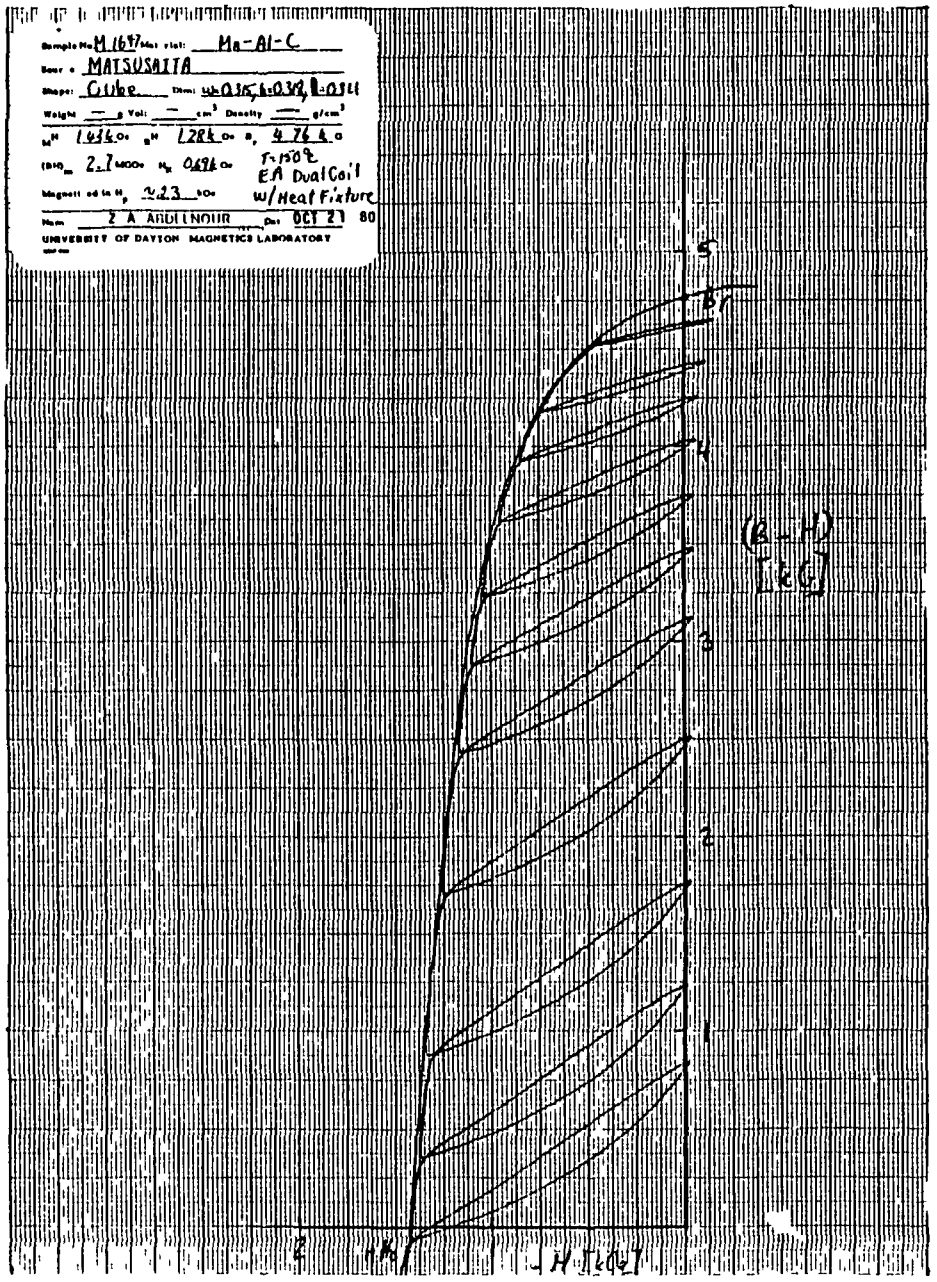

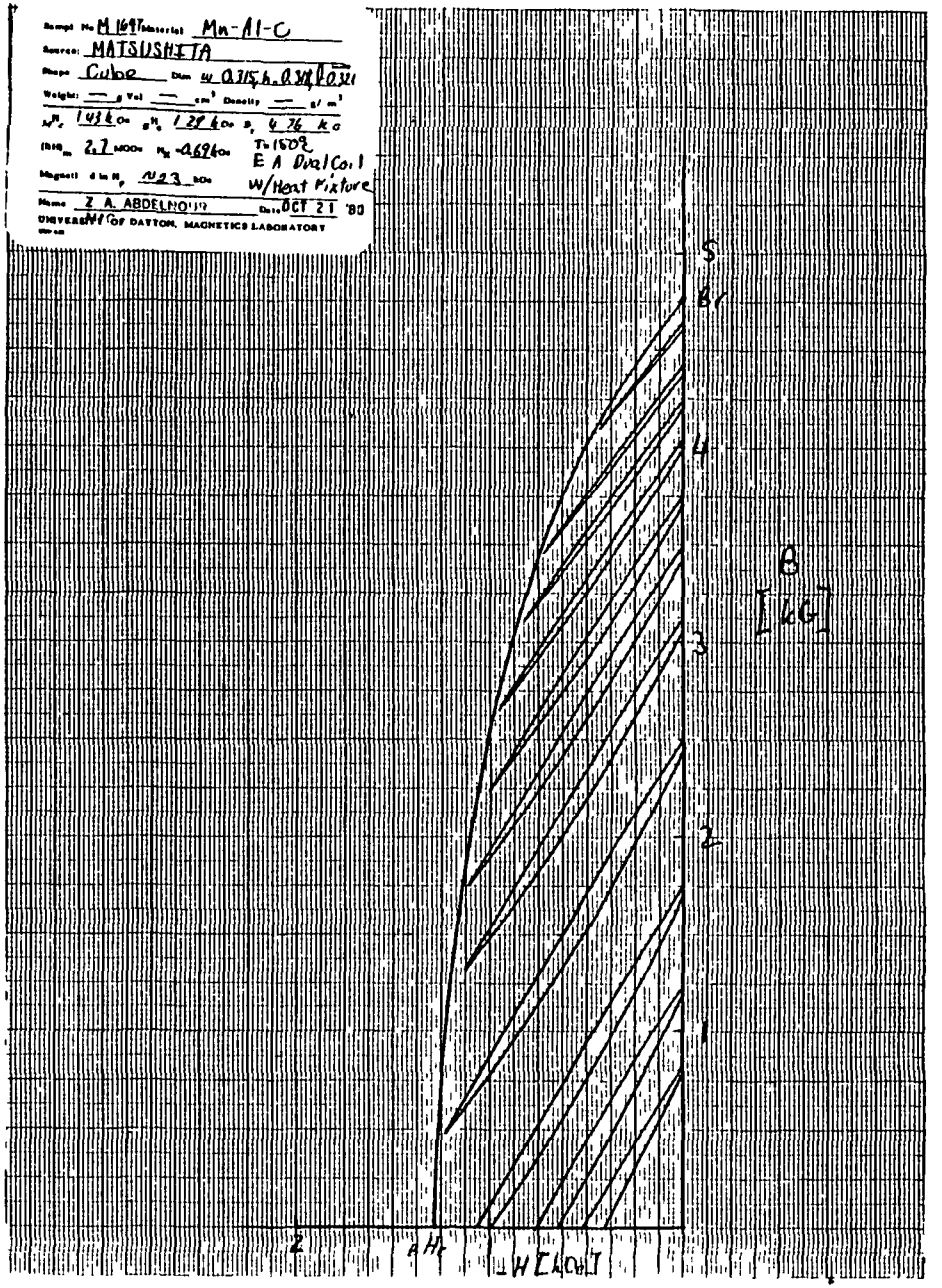

Fig. 72 Q-2 Recoil Loops, (B-H) & B for Cube M-1647 at +150°C.

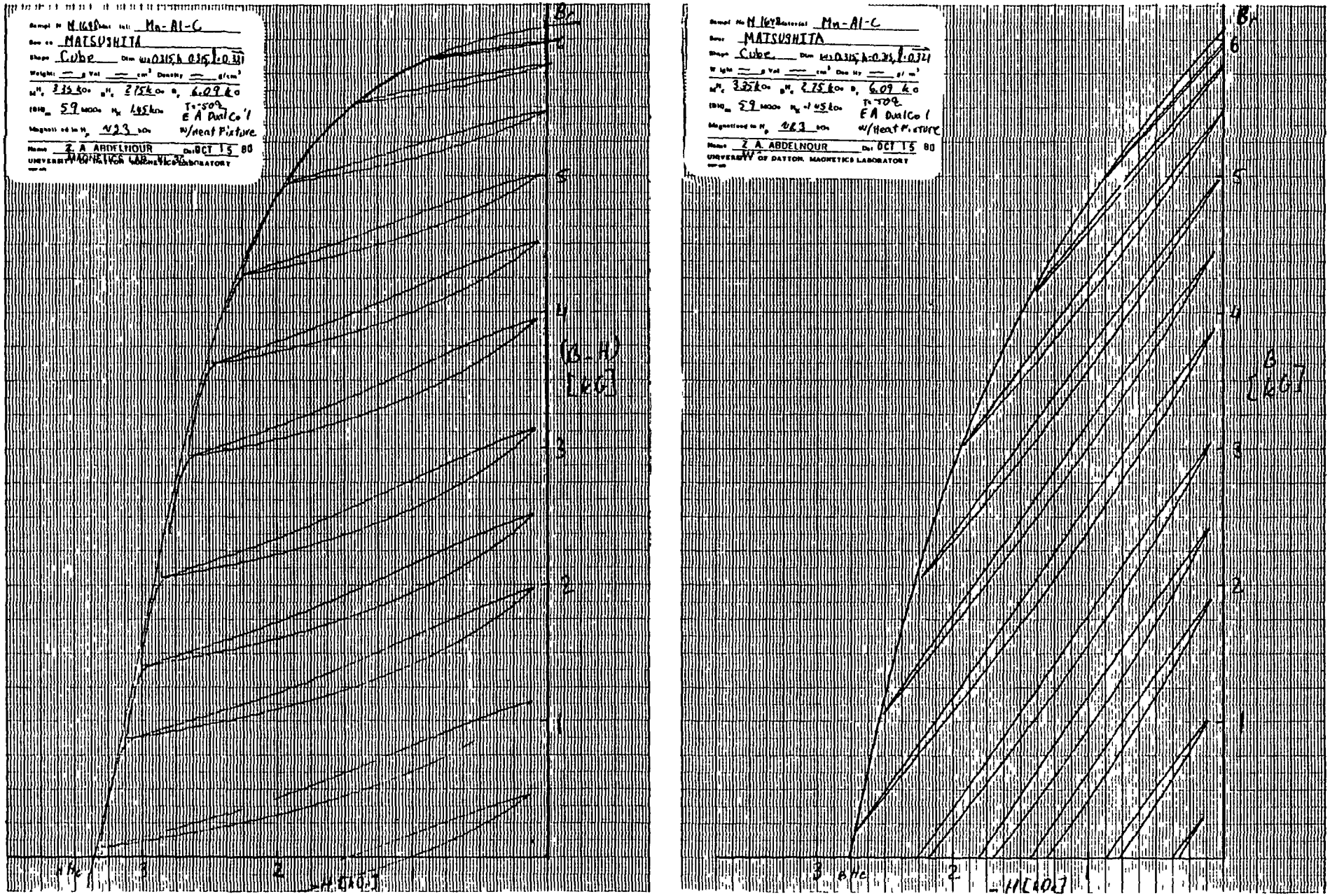

Fig. 73 Q-2 Recoil Loops, (B-H)&B for Cube M-1648 at -50°C.

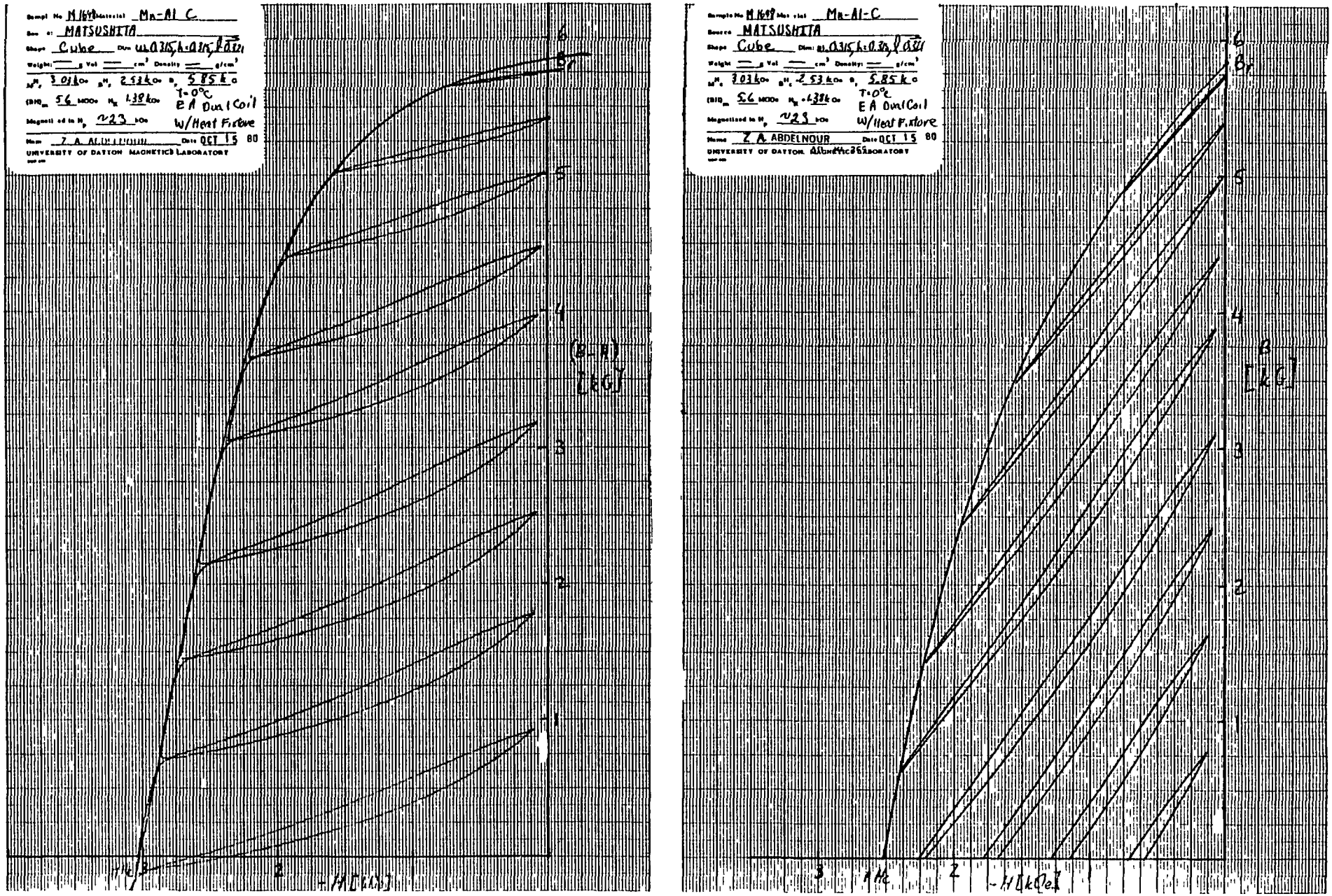

Fig. 74 Q-2 Recoil Loops, (B-H) & B for Cube M-1648 at 0°C.

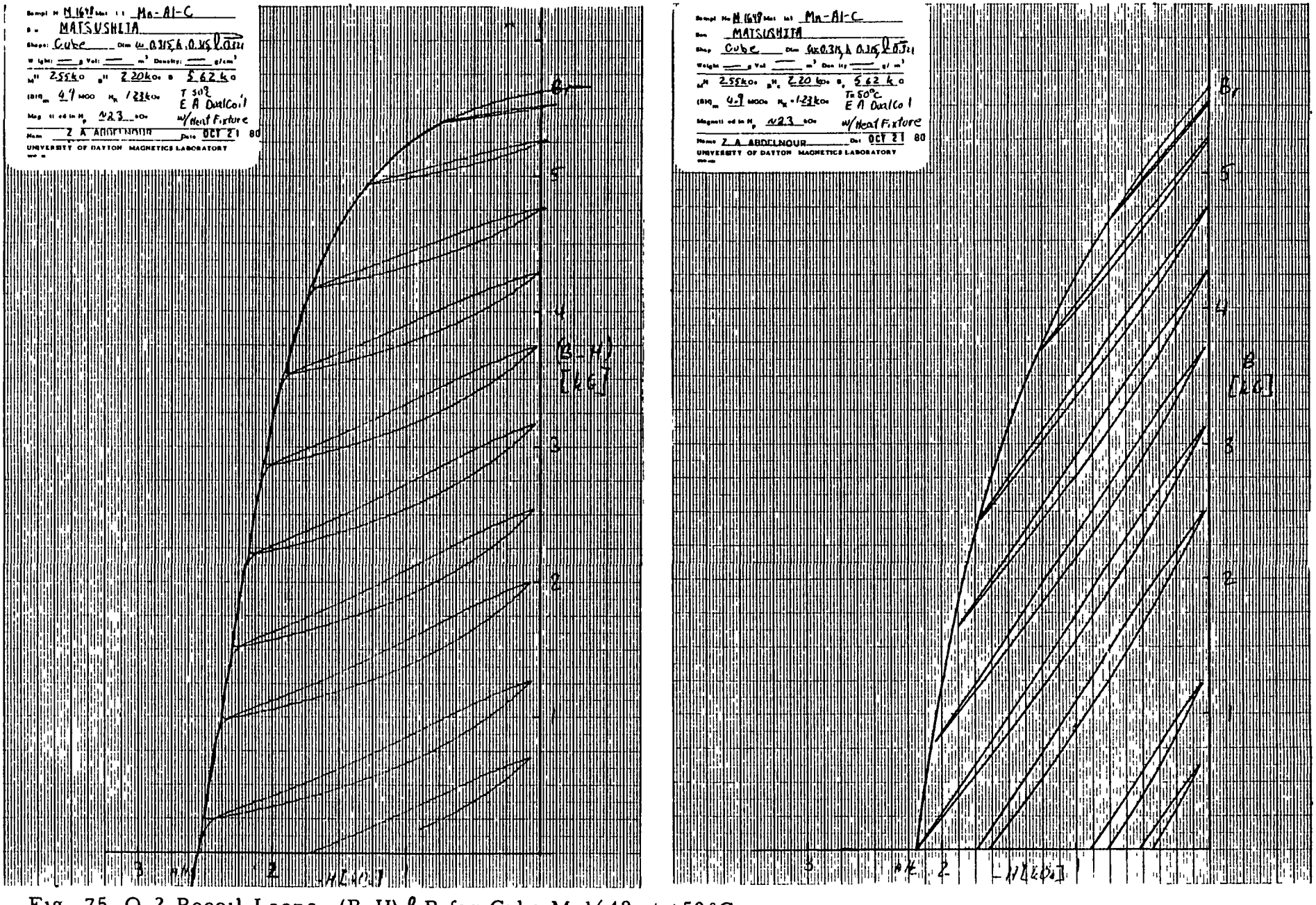

Fig. 75 Q-2 Recoil Loops, (B-H) & B for Cube M-1648 at +50 °C.

C-2

A-73

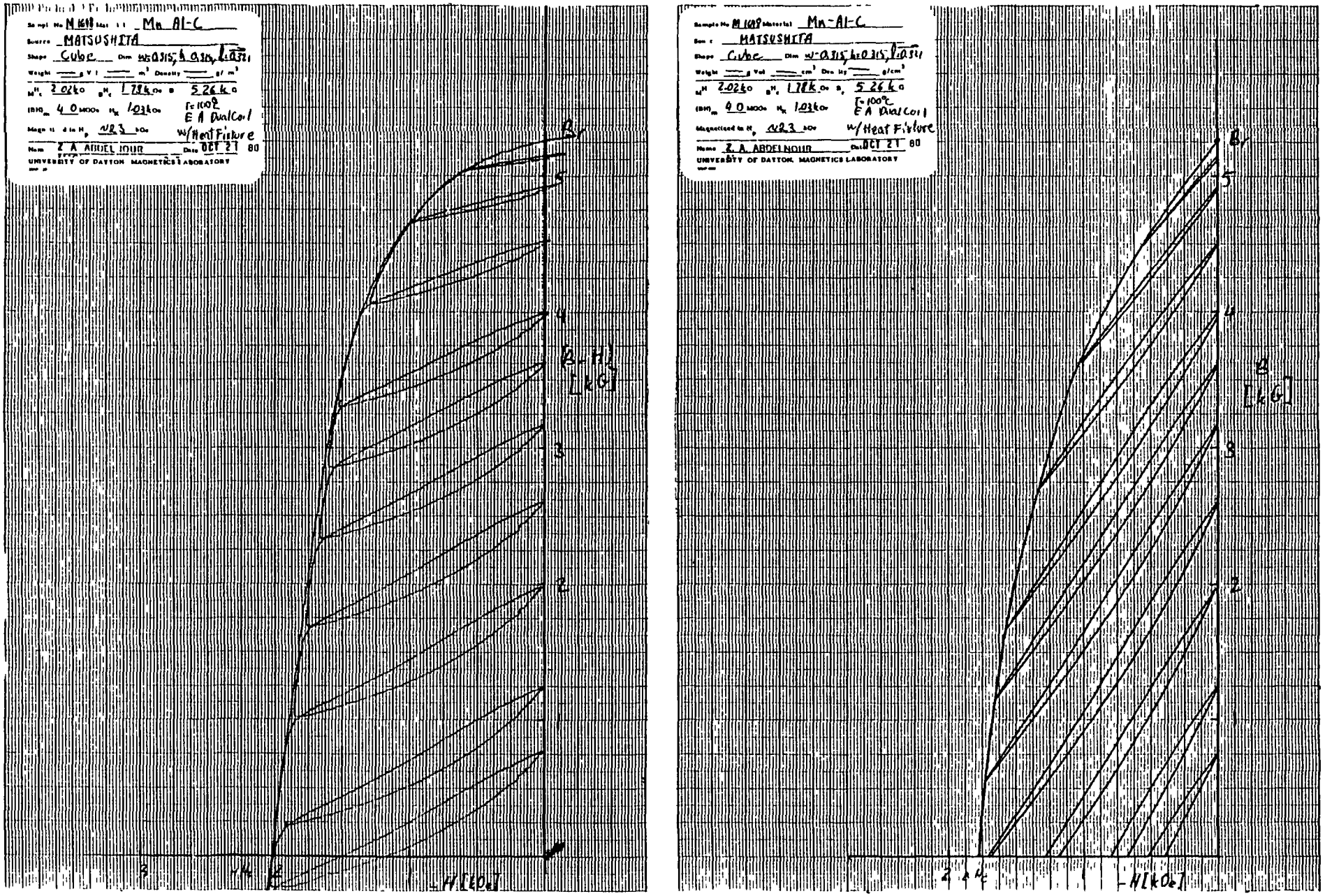

Fig. 76 Q-2 Recoil Loops, (B-H) & B for Cube M-1648 at +100°C.

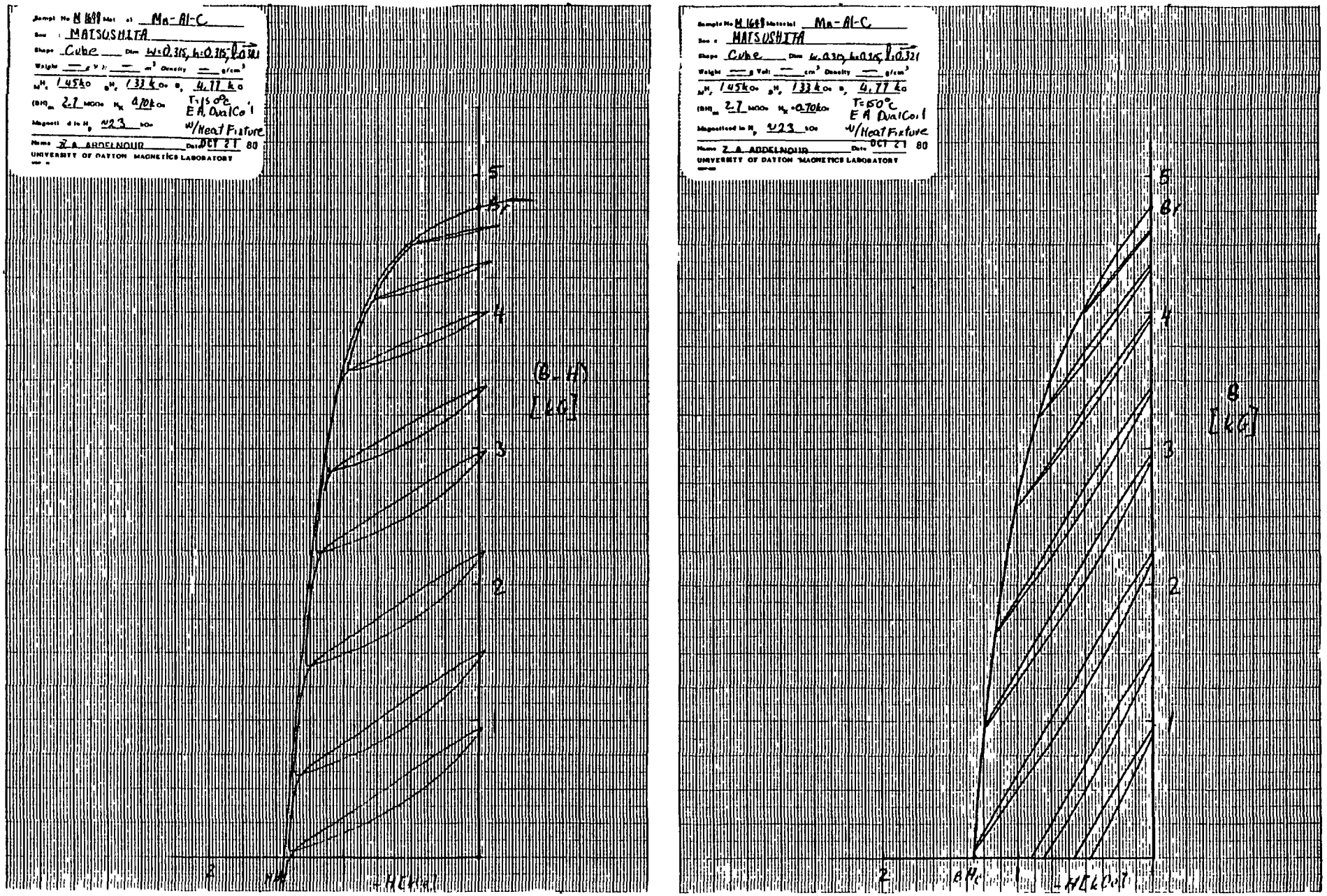

Fig. 77 Q-2 Recoil Loops, (B-H) &B for Cube M-1648 at +150°C.

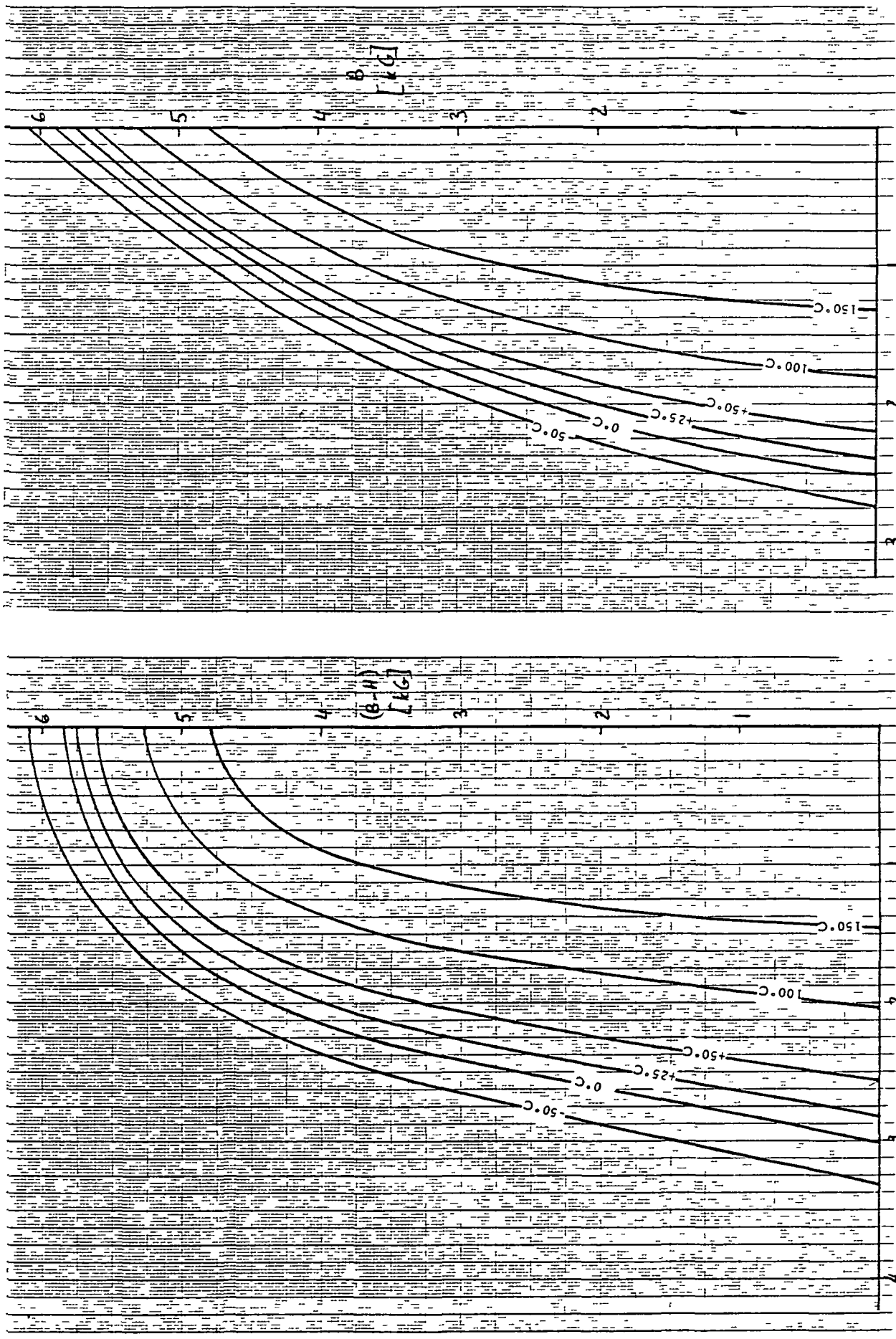

Fig. 78 Composite Q-2 Loops, (B-H) & B For Cube M-1646 At The Various Temperatures (-50°C, 0°C, 25°C, 50°C, 100°C and 150°C).

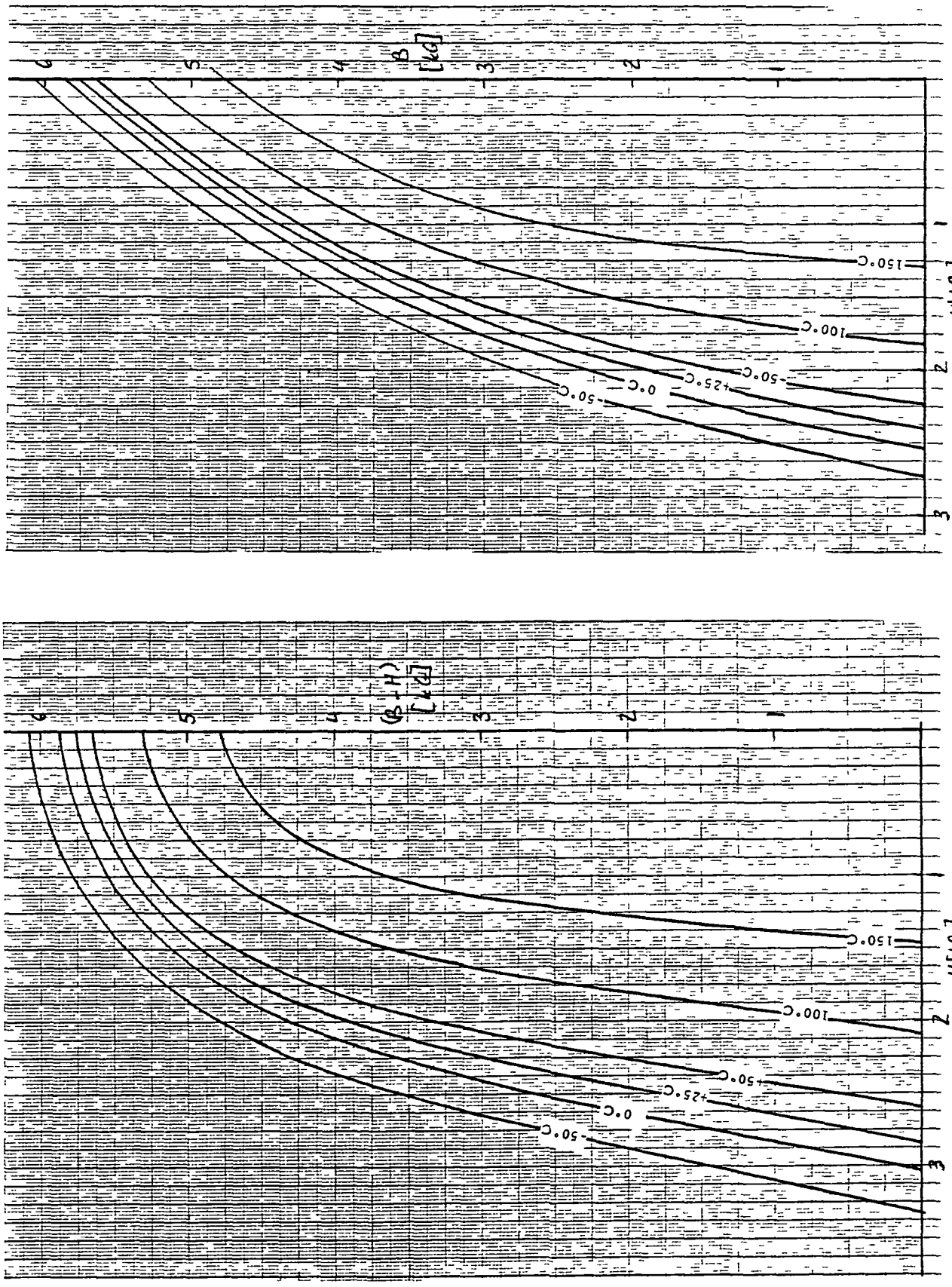

Fig. 79 Composite Q-2 Loops, (B-H) & B For Cube M-1647 At The Various Temperatures (-50°C, 0°C, 25°C, 50°C, 100°C and 150°C).

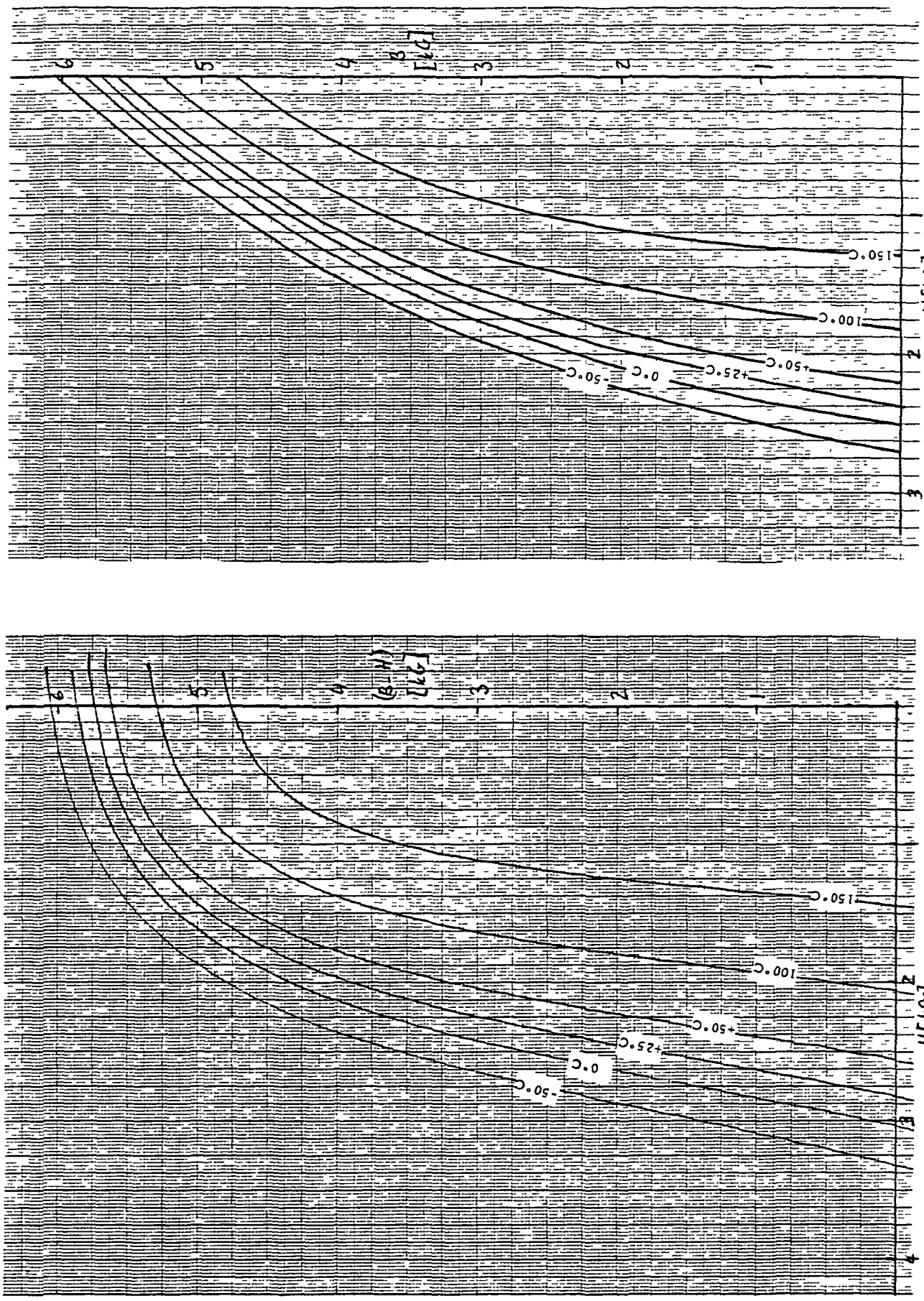

Fig. 80 Composite Q-2 Loops, (B-H) f B For Cube M-1648 At The Various Temperatures (-50°C, 0°C, 25°C, 50°C, 100°C and 150°C).

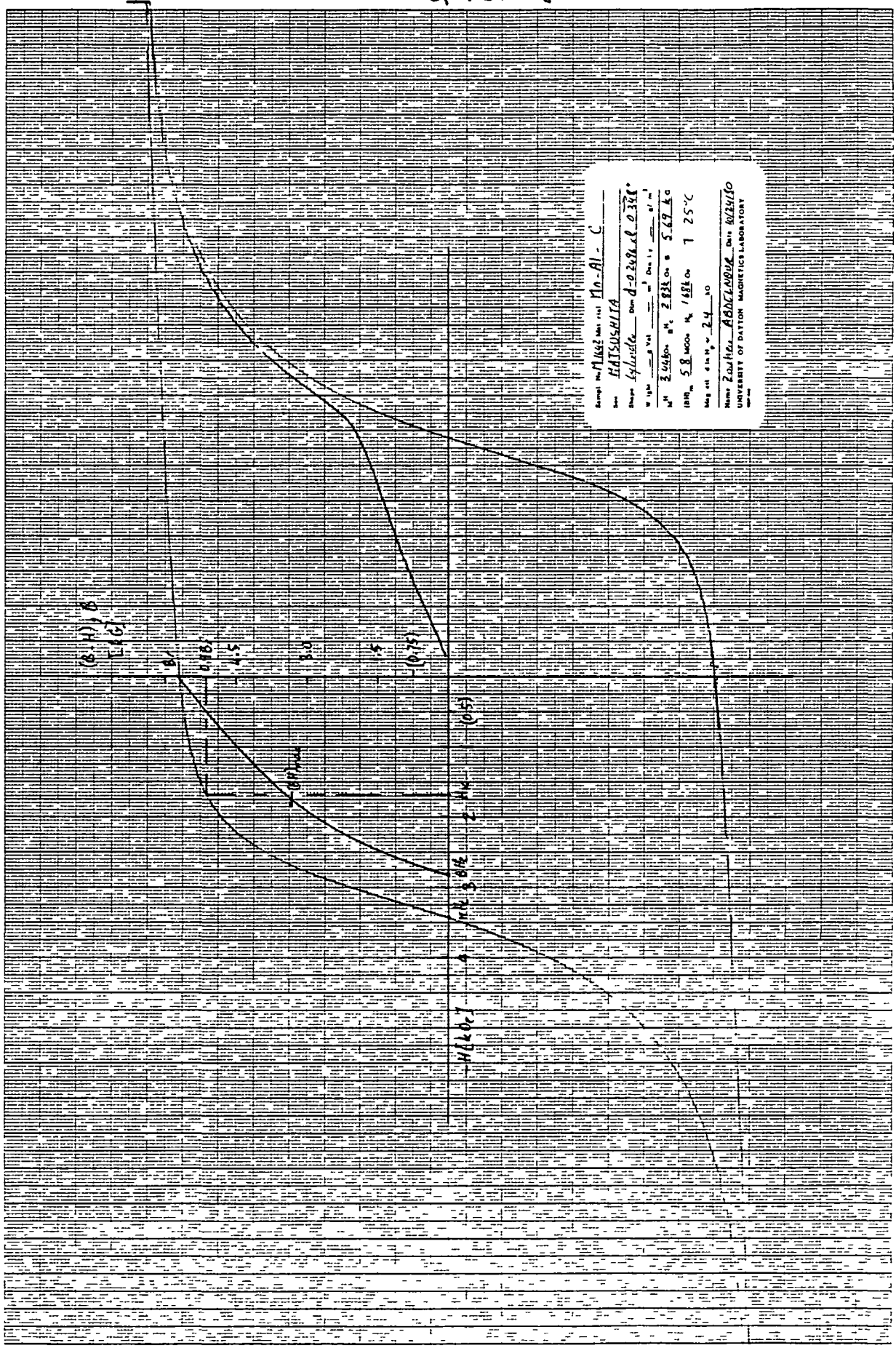

Fig. 81 Major Hysteresis Loops For Cylinder M-1642 at 25°C.

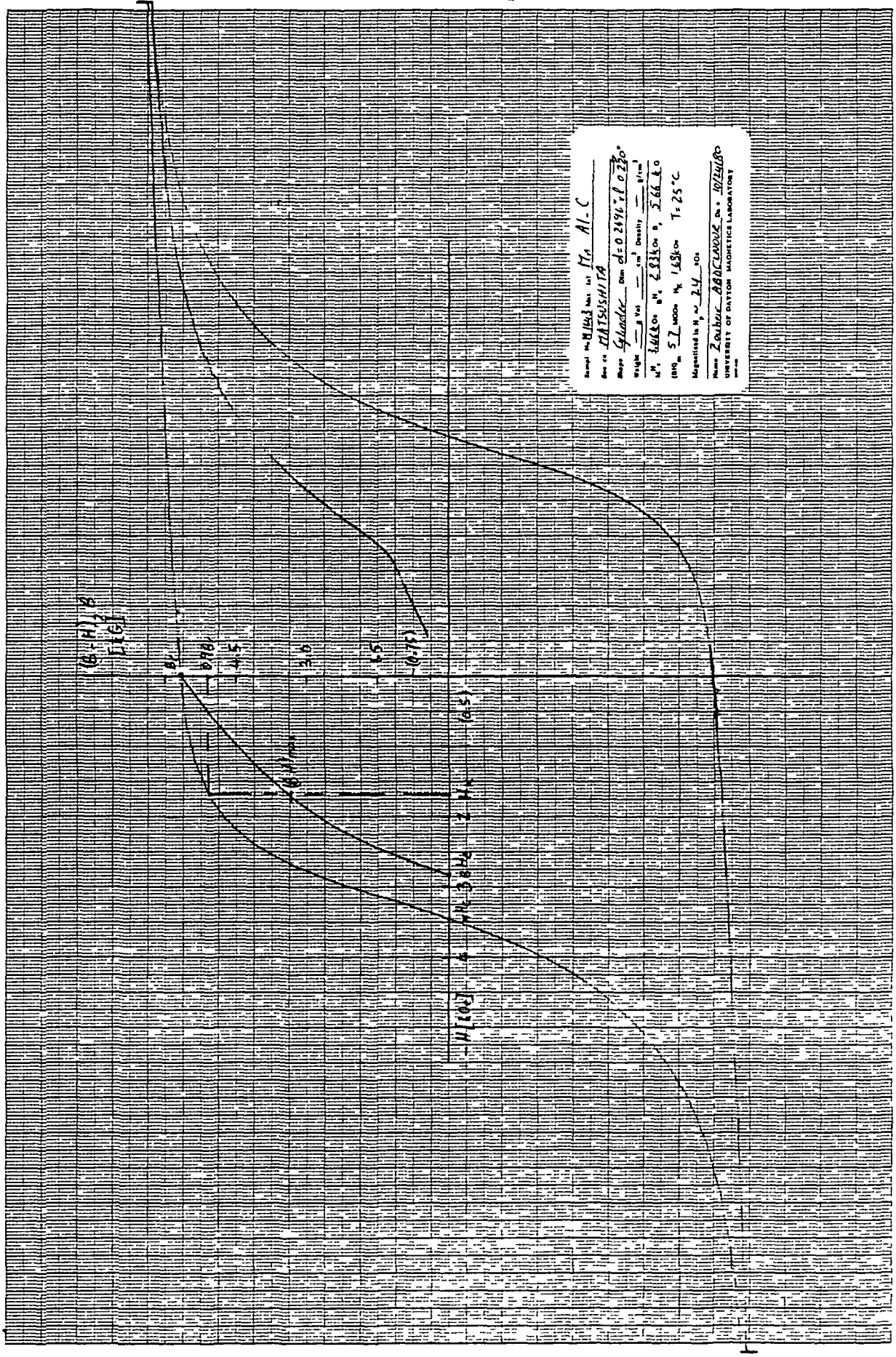

Fig. 82 Major Hysteresis Loops For Cylinder M-1643 at 25°C.

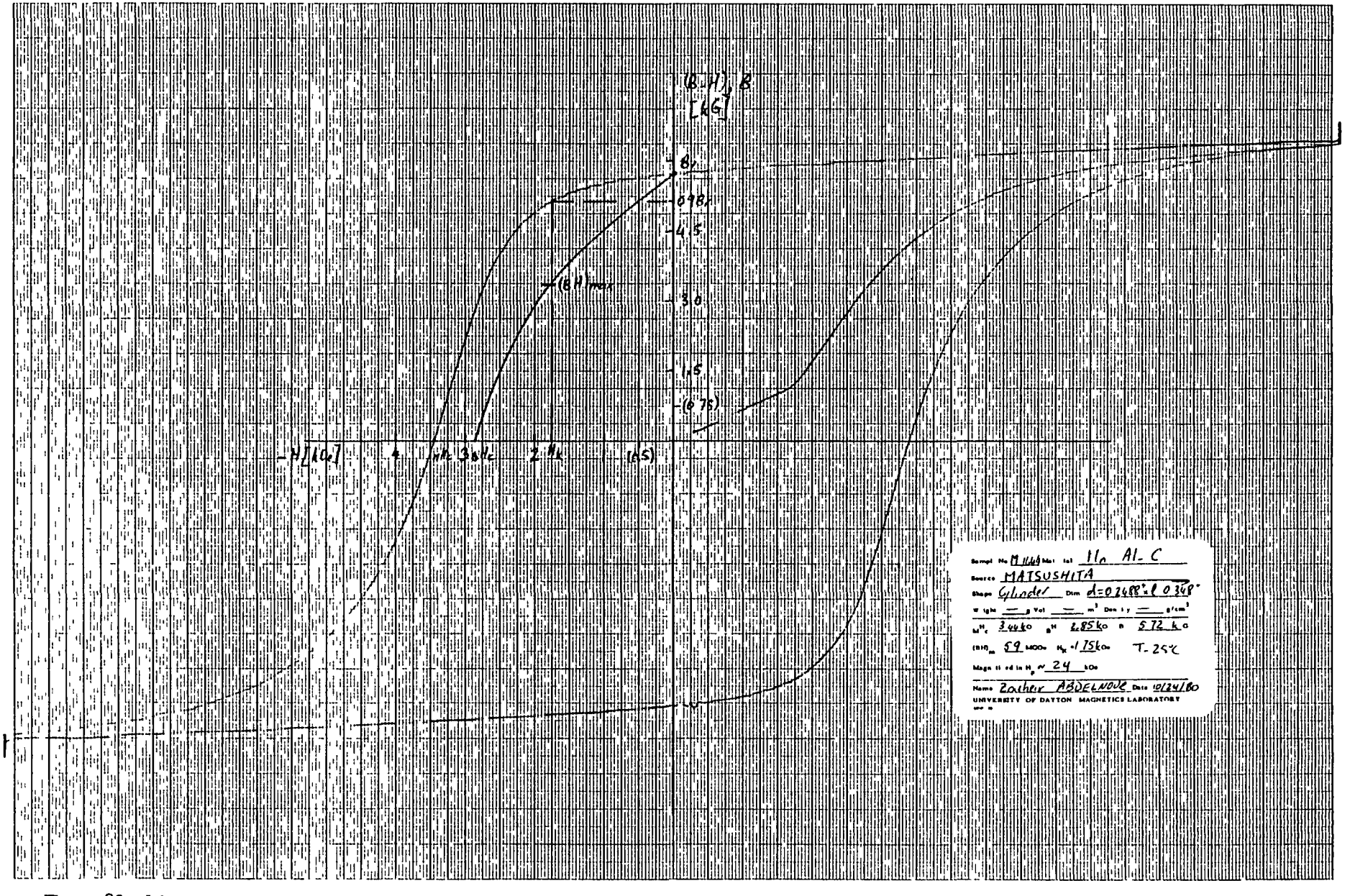

Fig. 83 Major Hysteresis Loops For Cylinder M-1644 at 25°C.

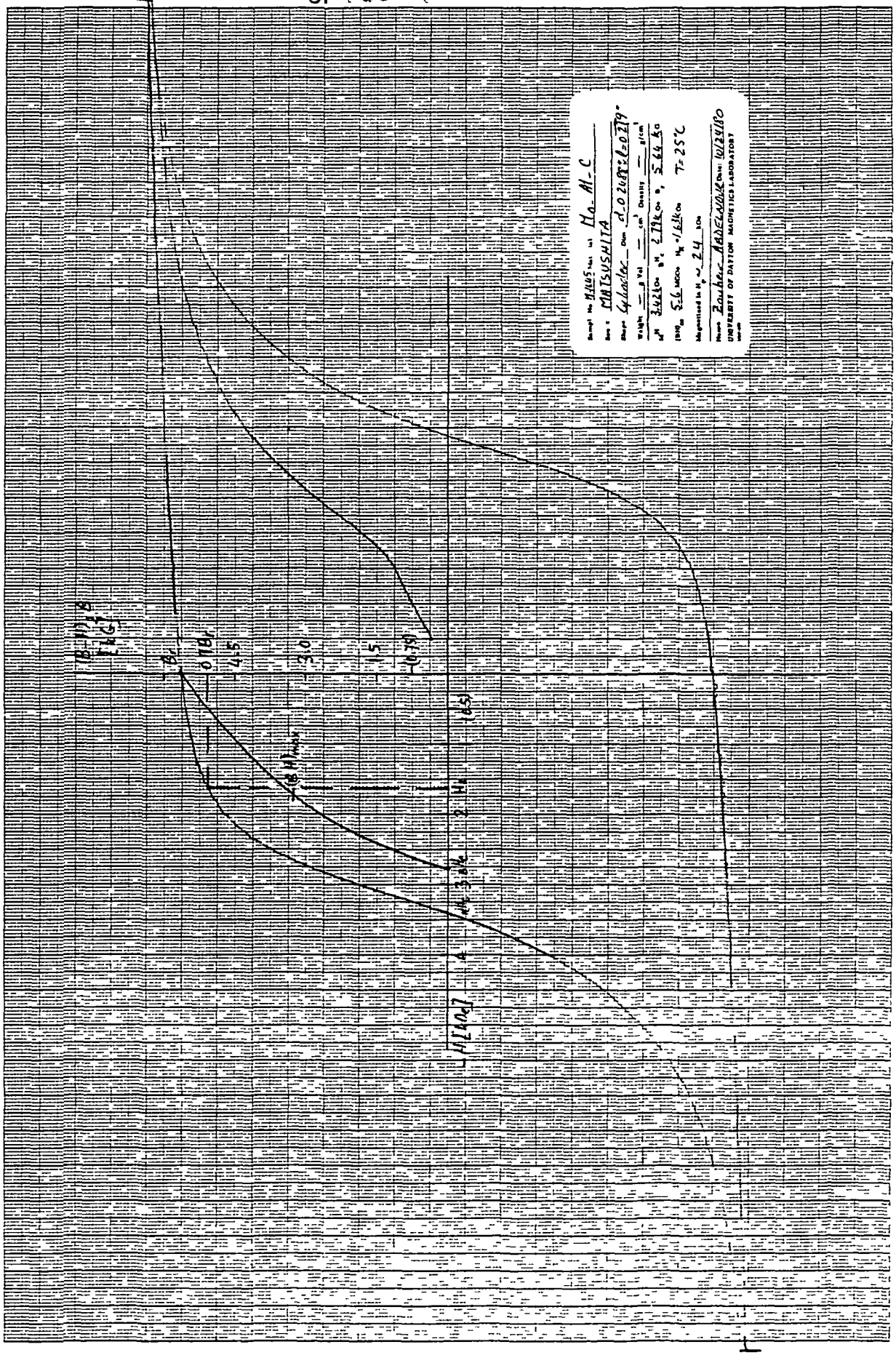

Fig. 84 Major Hysteresis Loops For Cylinder M-1645 at 25°C.